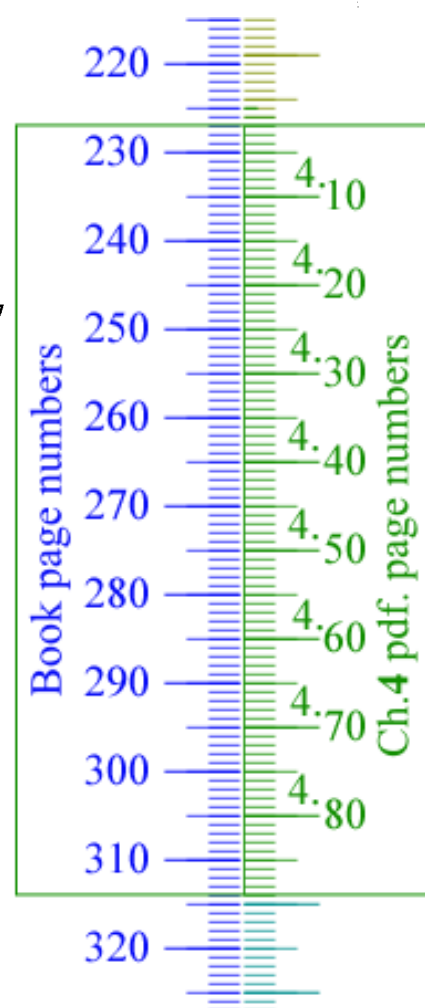


Principles of Symmetry, Dynamics, and Spectroscopy  
- W. G. Harter - Wiley (1993)

Chapter

**4 THEORY AND APPLICATIONS OF HIGHER FINITE SYMMETRY AND INDUCED REPRESENTATIONS**

- 4.1 Octahedral Symmetries and Their Characters / 227
    - A. Octahedral Group ( $O$ ) / 228
    - B. Full Octahedral Group ( $O_h$ ) / 234
    - C. Full Tetrahedral Symmetry  $T_d$  / 236
    - D. Partial Tetrahedral Symmetries  $T$  and  $T_h$  / 236
  - 4.2 Irreducible Representations of Octahedral Symmetry / 237
    - A. Subgroup Chains and Idempotent Splitting / 237
    - B. More Subgroup Correlations / 231
    - C. Conjugate and Normal Subgroups / 254
  - 4.3 Introduction to Symmetry Breaking and Induced Representations / 255
    - A. Octahedral Models and Induced Representations / 256
    - B. Model Solving and Induced Representation Reduction / 259
    - C. The Frobenius Reciprocity Theorem and Factored  $P$ -Operators / 264
    - D. Spontaneous or Internal Symmetry Breaking / 269
    - E. External Symmetry Breaking / 271
  - 4.4 Vibrations of Octahedral Hexafluoride Molecules / 286
    - A. Projection Analysis / 286
    - B. Solving Equations of Motion / 292
    - C. Classical Canonical Coordinates / 301
    - D. Elementary Quantum Theory of Vibrations / 302
- Additional Reading / 308  
Problems / 308



## CHAPTER 4

---

# THEORY AND APPLICATIONS OF HIGHER FINITE SYMMETRY AND INDUCED REPRESENTATIONS

---

All but five of the 32 crystal point symmetries (Recall Figure 3.1.1) have been analyzed in terms of cyclic groups  $C_2$ ,  $C_3$ , and  $C_4$  and dihedral groups  $D_2$ ,  $D_3$ , and  $D_4$ . The remaining five symmetries  $T$ ,  $T_h$ ,  $T_d$ ,  $O$ , and  $O_h$  are called tetrahedral, cubic, or octahedral symmetries. To analyze these one needs only to concentrate on two of them: the octahedral group  $O$  and its tetrahedral subgroup  $T$ . It will be shown that the group  $T_h$  is simply  $T_h = T \times C_i$ ,  $O_h$  is simply  $O \times C_i$ , and  $T_d$  is isomorphic to  $O$ .

The derivation and application of octahedral irreps can be done using the  $P$ -operator techniques discussed in the preceding chapters. However, there are some additional and important relations which help simplify the analysis of high symmetry. In this chapter the relations between subgroups  $C_n$  and  $D_n$  of octahedral symmetry will be exploited in the reduction of octahedral representations. The theory of induced representations will be introduced. This theory has become very important in understanding high-resolution laser spectra of symmetric molecules, among other things. Examples which will be treated in this section include the elements of spectral cluster theory and the classical vibrational spectra of  $SF_6$  and  $UF_6$  molecules. An introduction to the quantum theory of molecular vibrations is given also.

### 4.1 OCTAHEDRAL SYMMETRIES AND THEIR CHARACTERS

Let us begin with a synopsis of the point symmetries that may be found in a cubic crystal. They are also fairly common symmetries for polyatomic molecules.

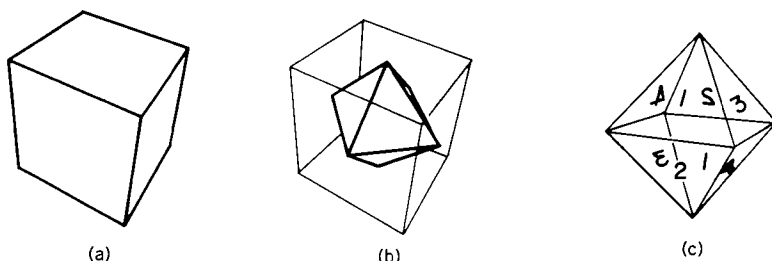


**Figure 4.1.1** Objects having octahedral ( $O$ ) symmetry. (a) The cube or hexahedron. (b) The octahedron. The cube is transformed into the octahedron by placing vertices of one in the center of the faces of the other. (c) ( $4! = 24$ ) permutations of four integers correspond to the 24 equivalent positions in which the octahedron may be placed.

### A. The Octahedral Group ( $O$ )

The rotational symmetry of a regular cube or hexahedron in Figure 4.1.1(a) or of a regular octahedron in Figures 4.1.1(b) and 4.1.1(c) is called  $O$  or octahedral symmetry. The symmetry of the octahedron can be stated by naming all its equivalent orientational positions, or by naming all the rotational operations which can change one position into another. For simple counting purposes the former is probably easier. The octahedron has eight equivalent faces to show. Since each one can be rotated to three equivalent positions there must be  $8 \cdot 3 = 24$  different rotational positions in all. (Equivalently, there are six cube faces or octahedron corners with four rotations for each, or 12 edges times two rotations each, all products which give the number 24.) It is interesting to note that each rotation corresponds to one of the  $24 = 4!$  permutations of the digits (1, 2, 3, 4) as depicted in Figure 4.1.1(c).

The labeling of the 24 symmetry operators is a little more difficult, but easy enough if done one class at a time. Figure 4.1.2 labels the operators from the class of (a) the identity 1, (b) the  $120^\circ$  rotations,  $r_j$  and  $r_j^2$ , (c) the  $180^\circ$  rotations  $R_j^2$  around  $\chi_1, \chi_2, \chi_3$  axes, (d) the  $90^\circ$  rotations,  $R_j$  and  $R_j^3$ , and (e) the  $180^\circ$  rotations  $i_j$  around edges. Each symbol next to an axis labels a counterclockwise rotation of the octahedron by a specific angle associated with its class. Axes are all meant to be fixed in the space of the laboratory rather than the body of the octahedron.

The  $O$ -group multiplication may be found easily using the Hamilton arc vectors described in Section 3.1.B. The octahedral arcs are shown for different classes in Figure 4.1.3(a). A stereogram of the superimposed arc paths is given below that in Figure 4.1.3(b). A projected view of hemisphere looking down the  $x_3$  or  $z$  axis is shown in Figure 4.1.4. Each of the 24 rotations is labeled on one or more arc vectors. For now you should ignore

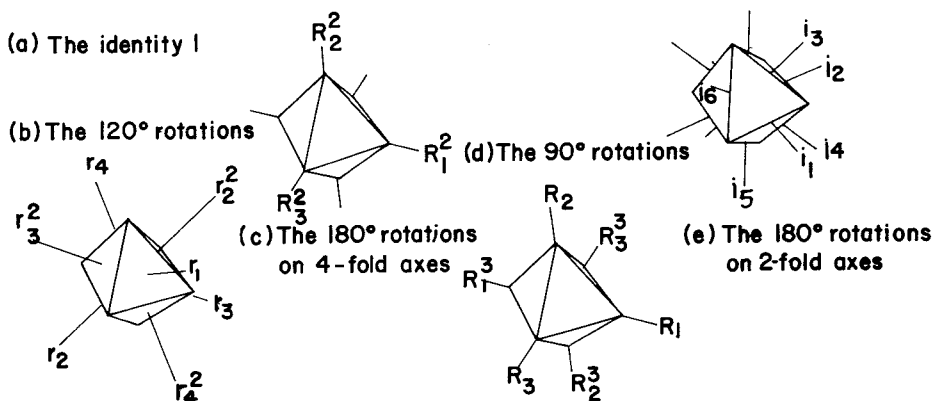


**Figure 4.1.2** The five classes of octahedral operations. (a) The identity class (no rotation). (b) The threefold rotations ( $120^\circ$ ). (c) The tetragonal twofold rotations ( $180^\circ$ ). (d) The fourfold rotations ( $90^\circ$ ). (e) The diagonal twofold rotations ( $180^\circ$ ).

the minus signs next to some labels. These will be used in Chapter 5 to treat spin- $\frac{1}{2}$  rotations.

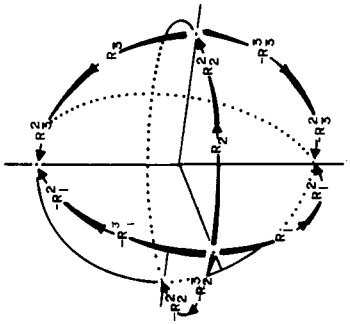
All  $(24)^2 = 576$  octahedral products  $R_b R_a = R_{ba}$  can be read from the diagram in Figure 4.1.4. The head-to-tail addition of the  $a$  vector to the  $b$  vector yield the  $ba$  vector, as indicated by the triangle above the diagram. Some products are already set up, as are, for example,  $r_3 R_2 = R_1$  or  $R_1^2 i_4 = R_3$ . Other products require adjustment of one or two vectors so the head of the  $a$  vector meets the tail of the  $b$  vector. The resulting octahedral multiplication table is given in the table section.

Relatively few multiplications are needed to construct the algebra of the octahedral classes:

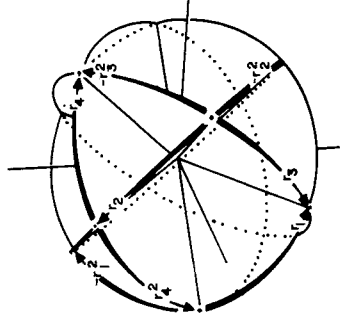
$$\begin{aligned}
 c_1 &= 1, \\
 c_r &= r_1 + r_2 + r_3 + r_4 + r_1^2 + r_2^2 + r_3^2 + r_4^2, \\
 c_{R^2} &= R_1^2 + R_2^2 + R_3^2, \\
 c_R &= R_1 + R_2 + R_3 + R_1^3 + R_2^3 + R_3^3, \\
 c_i &= i_1 + i_2 + i_3 + i_4 + i_5 + i_6.
 \end{aligned} \tag{4.1.1}$$

For example, only three multiplications are needed to determine the class membership of the 18 elements in the product

$$\begin{aligned}
 c_{R^2 c_i} &= R_1^2 i_1 + \cdots = R_2 + \cdots \\
 &+ R_2^2 i_1 + \cdots \quad i_2 + \cdots \\
 &+ R_3^2 i_1 + \cdots \quad R_3^3 + \cdots.
 \end{aligned} \tag{4.1.2}$$



THE 180° CLASS  
 $i$   $2$   $3$   $4$   $6$

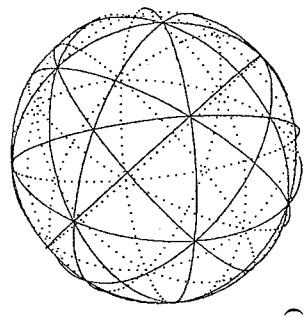
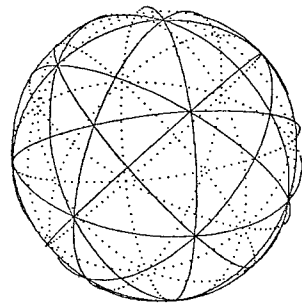


THE 120° CLASS  
 $r_1$   $r_2$   $r_3$   $r_4$   
 $r_1^2$   $r_2^2$   $r_3^2$   $r_4^2$

THE 90° CLASS  
 $R_1$   $R_2$   $R_3$   
 $R_1^2$   $R_2^2$   $R_3^2$

THE 180° CLASS

(a)



(b)

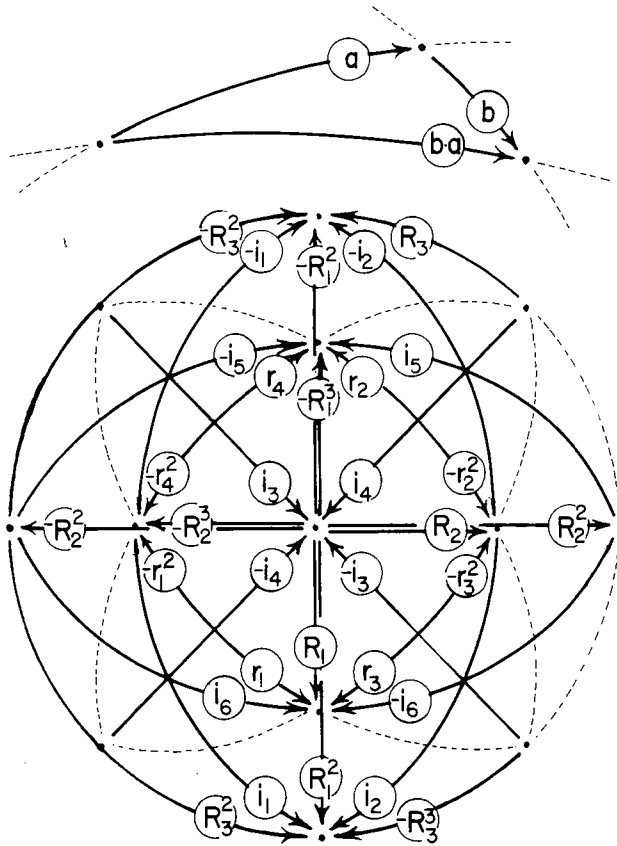


Figure 4.1.4 Octahedral group nomogram.

Since there are two members from  $c_R$  for each one from  $c_i$  in the first column of Eq. (4.1.2) one must conclude that the 18 products consist of 12  $R_j$ 's and 6  $i_j$ 's, or

$$c_{R^2}c_i = 2c_R + c_i = c_i c_{R^2}. \tag{4.1.3}$$

This simplification of any class product,

$$\begin{aligned} c_g c_h &= g_1 h_1 + g_2 h_1 + \dots = g_1 h_1 + t g_1 h_1 t^{-1} + \dots \\ &+ g_1 h_2 + g_2 h_2 + \dots \quad g_1 h_2 + t g_1 h_2 t^{-1} + \dots \\ &+ g_1 h_3 + g_2 h_3 + \dots \quad g_1 h_3 + t g_1 h_3 t^{-1} + \dots \\ &+ \dots \quad \dots \quad \dots \quad \dots, \end{aligned} \tag{4.1.4}$$

is always possible since the second column (or row) of the product is just a

transformation,

$$\begin{aligned}
 t g_1 h_j t^{-1} &= t g_1 t^{-1} t h_j t^{-1} \\
 &= g_2 \quad h'_j,
 \end{aligned}
 \tag{4.1.5}$$

of the first one. According to the definition of classes (see Section 3.2.A) the transformation converting  $g_1$  to  $g_2$  only rearranges the  $h_j$ 's in class  $c_h = t c_h t^{-1}$ . Hence the proportion of a given class found in each column (or row) of Eq. (4.1.4) must be equal.

The complete set of octahedral class products  $c_g c_h = c_h c_g$  are given by the following class algebra table:

<b>1</b>	$c_r$	$c_{R^2}$	$c_R$	$c_i$
$c_r$	$8\mathbf{1} + 4c_r + 8c_{R^2}$	$3c_r$	$4c_R + 4c_i$	$4c_R + 4c_i$
$c_R$		$3\mathbf{1} + 2c_{R^2}$	$c_R + 2c_i$	$2c_R + c_i$
$c_{R^2}$			$6\mathbf{1} + 3c_r + 2c_{R^2}$	$3c_r + 4c_{R^2}$
$c_i$				$6\mathbf{1} + 3c_r + 2c_{R^2}$

(4.1.6)

This class algebra can have no more than five linearly independent powers of any element. So it must be possible to construct a minimal equation for  $c_i$  by combining the six powers  $\{c_i^0, c_i, c_i^2, c_i^3, c_i^4, c_i^5\}$ :

$$\begin{aligned}
 c_i^0 &= \mathbf{1}, & c_i^3 &= 16c_R + 20c_i, \\
 c_i^1 &= c_i, & c_i^4 &= 48c_r + 64c_{R^2} + 20c_i^2, \\
 c_i^2 &= 6\mathbf{1} + 3c_r + 2c_{R^2}, & c_i^4 &= 120\mathbf{1} + 108c_r + 104c_{R^2}, \\
 c_i^5 &= 320c_R + 20c_i^4 + 256c_i \\
 &= 2400\mathbf{1} + 2160c_r + 2080c_{R^2} + 320c_R + 256c_i.
 \end{aligned}
 \tag{4.1.7}$$

Combining the expressions for  $c_i^3$  and  $c_i^5$  gives a minimal equation

$$\begin{aligned}
 c_i^5 - 40c_i^3 + 144c_i &= 0, \\
 (c_i^2 - 36)(c_i^2 - 4)c_i &= 0, \\
 (c_i + 6)(c_i - 6)(c_i + 2)(c_i - 2)c_i &= 0.
 \end{aligned}
 \tag{4.1.8}$$

[Note: For typographical convenience we write  $(c_i + r\mathbf{1})$  as  $(c_i + r)$ .] The roots  $\{2, -2, 0, 6, -6\}$  correspond to cubic irreps which are labeled  $(\alpha) =$

$\{T_2, T_1, E, A_1, A_2\}$ , respectively. The Equations (1.2.12) or (1.2.15) from Chapter 1 for idempotents then gives the following for the root  $c^{T_2} = 2$ :

$$\begin{aligned} \mathbb{P}^{T_2} &= \frac{(c_i + 2)(c_i - 0)(c_i - 6)(c_i + 6)}{(2 + 2)(2 - 0)(2 - 6)(2 + 6)} = [(c_i + 2)c_i(c_i^2 - 36)]/(-256) \\ &= [c_i^4 + 2c_i^3 - 36c_i^2 - 72c_i]/(-256) \\ &= [3\mathbf{1} - c_{R^2} - c_R + c_i]/8. \end{aligned} \tag{4.1.9}$$

The complete set of all-commuting idempotents is given now:

$$\begin{aligned} \mathbb{P}^{A_1} &= [\mathbf{1} + c_r + c_{R^2} + c_R + c_i]/24, \\ \mathbb{P}^{A_2} &= [\mathbf{1} + c_r + c_{R^2} - c_R - c_i]/24, \\ \mathbb{P}^E &= [2\mathbf{1} - c_r + 2c_{R^2}]/12, \\ \mathbb{P}^{T_1} &= [3\mathbf{1} - c_{R^2} + c_R - c_i]/8, \\ \mathbb{P}^{T_2} &= [3\mathbf{1} - c_{R^2} - c_R + c_i]/8. \end{aligned} \tag{4.1.10}$$

The coefficients in the brackets are the octahedral irrep characters  $\chi_j^\alpha$  according to the theory of Section (3.5.A). The character table is as follows:

	$g = \mathbf{1}$	$r, r^2$	$R^2$	$R, R^3$	$i$	
$\Gamma_1 = \chi_g^{A_1} =$	1	1	1	1	1	(4.1.11)
$\Gamma_2 = \chi_g^{A_2} =$	1	1	1	-1	-1	
$\Gamma_3 = \chi_g^E =$	2	-1	2	0	0	
$\Gamma_4 = \chi_g^{F_1} = \chi_g^{T_1} =$	3	0	-1	1	-1	
$\Gamma_5 = \chi_g^{F_2} = \chi_g^{T_2} =$	3	0	-1	-1	1	

This book will use the notation  $A, E,$  and  $T$  for the single ( $\chi_1^A \equiv l^A = 1$ ), double ( $\chi_1^E \equiv l^E = 2$ ), and triple ( $\chi_1^T \equiv l^T = 3$ ) dimensions of the respective irreps. The subscripts 1 and 2 indicate the even and odd character of  $90^\circ$  rotations  $R$  or  $R^3$ :

$$\begin{aligned} \chi_R^{A_1} &= 1 = \chi_R^{T_1}, \\ \chi_R^{A_2} &= -1 = \chi_R^{T_2}. \end{aligned} \tag{4.1.12}$$

Some alternative notation which occurs in the reference literature is indicated in Eq. (4.1.11).



### B. Full Octahedral Group ( $O_h$ )

The full octahedral group contains all the operations of  $O = \{1, r_1, r_2, \dots, R_1, R_2, \dots, i_1, i_2, \dots\}$  twice; once with inversion and once without. Since the inversion operator ( $I$ ) commutes with all rotation operators, one may write  $O_h$  as an outer product:

$$O_h = O \times C_i = O \times \{1, I\}. \tag{4.1.13}$$

The 48 elements of  $O_h$  are listed in Figure 4.1.5.  $O_h$  includes subgroups  $T$ ,  $T_h$ , and  $T_d$  as well as  $O$ . One way to account for the 48 operations is to consider all transformations of the orthogonal Cartesian unit vectors  $\{|x\rangle \equiv$

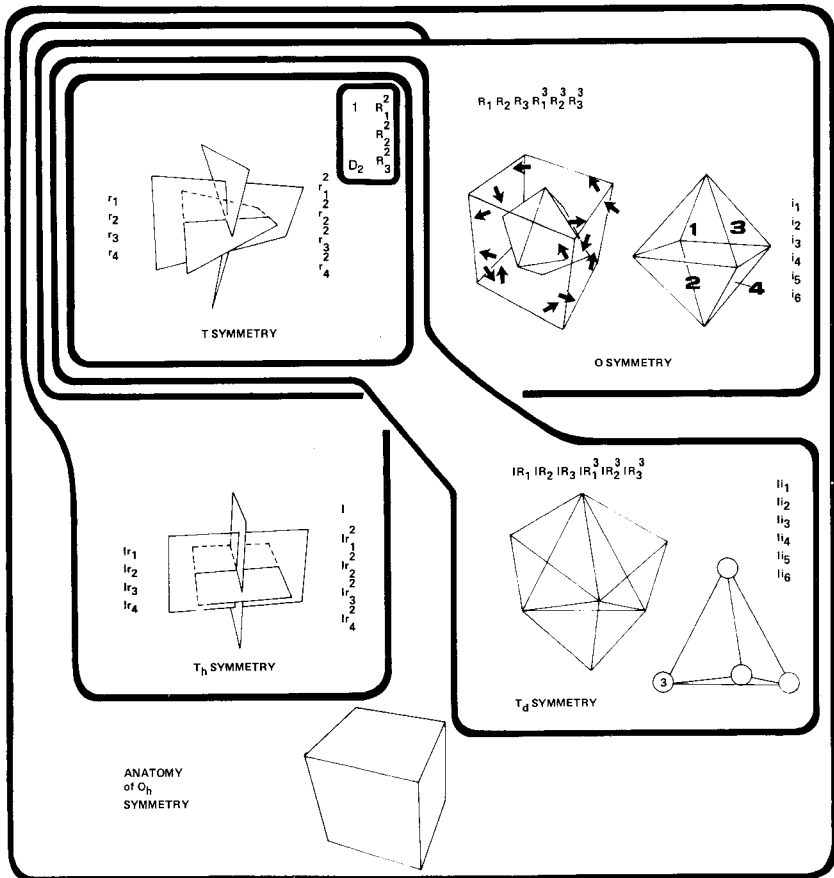


**Figure 4.1.5** The full octahedral group ( $O_h$ ) and four non-Abelian subgroups  $T$ ,  $T_h$ ,  $T_d$ , and  $O$ . The Abelian  $D_2$  subgroup of  $T$  is indicated also.

$|x_1\rangle, |y\rangle \equiv |x_2\rangle, |z\rangle \equiv |x_3\rangle$  which leave them pointing along Cartesian axes. This includes all  $3! = 6$  permutations. For example, the  $120^\circ$  rotation  $r_1$  gives

$$\{r_1|x_1\rangle = |x_2\rangle, r_1|x_2\rangle = |x_3\rangle, r_1|x_3\rangle = |x_1\rangle\}. \quad (4.1.14)$$

$O_h$  also includes  $2^3 = 8$  possible sign changes. For example, inversion  $I$  gives

$$\{I|x_1\rangle = -|x_1\rangle, I|x_2\rangle = -|x_2\rangle, I|x_3\rangle = -|x_3\rangle\}. \quad (4.1.15)$$

Altogether,  $O_h$  contains  $3! 2^3 = 48$  such operations. The geometrical significance of the operations will be discussed in the explanation of the tetrahedral subgroups and then again in Sections 4.2.A(a) and 4.2.A(b).

The full octahedral or  $O_h$  characters follow easily from those of  $O$  just as  $D_{4h}$  characters follow from those of  $D_4$ . The cross-product relation (4.1.13) is the key:

	$g = 1$	$r_1 \cdots$	$R_1^2 \cdots$	$R_1 \cdots$	$i_1 \cdots$	$I$	$Ir_1 \cdots$	$IR_1^2 \cdots$	$IR_1 \cdots$	$Ii_1 \cdots$
$(\alpha) = A_{1g}$	1	1	1	1	1	1	1	1	1	1
$A_{2g}$	1	1	1	-1	-1	1	1	1	-1	-1
$E_g$	2	-1	2	0	0	2	-1	2	0	0
$T_{1g}$	3	0	-1	1	-1	3	0	-1	1	-1
$T_{2g}$	3	0	-1	-1	1	3	0	-1	-1	1
$A_{1u}$	1	1	1	1	1	-1	-1	-1	-1	-1
$A_{2u}$	1	1	1	-1	-1	-1	-1	-1	1	1
$E_u$	2	-1	2	0	0	-2	1	-2	0	0
$T_{1u}$	3	0	-1	1	-1	-3	0	1	-1	1
$T_{2u}$	3	0	-1	-1	1	-3	0	1	1	-1

$$(4.1.16)$$

The  $g$  and  $u$  subindices stand for even (positive) and odd (negative) inversion parity, respectively. The following gives the form of the simple relation between  $O_h$  and  $O$  characters.

$$\begin{aligned} \chi_{R^{2g}}^{T_2} &= \chi_{R^2}^{T_2}, & \chi_{IR^{2g}}^{T_2} &= \chi_{R^2}^{T_2}, \\ \chi_{R^{2u}}^{T_2} &= \chi_{R^2}^{T_2}, & \xi_{IR^{2u}}^{T_2} &= -\chi_{R^2}^{T_2}. \end{aligned} \quad (4.1.17)$$

The same relation will hold between  $O_h$  and  $O$  irreps:

$$\begin{aligned} \mathcal{D}^{\alpha_g}(R) &= \mathcal{D}^\alpha(R), & \mathcal{D}^{\alpha_g}(IR) &= \mathcal{D}^\alpha(R), \\ \mathcal{D}^{\alpha_u}(R) &= \mathcal{D}^\alpha(R), & \mathcal{D}^{\alpha_u}(IR) &= -\mathcal{D}^\alpha(R). \end{aligned} \quad (4.1.18)$$

### C. Full Tetrahedral Symmetry $T_d$

The full symmetry of a regular tetrahedron is called  $T_d$ . It contains 24 operators  $\{1, r_j, \dots, r_j^2, \dots, R_j^2, \dots, IR_j, \dots, Ii_j, \dots\}$  listed in the  $T_d$  section of Figure 4.1.5. Note that the tetrahedron edges are face diagonals of a cube. The tetrahedron is invariant to reflections  $Ii_j$  through diagonal planes, but not the horizontal reflections  $IR_j^2$ . The tetrahedron is also invariant to  $90^\circ$  rotation inversions  $IR_j$  or  $IR_j^3$  around the Cartesian axes. Hence,  $T_d$  contains  $D_{2d}$  subgroups. Also  $T_d$  contains the  $120^\circ$  rotations  $r_i$  or  $r_i^2$  around (111) axes and  $180^\circ$  rotations  $R_i^2$  around the Cartesian axes.

The groups  $O$  and  $T_d$  are isomorphic. For each group product  $R_1R_2 = r_1$  or  $r_1i_1 = R_1^3$  in  $O$ , there is a corresponding product  $IR_1IR_2 = r_1$  or  $r_1Ii_1 = IR_1^3$  in  $T_d$ , respectively, since inversion  $I$  is all-commuting. Hence, the character table (4.1.11) serves as well for  $T_d$  if we relabel elements  $R_j$  and  $i_j$  as  $IR_j$  and  $Ii_j$ . Furthermore, by numbering the tetrahedron vertices as shown in Figure 4.1.5, the correspondence between  $T_d$  operations and the  $4!$  permutations of four integers is established.

### D. Partial Tetrahedral Symmetries $T$ and $T_h$

The purely rotational subgroup of  $T_d$  is called  $T$ , and it is the symmetry of the three twisted planes drawn in Figure 4.1.5. If the planes are flat and orthogonal the symmetry doubles to  $T_h$  shown in the same figure.  $T_h$  contains horizontal plane reflections  $IR_j^2$  as well as  $120^\circ$  rotation inversions  $Ir_j$  and  $Ir_j^2$ .  $T_h$  is an outer product of  $T$  and  $C_i$ :

$$T_h = T \times C_i = T \times \{1, I\}. \quad (4.1.19)$$

$T$  and  $T_h$  are the only non-Abelian crystal point groups that have any classes of elements separated from their inverses. The counterclockwise  $120^\circ$  rotations  $r_1r_2r_3r_4$  are now in a separate class from their inverses  $r_1^2r_2^2r_3^2r_4^2$ . No operation  $t$  in  $T$  or  $T_h$  exists such that  $t^{-1}r_it = r_i^2$ . This is one case where some "look-alike" elements do not belong to the same class.

Group  $T$  has four classes  $c_1, c_r, c_{r^2}$ , and  $c_{R^2}$ ; hence, it has four types of irreducible representations. The derivation of the all-commuting idempotents and the irrep character table (4.1.20) is left as an exercise.

$$\begin{array}{l} \chi_g^A = \\ \chi_g^E = \\ \chi_g^E = \\ \chi_g^T = \end{array} \begin{array}{cccc} g = 1 & r_1 \cdots & r_1^2 \cdots & R_1^2 \cdots \\ \begin{array}{|cccc} 1 & 1 & 1 & 1 \\ 1 & e^{2\pi i/3} & e^{-2\pi i/3} & 1 \\ 1 & e^{-2\pi i/3} & e^{2\pi i/3} & 1 \\ 3 & 0 & 0 & -1 \end{array} \end{array} \quad (4.1.20)$$

The  $T_h$  characters follow easily using Eq. (4.1.19).

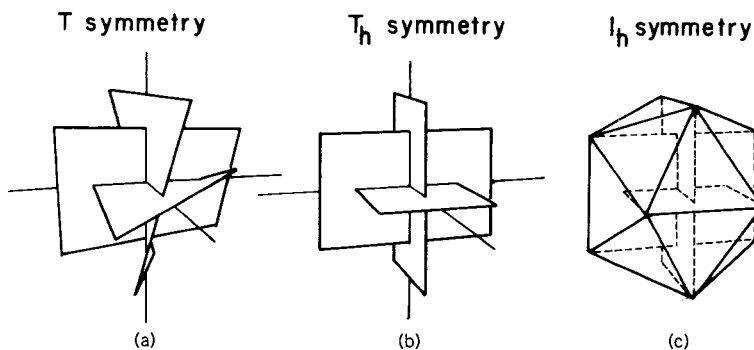


Figure 4.1.6 Examples of icosahedral ( $I_h$ ) symmetry and tetrahedral ( $T_h$ ) symmetry.

It should be evident from Figure 4.1.5 that  $T_h$  is not the symmetry of a tetrahedron. Instead, it is a subgroup of the highest point symmetry in three space. If the rectangles in the  $T_h$  portion of Figure 4.1.5 have a length:width "golden" ratio of

$$r = (1 + \sqrt{5})/2 = 1.618\dots,$$

then their vertices describe an ICOSAHEDRON. This 20-sided regular solid is shown in Figure 4.1.6. Icosahedral symmetry is not a crystal point group since it has fivefold symmetry axes. The importance of this symmetry in physics has been realized only recently with the discovery of the structure of viruses, quasi-crystals, and the molecule  $C_{60}$  which has the geodesic dome structure made famous by the architect Buckminster Fuller.  $C_{60}$  is called "buckminsterfullerene" in honor of Fuller's artistry.

## 4.2 IRREDUCIBLE REPRESENTATIONS OF OCTAHEDRAL SYMMETRY

The construction and labeling of octahedral symmetry representations will be treated now. By considering carefully the subgroups of  $O$  and  $O_h$  it is possible to simplify some of the octahedral group algebra.

### A. Subgroup Chains and Idempotent Splitting

The dimensions ( $l^\alpha$ ) of the  $O$  irreps  $\mathcal{D}^\alpha$  are determined by the characters

$$l^\alpha = \chi_1^\alpha = \text{Trace } \mathcal{D}^\alpha(1)$$

in Eqs. (4.1.10) and (4.10.11). Each all-commuting idempotent  $\mathbb{P}^\alpha$  can be split into  $l^\alpha$  irreducible idempotents  $P_j^\alpha \equiv P_{jj}^\alpha$ ,

$$\mathbb{P}^\alpha = P_1^\alpha + P_2^\alpha + \cdots + P_{l^\alpha}^\alpha, \quad (4.2.1)$$

according to the theory of Section 3.3. In the group  $O$  we expect the following splittings:

$$\mathbb{P}^E = P_1^E + P_2^E, \quad (4.2.1a)_x$$

$$\mathbb{P}^{T_1} = P_1^{T_1} + P_2^{T_1} + P_3^{T_1}, \quad (4.2.1b)_x$$

$$\mathbb{P}^{T_2} = P_1^{T_2} + P_2^{T_2} + P_3^{T_2}, \quad (4.2.1c)_x$$

while  $P^{A_1}$  and  $P^{A_2}$  remain unsplit since  $l^{A_1} = 1 = l^{A_2}$ .

One way to do this splitting is to use subgroup idempotents. Recall that we used the  $C_2$  subgroup idempotents to split the  $C_{3v}$  (or  $D_3$ ) all-commuting idempotent  $P^E$  [recall Eq. (3.3.3)]:

$$\begin{aligned} \mathbb{P}^E = \mathbb{P}^E \mathbf{1} &= \mathbb{P}^E(P^+ + P^-) \\ &= P_1^E + P_2^E. \end{aligned} \quad (4.2.2)$$

However, later on a different splitting was effected by  $C_3$  subgroup idempotents [recall Eq. (3.3.15)]:

$$\begin{aligned} \mathbb{P}^E = \mathbb{P}^E \mathbf{1} &= \mathbb{P}^E(P_{0_3} + P_{1_3} + P_{2_3}) \\ &= P_{1_3}^E + P_{2_3}^E. \end{aligned} \quad (4.2.3)$$

This choice led to circular or moving-wave eigenstates.

Octahedral symmetry has more subgroups and correspondingly more different types of idempotent splittings and wave solutions. Besides  $D_3$ , one may notice that  $D_4$  and  $T$  are subgroups of  $O$  according to Figure 3.1.1. If one chooses to split  $O$  with  $D_4$  idempotents then two subchoices remain. One is free to use  $D_4 \supset C_4$  defined idempotents [recall Eq. (3.6.4)],

$$\mathbb{P}^E = \mathbb{P}^E \mathbf{1} = P_{1_4}^E + P_{3_4}^E, \quad (4.2.4)$$

or else  $D_4 \supset D_2 \supset C_2$  defined idempotents [recall Eqs. (3.6.6)–(3.6.8)],

$$\mathbb{P}^E = \mathbb{P}^E \mathbf{1} = P_{B_1}^E + P_{B_2}^E. \quad (4.2.5)$$

Each choice for a chain of subgroups such as  $O \supset D_4 \supset D_2$ ,  $O \supset D_4 \supset C_4$ ,  $O \supset D_3 \supset C_2$ , or  $O \supset D_3 \supset C_3$  corresponds to different idempotent splittings and different (but equivalent) irreps. Let us consider each choice in turn.

**(a) Tetragonal Standing-Wave Irreps ( $O_h \supset D_{4h} \supset D_{2h}$ )** Suppose we require  $O$  irreps which are diagonal with respect to subgroup  $D_2 = \{1, R_1^2, R_2^2, R_3^2\}$ , and reduced with respect to tetragonal subgroup  $D_4 = \{1, R_3, R_3^2, R_1^2, R_2^2, i_3, i_4\}$ . These irreps are most commonly used in solid-state applications. The formal derivation of them involves splitting by the combination of idempotent relations for  $D_4$ :

$$\mathbf{1} = P^E + P^{A_1} + P^{A_2} + P^{B_1} + P^{B_2} \quad (4.2.6)$$

and  $D_2$ :

$$\mathbf{1} = p^{A_1} + p^{A_2} + p^{B_1} + p^{B_2}. \quad (4.2.7)$$

Here it will be necessary to label  $D_2$  idempotents with lower-case  $p$ ; for example, let

$$p^{B_2} = (\mathbf{1} - R_3^2 + R_2^2 - R_1^2)/4,$$

where  $D_2$  characters in Eq. (3.6.33) are used. This will distinguish them from  $D_4$  idempotents with the same superscript, such as

$$P^{B_2} = (\mathbf{1} + R_3^2 - R_3 - R_3^3 - R_1^2 - R_2^2 + i_3 + i_4)/8.$$

[ $P^{B_2}$  follows from  $D_4$  characters in Eq. (3.6.3).]

The splitting combination is

$$\begin{aligned} \mathbf{1} &= (P^E + P^{A_1} + P^{A_2} + P^{B_1} + P^{B_2})(p^{A_1} + p^{A_2} + p^{B_1} + p^{B_2}) \\ &= (P^E p^{B_1} + P^E p^{B_2} + P^{A_1} p^{A_1} + P^{A_2} p^{A_2} + P^{B_1} p^{A_1} + P^{B_2} p^{A_2}) \\ &= P_1^E + P_2^E + P^{A_1} + P^{A_2} + P^{B_1} + P^{B_2}. \end{aligned} \quad (4.2.8)$$

This involves six irreducible  $D_4$  idempotents. [Recall Eqs. (3.6.2) and (3.6.3).] Operating with this on the octahedral all-commuting idempotent  $\mathbb{P}^{T_1}$  gives the desired three-term splitting,

$$\begin{aligned} \mathbb{P}^{T_1} &= \mathbb{P}^{T_1} \mathbf{1} = \mathbb{P}^{T_1} (P_1^E + P_2^E + P^{A_1} + P^{A_2} + P^{B_1} + P^{B_2}) \\ &= P_1^{T_1} + P_2^{T_1} + 0 + P_3^{T_1} + 0 + 0, \end{aligned} \quad (4.2.9)$$

where some group multiplication algebra yields the irreducible idempotents:

$$P_1^{T_1} \equiv \mathbb{P}^{T_1} P_1^E = \mathbb{P}^{T_1} P^E p^{B_1} = (\mathbf{1} + R_1^2 - R_2^2 - R_3^2 + R_1 + R_1^3 - i_5 - i_6)/8, \tag{4.2.10a}$$

$$P_2^{T_1} \equiv \mathbb{P}^{T_1} P_2^E = \mathbb{P}^{T_1} P^E p^{B_2} = (\mathbf{1} - R_1^2 + R_2^2 - R_3^2 + R_2 + R_2^3 - i_1 - i_2)/8, \tag{4.2.10b}$$

$$P_3^{T_1} \equiv \mathbb{P}^{T_1} P^{A_2} = \mathbb{P}^{T_1} P^{A_2} p^{A_2} = (\mathbf{1} - R_1^2 - R_2^2 + R_3^2 + R_3 + R_3^3 - i_3 - i_4)/8. \tag{4.2.10c}$$

This formal idempotent production introduces the idea of SUBGROUP CHAIN LABELING of irrep idempotents and bases. Instead of blindly numbering them “one,” “two,” and “three,” one uses the previously established irrep labels of the subgroup chain  $D_4 \supset D_2$  to label the three  $T_1$  components. Let us label the  $T_1$  idempotents (4.2.10) as follows:

$$P_1^{T_1} \equiv P_{B_1}^{E \begin{matrix} [T_1] \\ \end{matrix}}, \quad P_2^{T_1} \equiv P_{B_2}^{E \begin{matrix} [T_1] \\ \end{matrix}}, \quad P_3^{T_1} \equiv P_{A_2}^{A_2 \begin{matrix} [T_1] \\ \end{matrix}}, \tag{4.2.11}$$

where each link in the descending chain of labels stands for a corresponding subgroup irrep in the  $O \supset D_4 \supset D_2$  chain.

$$P_m^{[\mu]} \equiv P_n^\nu \begin{matrix} [\mu] & [\mu] \text{ labels} & O \text{ irrep} \\ & \nu \text{ labels} & D_4 \text{ irrep} \\ & n \text{ labels} & D_2 \text{ irrep} \end{matrix} \tag{4.2.12}$$

This chain labeling tells exactly how the  $\mathscr{D}^{T_1}$  irrep is reduced or diagonalized when restricted or subduced ( $\downarrow$ ) to subgroups  $D_4$  or  $D_2$ .

$$\mathscr{D}^{T_1} \downarrow D_4 = \begin{pmatrix} \begin{pmatrix} \mathscr{D}^E \\ \end{pmatrix} & 0 \\ 0 & 0 & (D^{A_2}) \end{pmatrix}, \tag{4.2.13a}$$

$$\mathscr{D}^{T_1} \downarrow D_2 = \begin{pmatrix} (D^{B_1}) & 0 & 0 \\ 0 & (D^{B_2}) & 0 \\ 0 & 0 & (D^{A_2}) \end{pmatrix}. \tag{4.2.13b}$$

The irrep matrices  $\mathscr{D}_{(g)}^{T_1}$  may be derived formally from the irreducible idempotents  $P_j^{T_1}$  by constructing the guarded elements  $P_i^{T_1}gP_j^{T_1}$ , normalizing them, and using the elementary operator relation  $P_i^{T_1}gP_j^{T_1} = \mathscr{D}_{ij}^{T_1}(g)P_j^{T_1}$ . This was done for  $C_{3v}$  in Sections 3.4.A and 3.4.B. Also, this particular  $T_1$ -type representation can also be derived from simple Cartesian vector properties, as we will see shortly. The  $\mathscr{D}^{T_1}$  are listed below for all 24  $O$  operations.

$$\begin{array}{cccccc}
 \mathscr{D}^{T_1}(1) = & R_1^2 = & r_1 = & r_2 = & r_1^2 = & r_2^2 = \\
 \begin{vmatrix} 1 & \cdot & \cdot \\ \cdot & 1 & \cdot \\ \cdot & \cdot & 1 \end{vmatrix} & \begin{vmatrix} 1 & \cdot & \cdot \\ \cdot & -1 & \cdot \\ \cdot & \cdot & -1 \end{vmatrix} & \begin{vmatrix} \cdot & \cdot & 1 \\ 1 & \cdot & \cdot \\ \cdot & 1 & \cdot \end{vmatrix} & \begin{vmatrix} \cdot & \cdot & -1 \\ 1 & \cdot & \cdot \\ \cdot & -1 & \cdot \end{vmatrix} & \begin{vmatrix} \cdot & 1 & \cdot \\ \cdot & \cdot & 1 \\ 1 & \cdot & \cdot \end{vmatrix} & \begin{vmatrix} \cdot & 1 & \cdot \\ \cdot & \cdot & -1 \\ -1 & \cdot & \cdot \end{vmatrix} \\
 \\
 \mathscr{D}^{T_1}(R_3^2) = & R_2^2 = & r_4 = & r_3 = & r_3^2 = & r_4^2 = \\
 \begin{vmatrix} -1 & \cdot & \cdot \\ \cdot & -1 & \cdot \\ \cdot & \cdot & 1 \end{vmatrix} & \begin{vmatrix} -1 & \cdot & \cdot \\ \cdot & 1 & \cdot \\ \cdot & \cdot & -1 \end{vmatrix} & \begin{vmatrix} \cdot & \cdot & 1 \\ -1 & \cdot & \cdot \\ \cdot & -1 & \cdot \end{vmatrix} & \begin{vmatrix} \cdot & \cdot & -1 \\ -1 & \cdot & \cdot \\ \cdot & 1 & \cdot \end{vmatrix} & \begin{vmatrix} \cdot & -1 & \cdot \\ \cdot & \cdot & 1 \\ -1 & \cdot & \cdot \end{vmatrix} & \begin{vmatrix} \cdot & -1 & \cdot \\ \cdot & \cdot & -1 \\ 1 & \cdot & \cdot \end{vmatrix} \\
 \\
 \mathscr{D}^{T_1}(R_3) = & i_4 = & i_1 = & i_2 = & R_1^3 = & R_1 = \\
 \begin{vmatrix} \cdot & -1 & \cdot \\ 1 & \cdot & \cdot \\ \cdot & \cdot & 1 \end{vmatrix} & \begin{vmatrix} \cdot & -1 & \cdot \\ -1 & \cdot & \cdot \\ \cdot & \cdot & -1 \end{vmatrix} & \begin{vmatrix} \cdot & \cdot & 1 \\ \cdot & -1 & \cdot \\ 1 & \cdot & \cdot \end{vmatrix} & \begin{vmatrix} \cdot & \cdot & -1 \\ \cdot & -1 & \cdot \\ -1 & \cdot & \cdot \end{vmatrix} & \begin{vmatrix} 1 & \cdot & \cdot \\ \cdot & \cdot & 1 \\ \cdot & -1 & \cdot \end{vmatrix} & \begin{vmatrix} 1 & \cdot & \cdot \\ \cdot & \cdot & -1 \\ \cdot & 1 & \cdot \end{vmatrix} \\
 \\
 \mathscr{D}^{T_1}(R_3^3) = & i_3 = & R_2 = & R_3^3 = & i_6 = & i_5 = \\
 \begin{vmatrix} \cdot & 1 & \cdot \\ -1 & \cdot & \cdot \\ \cdot & \cdot & 1 \end{vmatrix} & \begin{vmatrix} \cdot & 1 & \cdot \\ 1 & \cdot & \cdot \\ \cdot & \cdot & -1 \end{vmatrix} & \begin{vmatrix} \cdot & \cdot & 1 \\ \cdot & 1 & \cdot \\ -1 & \cdot & \cdot \end{vmatrix} & \begin{vmatrix} \cdot & \cdot & -1 \\ \cdot & 1 & \cdot \\ 1 & \cdot & \cdot \end{vmatrix} & \begin{vmatrix} -1 & \cdot & \cdot \\ \cdot & \cdot & 1 \\ \cdot & 1 & \cdot \end{vmatrix} & \begin{vmatrix} -1 & \cdot & \cdot \\ \cdot & \cdot & -1 \\ \cdot & -1 & \cdot \end{vmatrix}
 \end{array} \tag{4.2.14}$$

The eight matrices in the first two columns belong to the subduced representation  $\mathscr{D}^{T_1} \downarrow D_4$ . Notice that they have the block-diagonal reduced form of Eq. (4.2.13a). The four matrices  $\mathscr{D}^{T_1} \downarrow D_2 = \{\dots \mathscr{D}(R_j^2)\}$  are in the diagonal form of Eq. (4.2.13b).

The octahedral irrep  $\mathscr{D}^{T_2}$  is very similar to  $\mathscr{D}^{T_1}$ . The character table (4.1.11) of  $O$  indicates that one can obtain  $\mathscr{D}^{T_2}$  from  $\mathscr{D}^{T_1}$  simply by a change of sign for the elements  $\{R_1, R_2, \dots, R_3^3, i_1, i_2, \dots, i_6\}$  in the "second half" of  $O$ , i.e., for the coset  $R_1T$  of subgroup  $T$ :

$$\mathscr{D}^{T_2}(R_j) = -\mathscr{D}^{T_1}(R_j), \quad \mathscr{D}^{T_2}(i_j) = -\mathscr{D}^{T_1}(i_j). \tag{4.2.15}$$

This definition of  $\mathscr{D}^{T_2}$  is quite convenient for many purposes. However, it changes the  $\mathscr{D}^E$  representation of the elements  $R_3, R_3^3, i_3$ , and  $i_4$  in subgroup  $D_4$ . Effectively, it introduces a phase change  $\{|^E_1\rangle, |^E_2\rangle\} \rightarrow \{|^E_1\rangle, -|^E_2\rangle\}$  in the  $E$  basis. When it is necessary to avoid this we shall use the



following “kosher”  $\mathscr{D}^{T_2}$  irrep:

$$\begin{aligned}
 \mathscr{D}^{T_2}(1) &= & R_1^2 &= & r_1 &= & r_2 &= & r_1^2 &= & r_2^2 &= \\
 \begin{vmatrix} 1 & \cdot & \cdot \\ \cdot & 1 & \cdot \\ \cdot & \cdot & 1 \end{vmatrix} & \begin{vmatrix} 1 & \cdot & \cdot \\ \cdot & -1 & \cdot \\ \cdot & \cdot & -1 \end{vmatrix} & \begin{vmatrix} \cdot & \cdot & 1 \\ -1 & \cdot & \cdot \\ \cdot & -1 & \cdot \end{vmatrix} & \begin{vmatrix} \cdot & \cdot & -1 \\ -1 & \cdot & \cdot \\ \cdot & 1 & \cdot \end{vmatrix} & \begin{vmatrix} \cdot & -1 & \cdot \\ \cdot & \cdot & -1 \\ 1 & \cdot & \cdot \end{vmatrix} & \begin{vmatrix} \cdot & -1 & \cdot \\ \cdot & \cdot & -1 \\ -1 & \cdot & \cdot \end{vmatrix} \\
 \mathscr{D}^{T_2}(R_3^2) &= & R_2^2 &= & r_4 &= & r_3 &= & r_3^2 &= & r_4^2 &= \\
 \begin{vmatrix} -1 & \cdot & \cdot \\ \cdot & -1 & \cdot \\ \cdot & \cdot & 1 \end{vmatrix} & \begin{vmatrix} -1 & \cdot & \cdot \\ \cdot & 1 & \cdot \\ \cdot & \cdot & -1 \end{vmatrix} & \begin{vmatrix} \cdot & \cdot & 1 \\ 1 & \cdot & \cdot \\ \cdot & 1 & \cdot \end{vmatrix} & \begin{vmatrix} \cdot & \cdot & -1 \\ 1 & \cdot & \cdot \\ \cdot & -1 & \cdot \end{vmatrix} & \begin{vmatrix} \cdot & 1 & \cdot \\ \cdot & \cdot & -1 \\ -1 & \cdot & \cdot \end{vmatrix} & \begin{vmatrix} \cdot & 1 & \cdot \\ \cdot & \cdot & -1 \\ 1 & \cdot & \cdot \end{vmatrix} \\
 \mathscr{D}^{T_2}(R_3) &= & i_4 &= & i_1 &= & i_2 &= & R_1^3 &= & R_1 &= \\
 \begin{vmatrix} \cdot & -1 & \cdot \\ 1 & \cdot & \cdot \\ \cdot & \cdot & -1 \end{vmatrix} & \begin{vmatrix} \cdot & -1 & \cdot \\ -1 & \cdot & \cdot \\ \cdot & \cdot & 1 \end{vmatrix} & \begin{vmatrix} \cdot & \cdot & -1 \\ \cdot & 1 & \cdot \\ -1 & \cdot & \cdot \end{vmatrix} & \begin{vmatrix} \cdot & \cdot & 1 \\ \cdot & 1 & \cdot \\ 1 & \cdot & \cdot \end{vmatrix} & \begin{vmatrix} -1 & \cdot & \cdot \\ \cdot & \cdot & 1 \\ \cdot & -1 & \cdot \end{vmatrix} & \begin{vmatrix} -1 & \cdot & \cdot \\ \cdot & \cdot & -1 \\ \cdot & 1 & \cdot \end{vmatrix} \\
 \mathscr{D}^{T_2}(R_3^3) &= & i_3 &= & R_2 &= & R_2^3 &= & i_6 &= & i_5 &= \\
 \begin{vmatrix} \cdot & 1 & \cdot \\ -1 & \cdot & \cdot \\ \cdot & \cdot & -1 \end{vmatrix} & \begin{vmatrix} \cdot & 1 & \cdot \\ 1 & \cdot & \cdot \\ \cdot & \cdot & 1 \end{vmatrix} & \begin{vmatrix} \cdot & \cdot & -1 \\ \cdot & -1 & \cdot \\ 1 & \cdot & \cdot \end{vmatrix} & \begin{vmatrix} \cdot & \cdot & 1 \\ \cdot & -1 & \cdot \\ -1 & \cdot & \cdot \end{vmatrix} & \begin{vmatrix} 1 & \cdot & \cdot \\ \cdot & \cdot & 1 \\ \cdot & 1 & \cdot \end{vmatrix} & \begin{vmatrix} 1 & \cdot & \cdot \\ \cdot & \cdot & -1 \\ \cdot & -1 & \cdot \end{vmatrix}
 \end{aligned}$$

(4.2.16)

The  $O \supset D_4 \supset D_2$  subgroup chain labeling of the  $T_2$  bases is given by the following:

$$P_1^{T_2} \equiv P_{B_1}^E, \quad P_2^{T_2} \equiv P_{B_2}^E, \quad P_3^{T_2} \equiv P_{A_2}^{B_2}. \quad (4.2.17)$$

The two-dimensional irrep  $\mathscr{D}^E$  of  $O$  can be produced formally by the same  $D_4$  splitting combination (4.2.8). The splitting of  $P^E$  goes as follows:

$$\begin{aligned}
 \mathbb{P}^E &= \mathbb{P}^E 1 = \mathbb{P}^E (P_1^E + P_2^E + P^{A_1} + P^{A_2} + P^{B_1} + P^{B_2}) \\
 &= 0 + 0 + P_1^E + 0 + P_2^E + 0, \quad (4.2.18a)
 \end{aligned}$$

where

$$P_1^E \equiv \mathbb{P}^E P^{A_1} = \mathbb{P}^E P^{A_1} P^{A_1} = 3(P^{A_1} \text{ (of } D_4) - \frac{1}{2}r_1 P^{A_1} - \frac{1}{2}r_1^2 P^{A_1})/4, \quad (4.2.18b)$$

$$P_2^E \equiv \mathbb{P}^E P^{B_1} = \mathbb{P}^E P^{B_1} P^{A_1} = 3(\overline{P^{B_1}} \text{ (of } D_4) - \frac{1}{2}r_1 P^{B_1} - \frac{1}{2}r_1^2 P^{B_1})/4. \quad (4.2.18c)$$

The following is a list of the  $\mathscr{D}^E$  irreps of  $O$  symmetry:

$$\begin{array}{l}
 \mathscr{D}^E(1) \quad R_1^2 = \begin{vmatrix} 1 & 0 \\ 0 & 1 \end{vmatrix} \quad r_1 = \begin{vmatrix} -1 & -\sqrt{3} \\ 2 & 2 \end{vmatrix} \quad r_2 = \begin{vmatrix} -1 & -\sqrt{3} \\ 2 & 2 \end{vmatrix} \quad r_1^2 = \begin{vmatrix} -1 & \sqrt{3} \\ 2 & 2 \end{vmatrix} \quad r_2^2 = \begin{vmatrix} -1 & \sqrt{3} \\ 2 & 2 \end{vmatrix} \\
 \mathscr{D}^E(R_3^2) \quad R_2^2 = \begin{vmatrix} 1 & 0 \\ 0 & 1 \end{vmatrix} \quad r_4 = \begin{vmatrix} -1 & -\sqrt{3} \\ 2 & 2 \end{vmatrix} \quad r_3 = \begin{vmatrix} -1 & -\sqrt{3} \\ 2 & 2 \end{vmatrix} \quad r_3^2 = \begin{vmatrix} -1 & \sqrt{3} \\ 2 & 2 \end{vmatrix} \quad r_4^2 = \begin{vmatrix} -1 & \sqrt{3} \\ 2 & 2 \end{vmatrix} \\
 \mathscr{D}^E(R_3) \quad i_4 = \begin{vmatrix} 1 & 0 \\ 0 & -1 \end{vmatrix} \quad i_1 = \begin{vmatrix} -1 & \sqrt{3} \\ 2 & 2 \end{vmatrix} \quad i_2 = \begin{vmatrix} -1 & \sqrt{3} \\ 2 & 2 \end{vmatrix} \quad R_1^3 = \begin{vmatrix} -1 & -\sqrt{3} \\ 2 & 2 \end{vmatrix} \quad R_1 = \begin{vmatrix} -1 & -\sqrt{3} \\ 2 & 2 \end{vmatrix} \\
 \mathscr{D}^E(R_3^3) \quad i_3 = \begin{vmatrix} 1 & 0 \\ 0 & -1 \end{vmatrix} \quad R_2 = \begin{vmatrix} -1 & \sqrt{3} \\ 2 & 2 \end{vmatrix} \quad R_2^2 = \begin{vmatrix} -1 & \sqrt{3} \\ 2 & 2 \end{vmatrix} \quad i_6 = \begin{vmatrix} -1 & -\sqrt{3} \\ 2 & 2 \end{vmatrix} \quad i_5 = \begin{vmatrix} -1 & -\sqrt{3} \\ 2 & 2 \end{vmatrix}
 \end{array}$$

(4.2.19)

Notice that the part which represents  $D_4 = \{1, R_3^2, R_3, R_3^3, R_1^2, R_2^2, i_3, i_4\}$  is diagonal:

$$\mathscr{D}^E \downarrow D_4 = \begin{pmatrix} D^{A_1} & 0 \\ 0 & D^{B_1} \end{pmatrix},$$

while  $D_2 = \{1, R_1^2, R_2^2, R_3^2\}$  is represented entirely by unit matrices:

$$\mathscr{D}^E \downarrow D_2 = \begin{pmatrix} D^{A_1} & 0 \\ 0 & D^{A_1} \end{pmatrix} = \begin{pmatrix} 1 & 0 \\ 0 & 1 \end{pmatrix}.$$

Notice also that each member of a  $D_2$  coset, such as  $r_1 D_2 = \{r_1 r_2 r_3 r_4\}$  is represented by the same matrix. In fact, the six cosets of  $D_2$  are each represented by one  $E$  irrep (3.3.7) of  $D_3$ .

The irreps of full octahedral symmetry differ from the  $O$  irreps only by  $(\pm)$  factors according to Eq. (4.1.18). Consider, for example, the irrep  $\mathscr{D}^{T_{1u}}$  given for  $Ir_1, i_4,$  and  $R_1^2$  in Figure 4.2.1. The matrices for  $i_4$  and  $R_1^2$  are the same as in Eq. (4.2.14). However, a  $u$  representation of any element with inversion attached has its sign changed from Eq. (4.2.14).

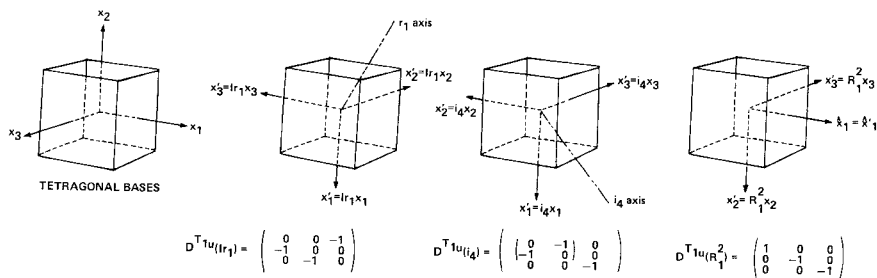


**Figure 4.2.1** Tetragonal vector bases and  $T_{1u}$  irreps of  $I_{r_1}$ ,  $i_4$ , and  $R_1^2$  operators (octahedral operators are defined in Figure 4.1.2).

The irrep  $\mathcal{D}^{T_{1u}}$  can be easily understood, since it represents the effect of  $O_h$  transformations on Cartesian unit vectors  $\{\hat{x} = \hat{x}_1, \hat{y} = \hat{x}_2, \hat{z} = \hat{x}_3\}$ . The effects of  $I_{r_1}$ ,  $i_4$ , and  $R_1^2$  are shown in Figure 4.2.1. It is easy to visualize a transformed unit vector such as

$$I_{r_1} |x_1\rangle = -|x_2\rangle,$$

which gives the corresponding  $T_{1u}$  irrep component

$$\mathcal{D}^{T_{1u}}(I_{r_1}) = \langle x_2 | I_{r_1} | x_1 \rangle = -1. \quad (4.2.20)$$

Notice also the difference between horizontal-plane reflections such as

$$\mathcal{D}^{T_{1u}}(I_{R_1^2}) = \begin{pmatrix} -1 & \cdot & \cdot \\ \cdot & 1 & \cdot \\ \cdot & \cdot & 1 \end{pmatrix}_{(D_{4h} \supset D_{2h})}, \quad (4.2.21)$$

which are diagonal in this representation, and diagonal-plane reflections such as

$$\mathcal{D}^{T_{1u}}(I_{i_4}) = \begin{pmatrix} \cdot & 1 & \cdot \\ 1 & \cdot & \cdot \\ \cdot & \cdot & 1 \end{pmatrix}_{(D_{4h} \supset D_{2h})}, \quad (4.2.22)$$

which are not.

The  $O_h \supset D_{4h} \supset D_{2h}$  subgroup chain labeling follows from that of  $O \supset D_4 \supset D_2$ . The labeling of the  $T_{1u}$  vector bases goes as follows:

$$|\hat{x}_1\rangle = \begin{vmatrix} T_{1u} \\ 1 \end{vmatrix} \equiv \begin{vmatrix} [T_{1u}] \\ E_{1u} \\ B_{1u} \end{vmatrix}, \quad |\hat{x}_2\rangle = \begin{vmatrix} T_{1u} \\ 2 \end{vmatrix} \equiv \begin{vmatrix} [T_{1u}] \\ E_{2u} \\ B_{2u} \end{vmatrix}, \quad |\hat{x}_3\rangle = \begin{vmatrix} T_{1u} \\ 3 \end{vmatrix} \equiv \begin{vmatrix} [T_{1u}] \\ A_{2u} \\ A_{2u} \end{vmatrix}. \quad (4.2.23)$$

**(b) Trigonal Standing-Wave Irreps ( $O_h \supset D_{3d} \supset C_{2v}$ )** Suppose we require  $O$  irreps which are diagonal with respect to subgroup  $C_2 = \{1, i_4\}$  and

reduced with respect to subgroup  $D_3 = \{1, r_1, r_1^2, i_2, i_4, i_5\}$ . The formal construction of these irreps involves splitting with the idempotent combination

$$\begin{aligned} 1 &= (P^E + P^{A_2} + P^{A_1})(P^A + P^B) \\ &= P^E P^A + P^E P^B + P^{A_2} P^B + P^{A_1} P^A \\ &= P_1^E + P_2^E + P^{A_2} + P^{A_1}, \end{aligned} \quad (4.2.24)$$

made from  $D_3$  and  $C_2$  operators.

For example, the following is the splitting of  $P^{T_1}$ :

$$\begin{aligned} P^{T_1} &= \mathbb{P}^{T_1}(P_1^E + P_2^E + P^{A_2} + P^{A_1}) \\ &= \mathbb{P}^{T_1} P_1^E + \mathbb{P}^{T_1} P_2^E + \mathbb{P}^{T_1} P^{A_2} + 0 \\ &= P_1^{T_1} + P_2^{T_1} + P_3^{T_1}. \end{aligned} \quad (4.2.25a)$$

This defines the  $D_3 \supset C_2$  subgroup correlation and base labeling

$$P_1^{T_1} \equiv \mathbb{P}^{T_1} P^E P^A, \quad P_2^{T_1} \equiv \mathbb{P}^{T_1} P^E P^B, \quad P_3^{T_1} \equiv \mathbb{P}^{T_1} P^{A_2} P^B. \quad (4.2.25b)$$

Another way to obtain trigonal  $\mathcal{O}^{T_1}$  representations involves the Cartesian unit vectors  $\{\hat{v}_1, \hat{v}_2, \hat{v}_3\}$  defined by

$$\hat{v}_1 = \begin{pmatrix} 1 \\ \sqrt{2} \\ -1 \\ 0 \end{pmatrix}, \quad \hat{v}_2 = \begin{pmatrix} 1 \\ \sqrt{6} \\ -2 \\ -\sqrt{6} \end{pmatrix}, \quad \hat{v}_3 = \begin{pmatrix} 1 \\ \sqrt{3} \\ 1 \\ \sqrt{3} \end{pmatrix}, \quad (4.2.26)$$

which are drawn in Figure 4.2.2. These are defined so  $\hat{v}_3$  points along the trigonal (111) direction or  $r_1$  axis, and  $\hat{v}_1$  lies along the  $i_4$  axis.  $\hat{v}_2$  is normal

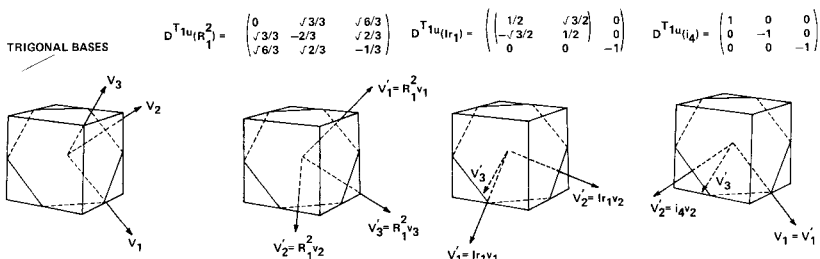


**Figure 4.2.2** Trigon vector bases and  $T_{1u}$  irreps of  $R_1^2$ ,  $Ir_1$ , and  $i_4$  operators.

to  $\hat{v}_1$  and  $\hat{v}_3$ . Clearly,  $\hat{v}_1$  and  $\hat{v}_2$  behave like  $E$  partners under  $120^\circ r_1$  rotations. Furthermore,  $\hat{v}_2$  and  $\hat{v}_3$  are antisymmetric ( $-$ ) to  $180^\circ i_4$  rotations, while  $\hat{v}_1$  is symmetric ( $+$ ). The full  $O_h \supset D_{3d} \supset C_{2v}$  labeling of these vector bases is

$$|v_1\rangle \equiv \begin{bmatrix} [T_{1u}] \\ 1 \end{bmatrix} = \begin{bmatrix} [T_{1u}] \\ E_u \\ A_u \end{bmatrix}, \quad |v_2\rangle \equiv \begin{bmatrix} T_{1u} \\ 2 \end{bmatrix} = \begin{bmatrix} [T_{1u}] \\ E_u \\ B_u \end{bmatrix}, \quad |v_3\rangle \equiv \begin{bmatrix} T_{1u} \\ 3 \end{bmatrix} = \begin{bmatrix} [T_{1u}] \\ A_{2u} \\ B_u \end{bmatrix}. \tag{4.2.27}$$

This is in agreement with Eq. (4.2.25b).

The vector transformations and  $\mathcal{D}^{T_{1u}}$  representations of  $R_1^2$ ,  $I_{r_1}$ , and  $i_4$  are shown in Figure 4.2.2. The entire trigonal representation  $\mathcal{D}^{T_1}$  of  $O$  is given in the following equation.

$\mathcal{D}^{T_1}(1) =$ $\begin{vmatrix} 1 & \cdot & \cdot \\ \cdot & 1 & \cdot \\ \cdot & \cdot & 1 \end{vmatrix}$	$i_4 = [12]$ $\begin{vmatrix} 1 & \cdot & \cdot \\ \cdot & -1 & \cdot \\ \cdot & \cdot & -1 \end{vmatrix}$	$R_1^2 = [13][24]$ $\begin{vmatrix} \cdot & \frac{\sqrt{3}}{3} & \frac{\sqrt{6}}{3} \\ \frac{\sqrt{3}}{3} & -2 & \frac{\sqrt{2}}{3} \\ \frac{\sqrt{6}}{3} & \frac{\sqrt{2}}{3} & -1 \end{vmatrix}$	$R_3 = [1423]$ $\begin{vmatrix} \cdot & -\frac{\sqrt{3}}{3} & -\frac{\sqrt{6}}{3} \\ \frac{\sqrt{3}}{3} & 2 & -\frac{\sqrt{2}}{3} \\ \frac{\sqrt{6}}{3} & -\frac{\sqrt{2}}{3} & 1 \end{vmatrix}$
$r_1 = [132]$ $\begin{vmatrix} \frac{-1}{2} & \frac{-\sqrt{3}}{2} & \cdot \\ \frac{\sqrt{3}}{2} & -1 & \cdot \\ \cdot & \cdot & 1 \end{vmatrix}$	$i_5 = [13]$ $\begin{vmatrix} -1 & -\sqrt{3} & \cdot \\ \frac{-1}{2} & \frac{-\sqrt{3}}{2} & \cdot \\ \frac{-\sqrt{3}}{2} & 1 & \cdot \\ \cdot & \cdot & -1 \end{vmatrix}$	$r_4 = [234]$ $\begin{vmatrix} 1 & -\sqrt{3} & \sqrt{6} \\ \frac{1}{2} & -\frac{\sqrt{3}}{6} & \frac{\sqrt{6}}{3} \\ -\frac{\sqrt{3}}{2} & -1 & \frac{\sqrt{2}}{3} \\ \cdot & -\frac{\sqrt{8}}{3} & -1 \end{vmatrix}$	$i_6 = [24]$ $\begin{vmatrix} -1 & \sqrt{3} & -\sqrt{6} \\ \frac{-1}{2} & \frac{\sqrt{3}}{6} & \frac{-\sqrt{6}}{3} \\ \frac{\sqrt{3}}{6} & -5 & -\frac{\sqrt{2}}{3} \\ -\frac{\sqrt{6}}{3} & -\frac{\sqrt{2}}{3} & 1 \end{vmatrix}$
$r_1^2 = [123]$ $\begin{vmatrix} -1 & \frac{\sqrt{3}}{2} & \cdot \\ \frac{-\sqrt{3}}{2} & -1 & \cdot \\ \cdot & \cdot & 1 \end{vmatrix}$	$i_2 = [23]$ $\begin{vmatrix} -1 & \sqrt{3} & \cdot \\ \frac{-1}{2} & \frac{\sqrt{3}}{2} & \cdot \\ \frac{\sqrt{3}}{2} & 1 & \cdot \\ \cdot & \cdot & -1 \end{vmatrix}$	$r_2^2 = [142]$ $\begin{vmatrix} -1 & -\sqrt{3} & \sqrt{6} \\ \frac{-1}{2} & -\frac{\sqrt{3}}{6} & \frac{\sqrt{6}}{3} \\ \frac{\sqrt{3}}{3} & 5 & \frac{\sqrt{2}}{3} \\ -\frac{\sqrt{6}}{3} & \frac{\sqrt{2}}{3} & -1 \end{vmatrix}$	$R_2^3 = [1342]$ $\begin{vmatrix} 1 & \sqrt{3} & -\sqrt{6} \\ \frac{1}{2} & \frac{\sqrt{3}}{6} & \frac{-\sqrt{6}}{3} \\ -\frac{\sqrt{3}}{2} & 1 & -\frac{\sqrt{2}}{3} \\ \cdot & \frac{\sqrt{8}}{3} & 1 \end{vmatrix}$

Notice that group operators which were diagonalized in the tetragonal irrep (4.2.14) become undiagonalized in (4.2.28), and vice versa. For example, the tetragonal irrep (4.2.21) of the horizontal-plane reflection becomes

$$\mathcal{D}^{T_{1u}}(IR_1^2) = \begin{pmatrix} \cdot & -\frac{\sqrt{3}}{3} & -\frac{\sqrt{6}}{3} \\ -\frac{\sqrt{3}}{3} & \frac{2}{3} & -\frac{\sqrt{2}}{3} \\ -\frac{\sqrt{6}}{3} & -\frac{\sqrt{2}}{3} & \frac{1}{3} \end{pmatrix} \quad (4.2.29)$$

( $D_{3d} \supset C_{2v}$ )

in the trigonal basis, but the trigonal irrep

$$\mathcal{D}^{T_{1u}}(Ii_4) = \begin{pmatrix} -1 & \cdot & \cdot \\ \cdot & 1 & \cdot \\ \cdot & \cdot & 1 \end{pmatrix} \quad (4.2.30)$$

( $D_{3d} \supset C_{2v}$ )

of the diagonal-plane reflection becomes diagonalized.

$R_2^2 = [14][23]$	$R_3^3 = [1324]$	$R_3^2 = [12][34]$	$i_3 = [34]$
$\begin{vmatrix} \cdot & -\frac{\sqrt{3}}{3} & -\frac{\sqrt{6}}{3} \\ -\frac{\sqrt{3}}{3} & -2 & \frac{\sqrt{2}}{2} \\ -\frac{\sqrt{6}}{3} & \frac{\sqrt{2}}{3} & -1 \end{vmatrix}$	$\begin{vmatrix} \cdot & \frac{\sqrt{3}}{3} & \frac{\sqrt{6}}{3} \\ -\frac{\sqrt{3}}{3} & 2 & -\frac{\sqrt{2}}{3} \\ -\frac{\sqrt{6}}{3} & -\frac{\sqrt{2}}{3} & \frac{1}{3} \end{vmatrix}$	$\begin{vmatrix} -1 & \cdot & \cdot \\ \cdot & \frac{1}{3} & -\frac{\sqrt{8}}{3} \\ \cdot & -\frac{\sqrt{8}}{3} & -1 \end{vmatrix}$	$\begin{vmatrix} -1 & \cdot & \cdot \\ \cdot & -\frac{1}{3} & \frac{\sqrt{8}}{3} \\ \cdot & \frac{\sqrt{8}}{3} & \frac{1}{3} \end{vmatrix}$
$r_2 = [124]$	$R_1 = [1234]$	$r_3 = [143]$	$R_1^3 = [1432]$
$\begin{vmatrix} -1 & \frac{\sqrt{3}}{2} & -\frac{\sqrt{6}}{3} \\ -\frac{\sqrt{3}}{3} & \frac{5}{6} & \frac{\sqrt{2}}{3} \\ \frac{\sqrt{6}}{3} & \frac{\sqrt{2}}{3} & -1 \end{vmatrix}$	$\begin{vmatrix} \frac{1}{2} & -\frac{\sqrt{3}}{6} & \frac{\sqrt{6}}{3} \\ \frac{\sqrt{3}}{2} & \frac{1}{6} & -\frac{\sqrt{2}}{3} \\ \cdot & \frac{\sqrt{8}}{3} & \frac{1}{3} \end{vmatrix}$	$\begin{vmatrix} \frac{1}{2} & \frac{\sqrt{3}}{2} & \cdot \\ \frac{\sqrt{3}}{6} & -\frac{1}{6} & -\frac{\sqrt{8}}{3} \\ -\frac{\sqrt{6}}{3} & \frac{\sqrt{2}}{3} & -1 \end{vmatrix}$	$\begin{vmatrix} \frac{1}{2} & \frac{\sqrt{3}}{2} & \cdot \\ -\frac{\sqrt{3}}{6} & \frac{1}{6} & \frac{\sqrt{8}}{3} \\ \frac{\sqrt{6}}{3} & -\frac{\sqrt{2}}{3} & \frac{1}{3} \end{vmatrix}$
$r_3^2 = [134]$	$i_1 = [14]$	$r_4^2 = [243]$	$R_2 = [1243]$
$\begin{vmatrix} \frac{1}{2} & \frac{\sqrt{3}}{6} & -\frac{\sqrt{6}}{3} \\ \frac{\sqrt{3}}{2} & -\frac{1}{6} & \frac{\sqrt{2}}{3} \\ \cdot & -\frac{\sqrt{8}}{3} & -1 \end{vmatrix}$	$\begin{vmatrix} -1 & -\frac{\sqrt{3}}{6} & \frac{\sqrt{6}}{3} \\ -\frac{\sqrt{3}}{6} & -\frac{5}{6} & -\frac{\sqrt{2}}{3} \\ \frac{\sqrt{6}}{3} & -\frac{\sqrt{2}}{3} & \frac{1}{3} \end{vmatrix}$	$\begin{vmatrix} \frac{1}{2} & -\frac{\sqrt{3}}{2} & \cdot \\ -\frac{\sqrt{3}}{6} & -\frac{1}{6} & -\frac{\sqrt{8}}{3} \\ \frac{\sqrt{6}}{3} & \frac{\sqrt{2}}{3} & -1 \end{vmatrix}$	$\begin{vmatrix} \frac{1}{2} & -\frac{\sqrt{3}}{2} & \cdot \\ \frac{\sqrt{3}}{6} & \frac{1}{6} & \frac{\sqrt{8}}{3} \\ -\frac{\sqrt{6}}{3} & -\frac{\sqrt{2}}{3} & \frac{1}{3} \end{vmatrix}$

(4.2.28)

The transformation matrix which relates the  $T_{1u}$  irreps represented in tetragonal bases to trigonal irreps is

$$\mathcal{F}(4 \leftarrow 3) = \begin{pmatrix} \langle x_1|v_1 \rangle & \langle x_1|v_2 \rangle & \langle x_1|v_3 \rangle \\ \langle x_2|v_1 \rangle & \langle x_2|v_2 \rangle & \langle x_2|v_3 \rangle \\ \langle x_3|v_1 \rangle & \langle x_3|v_2 \rangle & \langle x_3|v_3 \rangle \end{pmatrix} = \begin{pmatrix} \frac{1}{\sqrt{2}} & \frac{1}{\sqrt{6}} & \frac{1}{\sqrt{3}} \\ -\frac{1}{\sqrt{2}} & \frac{1}{\sqrt{6}} & \frac{1}{\sqrt{3}} \\ 0 & -\frac{2}{\sqrt{6}} & \frac{1}{\sqrt{3}} \end{pmatrix}. \quad (4.2.31)$$

The three columns of  $\mathcal{F}(4 \leftarrow 3)$  are the vectors (4.2.26). The equivalence transformation between the trigonal ( $D_{3d} \supset C_{2v}$ ) and tetragonal ( $D_{4h} \supset D_{2h}$ ) matrices has the following form:

$$\begin{aligned} \mathcal{F}(4 \leftarrow 3)(\mathcal{D}^{T_{1u}})_{(D_{3d} \supset C_{2v})} \mathcal{F}^\dagger(4 \leftarrow 3) &= (\mathcal{D}^{T_{1u}})_{(D_{4h} \supset D_{2h})}, \\ \mathcal{F}(4 \leftarrow 3)^\dagger (\mathcal{D}^{T_{1u}})_{(D_{4h} \supset D_{2h})} \mathcal{F}(4 \leftarrow 3) &= (\mathcal{D}^{T_{1u}})_{(D_{3d} \supset C_{2v})}. \end{aligned} \quad (4.2.32)$$

The trigonal  $\mathcal{D}^{T_2}$  irreps can be obtained by simply changing the signs of half the matrices according to Eq. (4.2.15). However, if one requires "kosher"  $D_3 \supset C_2$  subgroup labeling, then the irreps in the table section in the back of this book should be used. The  $O_h \supset D_{3d} \supset C_{2v}$  labeling of these is

$$\left| \begin{matrix} T_{2p} \\ 1 \end{matrix} \right\rangle = \left| \begin{matrix} [T_{2p}] \\ A_{1p} \\ A_p \end{matrix} \right\rangle, \quad \left| \begin{matrix} T_{2p} \\ 2 \end{matrix} \right\rangle = \left| \begin{matrix} [T_{2p}] \\ E_p \\ A_p \end{matrix} \right\rangle, \quad \left| \begin{matrix} T_{2p} \\ 3 \end{matrix} \right\rangle = \left| \begin{matrix} [T_{2p}] \\ E_p \\ B_p \end{matrix} \right\rangle, \quad (4.2.33)$$

where  $p = g$  or  $u$  is the inversion parity.

The trigonal  $E$ -type irreps have the same form as the tetragonal irreps (4.2.19). The  $E$  bases can be labeled

$$\left| \begin{matrix} E_p \\ 1 \end{matrix} \right\rangle \equiv \left| \begin{matrix} [E_p] \\ A_{1p} \\ A_{1p} \end{matrix} \right\rangle_{(D_{4h} D_{2h})} = \left| \begin{matrix} [E_p] \\ E_p \\ A_p \end{matrix} \right\rangle_{(D_{3d} C_{2v})}, \quad \left| \begin{matrix} E_p \\ 2 \end{matrix} \right\rangle \equiv \left| \begin{matrix} [E_p] \\ B_{1p} \\ A_{1p} \end{matrix} \right\rangle_{(D_{4h} D_{2h})} = \left| \begin{matrix} [E_p] \\ E_p \\ B_p \end{matrix} \right\rangle_{(D_{3d} C_{2v})}, \quad (4.2.34)$$

where  $p = u$  or  $g$  is inversion parity. They go equally well with  $D_4 \supset D_2$  or  $D_3 \supset C_2$  subgroup chains.

**(c) Tetragonal Moving-Wave Irreps ( $O \supset D_4 \supset C_4$ )** The introduction of magnetic fields and molecular rotations will require that cyclic rotation groups be represented by diagonal matrices. A simple transformation of the tetragonal irreps in Section 4.2.A(a) causes the irreps of the cyclic subgroup  $C_4 = \{1, R_3, R_3^2, R_3^3\}$  to be diagonal. For example, the  $\mathcal{D}^{T_1}$  irrep takes the following form:





The transformation which disagonalizes  $\mathcal{D}^{T_1}(R_3)$  from Eq. (4.2.14) is

$$\mathcal{F}^\dagger \begin{pmatrix} 0 & -1 & \cdot \\ 1 & 0 & \cdot \\ \cdot & \cdot & 1 \end{pmatrix} \mathcal{F} = \begin{pmatrix} i & \cdot & \cdot \\ \cdot & -i & \cdot \\ \cdot & \cdot & 1 \end{pmatrix} = \mathcal{D}^{T_1^0}(R_3), \quad (4.2.36)$$

$$\mathcal{F} = \begin{pmatrix} \langle x_1 |_{1_4}^E \rangle & \langle x_1 |_{3_4}^E \rangle & \cdot \\ \langle x_2 |_{1_4}^E \rangle & \langle x_2 |_{3_4}^E \rangle & \cdot \\ \cdot & \cdot & \langle x_3 |_{0_4}^{A_2} \rangle \end{pmatrix} = \begin{pmatrix} -1 & 1 & \cdot \\ \sqrt{2} & \sqrt{2} & \cdot \\ -i & -i & \cdot \\ \sqrt{2} & \sqrt{2} & \cdot \\ \cdot & \cdot & 1 \end{pmatrix}.$$

You may recall seeing this form of transformation before [viz., Eqs. (3.4.24)], and one should certainly expect to see it again. It is the transformation between standing-wave or linear  $(x, y)$  polarization states and moving-wave or circular  $(x \pm iy)$  polarization states. The following is the labeling of the circular  $T$  states by subgroup chain  $O \supset D_4 \supset C_4$ .

$$\begin{vmatrix} T_1 \\ 1_4 \end{vmatrix} = \begin{vmatrix} [T_1] \\ E \\ 1_4 \end{vmatrix}, \quad \begin{vmatrix} T_1 \\ 3_4 \end{vmatrix} = \begin{vmatrix} [T_1] \\ E \\ 3_4 \end{vmatrix}, \quad \begin{vmatrix} T_1 \\ 0_4 \end{vmatrix} = \begin{vmatrix} [T_1] \\ A_2 \\ 0_4 \end{vmatrix}. \quad (4.2.37)$$

The corresponding labeling for the  $T_2$  bases is similar.

$$\begin{vmatrix} T_2 \\ 1_4 \end{vmatrix} = \begin{vmatrix} [T_2] \\ E \\ 1_4 \end{vmatrix}, \quad \begin{vmatrix} T_2 \\ 3_4 \end{vmatrix} = \begin{vmatrix} [T_2] \\ E \\ 3_4 \end{vmatrix}, \quad \begin{vmatrix} T_2 \\ 2_4 \end{vmatrix} = \begin{vmatrix} [T_2] \\ B_2 \\ 2_4 \end{vmatrix}. \quad (4.2.38)$$

The third  $T_2$  component belongs to  $2_4$  waves angular quantum  $m = 2 \bmod 4$ . The first two components belong to  $(m = \pm 1 \bmod 4)$  waves, as do the corresponding  $T_1$  components.

The corresponding labeling of the  $E$ ,  $A_2$ , and  $A_1$  bases is as follows:

$$\begin{vmatrix} E \\ 0_4 \end{vmatrix} = \begin{vmatrix} [E] \\ A_1 \\ 0_4 \end{vmatrix}, \quad \begin{vmatrix} E \\ 2_4 \end{vmatrix} = \begin{vmatrix} [E] \\ B_1 \\ 2_4 \end{vmatrix}, \quad |A_2\rangle = \begin{vmatrix} [A_2] \\ B_1 \\ 2_4 \end{vmatrix}, \quad |A_1\rangle = \begin{vmatrix} [A_1] \\ A_1 \\ 0_4 \end{vmatrix}.$$

(4.2.39)

(4.2.40)

(4.2.41)

Notice that the  $E$ - and  $A_{1,2}$ -type bases do not require transformation from their standing-wave forms, since these are already diagonal representations of  $C_4$ .

**(d) Trigonal Moving-Wave Irreps ( $O \supset D_3 \supset C_3$ )** The standing-to-moving-wave transformation can be used to diagonalize the representations of cyclic subgroup  $C_3 = \{1, r_1, r_1^2\}$ . This produces complex irreps listed Table F.2.7.

**(e) Idempotent Splitting Corresponds to Level Splitting** Each class idempotent  $\mathbb{P}^\alpha$  is a sum of  $l^\alpha$  irreducible idempotents  $P_{ii}^\alpha \equiv P_i^\alpha$  ( $i = 1 \cdots l^\alpha$ ). Each  $P_i^\alpha$  can be thought of as a projection operator for a single state  $\Psi_i^\alpha$  belonging to one of  $l^\alpha$  degenerate energy levels  $\varepsilon_i^\alpha$  in an ( $\alpha$ )-type multiplet. For example,  $O$  symmetry gives rise to  $T_1$ -type triplets,  $T_2$ -type triplets,  $E$ -type doublets, and  $A_1$ - or  $A_2$ -type singlets.

If we reduce the  $O$  symmetry to one of its subgroups such as  $D_4$ ,  $D_2$ , or  $C_4$  then each of these levels may split according to the way that their corresponding class idempotents split. For example, the  $O \supset D_4$  splitting relation (4.2.9) gives the following (nonzero) terms:

$$\begin{aligned} \mathbb{P}^{T_1} &= \mathbb{P}^{T_1} P_1^E + \mathbb{P}^{T_1} P_2^E + \mathbb{P}^{T_1} P^{A_2} = \mathbb{P}^{T_1} P^E + \mathbb{P}^{T_1} P^{A_2} \\ &= P_{11}^{T_1} + P_{22}^{T_1} + P_{33}^{T_1}. \end{aligned}$$

The first line corresponds to a  $T_1$  triplet level splitting into an  $E$ -type doublet and an  $A_2$ -type singlet under  $D_4$  symmetry. The  $E$ -type doublet remains degenerate until we reduce the symmetry to one of the  $D_4$  subgroups  $D_2$ ,  $C_4$ , or lower. If  $C_4$  is used the resulting pair of levels emerging from an  $E$  doublet are labeled  $1_4$  and  $3_4$  according to (4.2.4), while  $D_4 \supset D_2$  symmetry breaking would split  $E$  into  $B_1$ - and  $B_2$ -type levels according to (4.2.5).

A level-splitting diagram which traces all the level correlations of the  $O \supset D_4 \supset D_2$  chain is shown in Figure 4.2.3(a). The companion figure [4.2.3(b)] traces the  $O \supset D_4 \supset C_4$  correlations. Without their labels the two figures appear identical! However, we have noted that the  $C_4$  symmetry breaking gives moving-wave states and is analogous to magnetic Zeeman or rotational Coriolis splitting. The  $D_2$  symmetry breaking, on the other hand, gives standing-wave states and is analogous to electric Stark or anisotropy splitting. It is helpful to use the level-splitting diagrams to keep track of both the mathematics and physics associated with idempotent splitting and subgroup correlations. Another way to do this uses correlation tables as shown in the following section.

## B. More Subgroup Correlations

There are quite a few more possible  $O_h$  subgroup chains besides the four main types discussed in the preceding section. However, one or more of the four types of irreps can easily be adapted to most other labeling schemes.

The "road map" for any link in a subgroup chain is the CORRELATION TABLE. The correlation table was introduced in Eqs. (3.6.27) for hexagonal

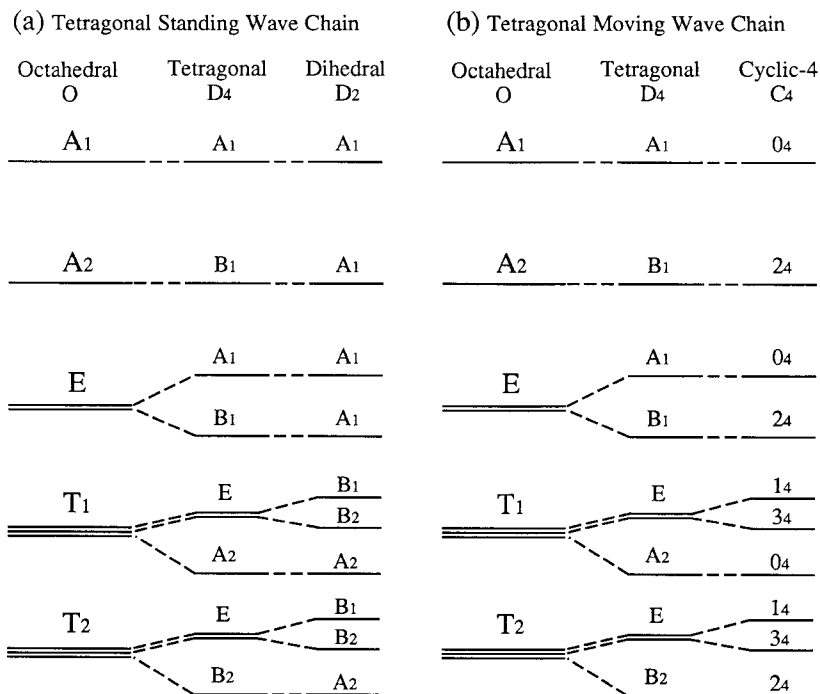


Figure 4.2.3 Level-splitting diagram for two of the tetragonal subgroup chains in octahedral symmetry.

or  $D_6$  subgroups. A correlation table lists the frequencies  $f^A$  of irreps  $D^A$  of subgroup  $H$  in a *subduced* irrep  $\mathcal{D}^\alpha \downarrow H$  of a larger group  $G \supset H$ . These frequencies can be obtained by comparing character tables of  $G$  and  $H$  and using the theory of Section 3.5.B(a).

For example, the  $O \supset D_4$  and  $O \supset C_4$  correlations used in the preceding section are summed up by the following tables:

$\downarrow D_4$	$A_1$	$A_2$	$B_1$	$B_2$	$E$
$\mathcal{D}^{A_1}$	1	·	·	·	·
$\mathcal{D}^{A_2}$	·	·	1	·	·
$\mathcal{D}^E$	1	·	1	·	·
$\mathcal{D}^{T_1}$	·	1	·	·	1
$\mathcal{D}^{T_2}$	·	·	·	1	1

(4.2.42a)

$\downarrow C_4$	$0_4$	$1_4$	$2_4$	$3_4$
$\mathcal{D}^{A_1}$	1	·	·	·
$\mathcal{D}^{A_2}$	·	·	1	·
$\mathcal{D}^E$	1	·	1	·
$\mathcal{D}^{T_1}$	1	1	·	1
$\mathcal{D}^{T_2}$	·	1	1	1

(4.2.42b)

Comparison of the  $C_4$  characters

$$\begin{array}{l} \chi^{0_4} = \\ \chi^{1_4} = \\ \chi^{2_4} = \\ \chi^{3_4} = \end{array} \begin{array}{c} g = 1 \quad R \quad R^2 \quad R^3 \\ \left[ \begin{array}{cccc} 1 & 1 & 1 & 1 \\ 1 & -i & -1 & i \\ 1 & -1 & 1 & -1 \\ 1 & i & -1 & -i \end{array} \right] \end{array}, \quad (4.2.43)$$

with the  $O$ -character table (4.1.11) yielding the  $O \supset C_4$  correlations (4.2.42b). For example, the  $\mathscr{D}^{T_1} \downarrow C_4$  characters are

$$\chi_g^{T_1} = \begin{array}{c} g = 1 \quad R \quad R^2 \quad R^3 \\ \left[ \begin{array}{cccc} 3 & 1 & -1 & 1 \end{array} \right] \end{array}$$

from the  $O$  table. It is easy to see that

$$\chi_g^{T_1} = \chi^{0_4} + \chi^{1_4} + \chi^{3_4}$$

for each  $g$  in the  $C_4$  table (4.2.43). This gives the  $T_1$  row of (4.2.42b).

The trigonal  $O \supset D_3$  and  $O \supset C_3$  correlations are found in the same way:

$$\begin{array}{l} \downarrow D_3 \\ \mathscr{D}^{A_1} \\ \mathscr{D}^{A_2} \\ \mathscr{D}^E \\ \mathscr{D}^{T_1} \\ \mathscr{D}^{T_2} \end{array} \begin{array}{c} A_1 \quad A_2 \quad E \\ \left[ \begin{array}{ccc} 1 & \cdot & \cdot \\ \cdot & 1 & \cdot \\ \cdot & \cdot & 1 \\ \cdot & 1 & 1 \\ 1 & \cdot & 1 \end{array} \right] \end{array},$$

(4.2.44a)

$$\begin{array}{l} \downarrow C_3 \\ \mathscr{D}^{A_1} \\ \mathscr{D}^{A_2} \\ \mathscr{D}^E \\ \mathscr{D}^{T_1} \\ \mathscr{D}^{T_2} \end{array} \begin{array}{c} 0_3 \quad 1_3 \quad 2_3 \\ \left[ \begin{array}{ccc} 1 & \cdot & \cdot \\ 1 & \cdot & \cdot \\ \cdot & 1 & 1 \\ 1 & 1 & 1 \\ 1 & 1 & 1 \end{array} \right] \end{array}.$$

(4.2.44b)

For a number of applications it will be convenient to have correlation tables for subgroup chains involving  $O_h \supset C_{2v}$ ,  $O_h \supset C_{3v}$ , and  $O_h \supset C_{4v}$ . The character table of  $C_{2v}$  has the  $C_2 \times C_2$  form as explained in Sections 2.10 and 2.11:

$$\begin{array}{l} \chi_g^{A'} = \\ \chi_g^{B'} = \\ \chi_g^{A''} = \\ \chi_g^{B''} = \end{array} \begin{array}{c} g = 1 \quad i_4 \quad IR_3^2 \quad Ii_3 \\ \left[ \begin{array}{cccc} 1 & 1 & 1 & 1 \\ 1 & -1 & 1 & -1 \\ 1 & 1 & -1 & -1 \\ 1 & -1 & -1 & 1 \end{array} \right] \end{array}. \quad (4.2.45)$$

The  $C_{3v}$  and  $C_{4v}$  characters were given by their isomorphic  $D_3$  and  $D_4$  characters in Eqs. (3.5.8) and (3.6.3), respectively. By comparing these with  $O_h$  characters one easily derives the following correlations:

$$\downarrow C_{2v} \begin{array}{c} A' \\ B' \\ A'' \\ B'' \end{array} \begin{array}{|c|c|c|c|} \hline \mathscr{D}^{A_{1g}} & 1 & \cdot & \cdot & \cdot \\ \hline \mathscr{D}^{A_{2g}} & \cdot & 1 & \cdot & \cdot \\ \hline \mathscr{D}^{E_g} & 1 & 1 & \cdot & \cdot \\ \hline \mathscr{D}^{T_{1g}} & \cdot & 1 & 1 & 1 \\ \hline \mathscr{D}^{T_{2g}} & 1 & \cdot & 1 & 1 \\ \hline \mathscr{D}^{A_{1u}} & \cdot & \cdot & 1 & \cdot \\ \hline \mathscr{D}^{A_{2u}} & \cdot & \cdot & \cdot & 1 \\ \hline \mathscr{D}^{E_u} & \cdot & \cdot & 1 & 1 \\ \hline \mathscr{D}^{T_{1u}} & 1 & 1 & \cdot & 1 \\ \hline \mathscr{D}^{T_{2u}} & 1 & 1 & 1 & \cdot \\ \hline \end{array}$$

(4.2.46a)

$$\downarrow C_{3v} \begin{array}{c} A' \\ A'' \\ E \end{array} \begin{array}{|c|c|c|} \hline \mathscr{D}^{A_{1g}} & 1 & \cdot & \cdot \\ \hline \mathscr{D}^{A_{2g}} & \cdot & 1 & \cdot \\ \hline \mathscr{D}^{E_g} & \cdot & \cdot & 1 \\ \hline \mathscr{D}^{T_{1g}} & \cdot & 1 & 1 \\ \hline \mathscr{D}^{T_{2g}} & 1 & \cdot & 1 \\ \hline \mathscr{D}^{A_{1u}} & \cdot & 1 & \cdot \\ \hline \mathscr{D}^{A_{2u}} & 1 & \cdot & \cdot \\ \hline \mathscr{D}^{E_u} & \cdot & \cdot & 1 \\ \hline \mathscr{D}^{T_{1u}} & 1 & \cdot & 1 \\ \hline \mathscr{D}^{T_{2u}} & \cdot & 1 & 1 \\ \hline \end{array}$$

(4.2.46b)

$$\downarrow C_{4v} \begin{array}{c} A' \\ B' \\ A'' \\ B'' \\ E \end{array} \begin{array}{|c|c|c|c|c|} \hline \mathscr{D}^{A_{1g}} & 1 & \cdot & \cdot & \cdot & \cdot \\ \hline \mathscr{D}^{A_{2g}} & \cdot & 1 & \cdot & \cdot & \cdot \\ \hline \mathscr{D}^{E_g} & 1 & 1 & \cdot & \cdot & \cdot \\ \hline \mathscr{D}^{T_{1g}} & \cdot & \cdot & 1 & \cdot & 1 \\ \hline \mathscr{D}^{T_{2g}} & \cdot & \cdot & \cdot & 1 & 1 \\ \hline \mathscr{D}^{A_{1u}} & \cdot & \cdot & 1 & \cdot & \cdot \\ \hline \mathscr{D}^{A_{2u}} & \cdot & \cdot & \cdot & 1 & \cdot \\ \hline \mathscr{D}^{E_u} & \cdot & \cdot & 1 & 1 & \cdot \\ \hline \mathscr{D}^{T_{1u}} & 1 & \cdot & \cdot & \cdot & 1 \\ \hline \mathscr{D}^{T_{2u}} & \cdot & 1 & \cdot & \cdot & 1 \\ \hline \end{array}$$

(4.2.46c)

### C. Conjugate and Normal Subgroups

When correlating a  $C_{nv}$  or  $D_n$  subgroup it is sometimes necessary to specify which subgroup. For example, consider the two subgroups  $\{1, R_3^2, i_3, i_4\}$  and  $\{1, R_3^2, R_1^2, R_2^2\}$ . Both subgroups contain three 180° rotations around orthogonal axes. Both should be labeled  $D_2$  and both have the same set of irreps:

$$\begin{aligned} D'_2 &= \{1 \quad R_3^2 \quad i_3 \quad i_4\} \\ D_2 &= \{1 \quad R_3^2 \quad R_1^2 \quad R_2^2\} \\ \begin{array}{l} A_1 \\ B_1 \\ A_2 \\ B_2 \end{array} & \begin{array}{|c|c|c|c|} \hline 1 & 1 & 1 & 1 \\ \hline 1 & -1 & 1 & -1 \\ \hline 1 & 1 & -1 & -1 \\ \hline 1 & -1 & -1 & 1 \\ \hline \end{array} \end{aligned} \tag{4.2.47}$$

However, they have quite different correlations with the octahedral irreps as the following tables show:

$$\downarrow \{1R_3^2i_3i_4\} \begin{array}{c} A_1 \\ B_1 \\ A_2 \\ B_2 \end{array} \begin{array}{|c|c|c|c|} \hline \mathscr{D}^{A_1} & 1 & \cdot & \cdot & \cdot \\ \hline \mathscr{D}^{A_2} & \cdot & \cdot & 1 & \cdot \\ \hline \mathscr{D}^E & 1 & \cdot & 1 & \cdot \\ \hline \mathscr{D}^{T_1} & \cdot & 1 & 1 & 1 \\ \hline \mathscr{D}^{T_2} & 1 & 1 & \cdot & 1 \\ \hline \end{array}$$

(4.2.48a)

$$\downarrow \{1R_3^2R_2^2R_1^2\} \begin{array}{c} A_1 \\ B_1 \\ A_2 \\ B_2 \end{array} \begin{array}{|c|c|c|c|} \hline \mathscr{D}^{A_1} & 1 & \cdot & \cdot & \cdot \\ \hline \mathscr{D}^{A_2} & 1 & \cdot & \cdot & \cdot \\ \hline \mathscr{D}^E & 2 & \cdot & \cdot & \cdot \\ \hline \mathscr{D}^{T_1} & \cdot & 1 & 1 & 1 \\ \hline \mathscr{D}^{T_2} & \cdot & 1 & 1 & 1 \\ \hline \end{array}$$

(4.2.48b)

The  $D'_2$  subgroup containing  $i_3$  and  $i_4$  could be used by itself to label each  $O$  irrep uniquely. The other  $D_2$  subgroup cannot provide  $E$ -irrep labeling, since  $E$  is correlated twice with the same irrep  $A_1$ . Indeed, the labeling chain  $O \supset D_4 \supset D_2$  discussed in Section 4.2.A(b) requires the  $D_4$  link in order to work for all  $O$  irreps.

Whenever we choose a particular subgroup  $H$  for labeling we generally ignore several CONJUGATE SUBGROUPS  $H' = tHt^{-1}$ ,  $H'' = uHu^{-1}$ , ... obtained by transforming  $H$  by group operators. For example,  $D'_2 = \{1, R_3^2, i_3, i_4\}$  has two other distinct conjugate subgroups  $D_2^{R_1} = \{1, R_2^2, i_1, i_2\}$  and  $D_2^{R_2} = \{1, R_1^2, i_5, i_6\}$ . Most of the subgroups of octahedral symmetry have several conjugates. By focusing on one choice from several conjugates we single out a particular axis or direction in the octahedral symmetry. However, each choice must give the same correlation table. This is true since the correlations depend only on the characters which are independent of transformations  $g' = tgt^{-1}$  within classes.

The other subgroup  $D_2 = \{1, R_1^2, R_2^2, R_3^2\}$  is an example of a self-conjugate or NORMAL subgroup of the octahedral group. A normal subgroup  $N \subset G$  is one for which  $gNg^{-1} = N$  for all transformations  $g$  in  $G$ . Normal subgroups are distinguished by being "unique" in their group.

### 4.3 INTRODUCTION TO SYMMETRY BREAKING AND INDUCED REPRESENTATIONS

Many spectroscopic applications of symmetry analysis involve effects in which higher-symmetry systems are changed into lower-symmetry ones. These effects are called SYMMETRY-BREAKING EFFECTS, and there are two basic types of symmetry breaking. One type is EXTERNAL or "applied" symmetry breaking, wherein a system of higher symmetry is perturbed by an outside force of lower symmetry. This perturbation generally causes splitting of spectral degeneracy, as in the example of Zeeman splitting in Figure 3.6.3 or band-gap splitting in Figure 2.7.7. Another type is INTERNAL or "spontaneous" symmetry breaking, in which a system tends to "stick" in a low-symmetry state when resonance or tunneling between equivalent states becomes negligible. This sticking generally goes along with *increased* spectral degeneracy, as in the example of  $\text{NH}_3$  with  $S = 0$  in Figure 2.12.7, or band collapse represented in Figure 2.12.1(c).

Either type of symmetry breaking involves the subgroup correlations which were introduced in Section 4.2 and the preceding chapter. In this section some applications will exhibit the relationship between the two opposing types of symmetry breaking: one which reduces spectral degeneracy, and the other which increases it. This will involve a relation between *subduced* representations ( $\mathcal{D}^\alpha \downarrow H$ ) and new type of representation called the *induced* representation, denoted by  $(D^A \uparrow G)$ .

### A. Octahedral Models and Induced Representations

Let us consider two different physical problems which are mathematically very similar. One problem is classical and involves an octahedral arrangement of six vibrating masses constrained to slide on coordinate axes  $\{\pm x, \pm y, \pm z\}$ , as shown in Figure 4.3.1(a). The other problem is quantum mechanical and involves a particle which spends most of its time in any of the six potential valleys centered around the  $\{\pm x, \pm y, \pm z\}$  axes in Figure 4.3.1(b). The figure shows a plot of the potential versus angular direction with high-potential directions indicated by mountains and low ones by valleys. In Chapters 5–7 we will study such angular potentials in greater detail, but for now a qualitative picture of one example is all that is needed.

In either problem there will be six base states  $\{|1\rangle, |2\rangle, \dots, |6\rangle\}$ . In the spring-mass problem ket  $|j\rangle$  means mass  $j$  is stretched one unit outward from its equilibrium position, while the other masses are fixed at their respective equilibrium or resting points. In the quantum-mechanical problem ket  $|j\rangle$  stands for a state for which the probability of finding the particle in the  $j$ th valley is unity. In other words, the wave function

$$\langle \theta \phi | j \rangle = \psi_j(\theta \phi) \tag{4.3.1}$$

of the  $j$ th base state is localized around the polar angles of the  $j$ th axis or valley in Figure 4.3.1(b).

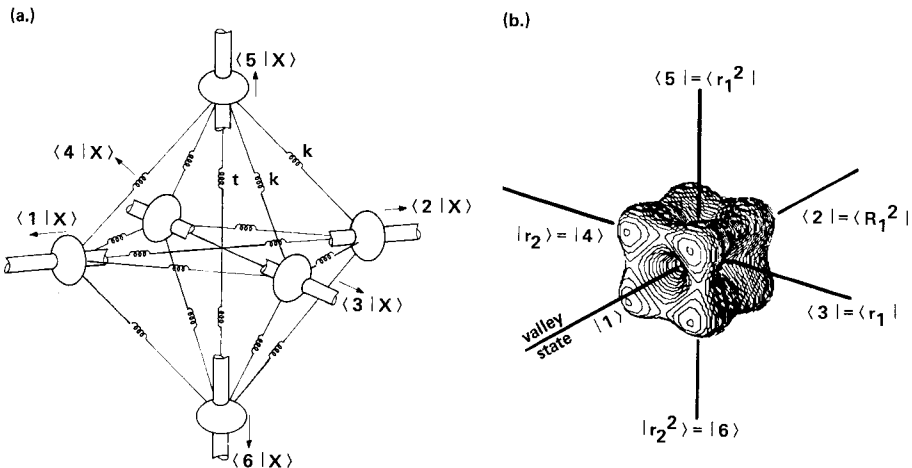


**Figure 4.3.1** Examples of physical systems with octahedral symmetry. (a) Coupled oscillating beads sliding on octahedral axes are described by six classical coordinates  $x_j = \langle j | x \rangle$ . (b) A six-state quantum system could describe a particle capable of tunneling between six equivalent potential valleys.

Either problem involves eigensolutions of matrices which have virtually the same form. The spring-mass problem involves an acceleration matrix:

$$- \begin{pmatrix} \langle 1|\mathbf{a}|1\rangle & \langle 1|\mathbf{a}|2\rangle & \cdots & \langle 1|\mathbf{a}|6\rangle \\ \langle 2|\mathbf{a}|1\rangle & \langle 2|\mathbf{a}|2\rangle & \cdots & \langle 2|\mathbf{a}|6\rangle \\ \cdot & & & \\ \cdot & & & \\ \cdot & & & \\ \langle 6|\mathbf{a}|1\rangle & \langle 6|\mathbf{a}|2\rangle & \cdots & \langle y|\mathbf{a}|6\rangle \end{pmatrix} = \begin{pmatrix} h & t & s & s & s & s \\ t & h & s & s & s & s \\ s & s & h & t & s & s \\ s & s & t & h & s & s \\ s & s & s & s & h & t \\ s & s & s & s & t & h \end{pmatrix}, \quad (4.3.2a)$$

where components

$$\begin{aligned} h &= 2k + t, \\ s &= k/2 \end{aligned} \quad (4.3.2b)$$

are related to spring constants  $k$  and  $t$  of nearest- and next-nearest-neighbor connections, respectively, in Figure 4.3.1(a). The quantum problem involves a Hamiltonian matrix:

$$\begin{pmatrix} \langle 1|\mathbf{H}|1\rangle & \langle 1|\mathbf{H}|2\rangle & \cdots & \langle 1|\mathbf{H}|6\rangle \\ \langle 2|\mathbf{H}|1\rangle & \langle 2|\mathbf{H}|2\rangle & \cdots & \langle 2|\mathbf{H}|6\rangle \\ \cdot & & & \cdot \\ \cdot & & & \cdot \\ \cdot & & & \cdot \\ \langle 6|\mathbf{H}|1\rangle & \langle 6|\mathbf{H}|2\rangle & \cdots & \langle 6|\mathbf{H}|6\rangle \end{pmatrix} = \begin{pmatrix} H & T & S & S & S & S \\ T & H & S & S & S & S \\ S & S & H & T & S & S \\ S & S & T & H & S & S \\ S & S & S & S & H & T \\ S & S & S & S & T & H \end{pmatrix}. \quad (4.3.3)$$

The diagonal components are the energy-expectation values  $H$  of the localized wave functions (4.3.1). The off-diagonal components  $S$  and  $T$  are tunneling amplitudes between nearest- and next-nearest-neighboring valleys, respectively, in Figure 4.3.1(b).

Instead of labeling the bases  $\{|1\rangle, |2\rangle, \dots, |6\rangle\}$  with numbers, let us use octahedral group operators. Let each state be labeled as follows:

$$|g\rangle = g|1\rangle, \quad (4.3.4)$$

by the operation  $g$  which converts the first state,

$$|1\rangle = \mathbf{1}|1\rangle, \quad (4.3.5)$$

into the  $g$ th state  $|g\rangle$ . This group labeling scheme has been used in Chapters 2 and 3. However, now there are four times as many octahedral operations as



there are base vectors. Indeed, the first state  $|1\rangle$  of the spring-mass problem could be labeled by  $R_3$ ,  $R_3^2$ , and  $R_3^3$  as well as by  $\mathbf{1}$ . State  $|1\rangle$  is unchanged by 3-axis rotations, since it is just a displacement along this axis:

$$|1\rangle = \mathbf{1}|1\rangle = R_3|1\rangle = R_3^2|1\rangle = R_3^3|1\rangle. \tag{4.3.6}$$

In other words the first spring-mass state  $|1\rangle$  is invariant to its local  $C_4 = \{1, R_3, R_3^2, R_3^3\}$  axial subgroup. Let us rewrite this using the invariant  $C_4$  idempotent,

$$P^A \equiv P^{0_4} = (\mathbf{1} + R_3 + R_3^2 + R_3^3)/4,$$

as follows:

$$|1\rangle = P^{0_4}|1\rangle = (\mathbf{1} + R_3 + R_3^2 + R_3^3)|1\rangle/4. \tag{4.3.7}$$

The relations (4.3.6) or (4.3.7) will be called **LOCAL SYMMETRY CONDITIONS** of  $|1\rangle$ . They imply that each of the other states  $|g\rangle = g|1\rangle$  could be labeled

$$\begin{aligned} |g\rangle &= g|1\rangle = gR_3|1\rangle = gR_3^2|1\rangle = gR_3^3|1\rangle, \\ |g\rangle &= |gR_3\rangle = |gR_3^2\rangle = |gR_3^3\rangle, \end{aligned} \tag{4.3.8}$$

i.e., by any element  $gR_3^h$  in the  $g$ th coset  $gC_4$  of the local subgroup.

In Figure 4.3.1(a) we have chosen one element  $g$  from each coset:

$$\begin{aligned} R_1^2(\mathbf{1}, R_3, R_3^2, R_3^3) &= (R_1^2, i_4, R_2^2, i_3), \\ r_1(\mathbf{1}, R_3, R_3^2, R_3^3) &= (r_1, i_1, r_4, R_2), \\ r_2(\mathbf{1}, R_3, R_3^2, R_3^3) &= (r_2, i_2, r_3, R_2^3), \\ r_1^2(\mathbf{1}, R_3, R_3^2, R_3^3) &= (r_1^2, R_1^3, r_3^2, i_6), \\ r_2^2(\mathbf{1}, R_3, R_3^2, R_3^3) &= (r_2^2, R_1, r_4^2, i_5), \end{aligned} \tag{4.3.9}$$

of  $C_4 = \{\mathbf{1}, R_3, R_3^2, R_3^3\}$  to label the base states

$$\{|1\rangle = |1\rangle, |2\rangle = |R_1^2\rangle, |3\rangle = |r_1\rangle, |4\rangle = |r_2\rangle, |5\rangle = |r_1^2\rangle, |6\rangle = |r_2^2\rangle\}. \tag{4.3.10}$$

Furthermore, let us suppose that the base states of the quantum problem satisfy the  $0_4$  local symmetry conditions as well. Then they can be labeled just like the classical bases as indicated in Figure 4.3.1(b). Imposing these conditions implies that the wave functions (4.3.1) in the valleys have the fourfold ( $0_4$ ) symmetry of their locality. Later on we shall consider wave functions having other types of local symmetry.

Vectors (4.3.10) which satisfy  $0_4$  local symmetry conditions are the basis of what is called an INDUCED REPRESENTATION  $\mathcal{F} = D^{0_4} \uparrow O$  of octahedral group  $O$  induced by irrep  $D^{0_4}$  of subgroup  $C_4$ . Let us construct the induced representation of octahedral rotation  $i_4$ , for example. Operation on bases (4.3.10) gives

$$\begin{aligned}
 i_4|1\rangle &= i_4|1\rangle, & i_4|2\rangle &= i_4R_1^2|1\rangle, & i_4|3\rangle &= i_4r_1|1\rangle, & i_4|4\rangle &= i_4r_2|1\rangle, & i_4|5\rangle &= i_4r_1^2|1\rangle, & i_4|6\rangle &= i_4r_2^2|1\rangle, \\
 &= R_1^2|1\rangle, & &= R_3^3|1\rangle, & &= i_5|1\rangle, & &= i_6|1\rangle, & &= i_2|1\rangle, & &= i_1|1\rangle, \\
 &= |2\rangle, & &= |1\rangle, & &= |6\rangle, & &= |5\rangle, & &= |4\rangle, & &= |3\rangle,
 \end{aligned}
 \tag{4.3.11}$$

where the octahedral multiplication nomogram, Eqs. (4.3.9) and (4.3.8), were used in turn. Expressing these results in matrix form gives

$$\begin{aligned}
 \mathcal{F}^{0_4 \uparrow 0}(i_4) &= \begin{pmatrix} \langle 1|i_4|1\rangle & \langle 1|i_4|2\rangle & \cdots & \langle 1|i_4|6\rangle \\ \langle 2|i_4|1\rangle & \langle 2|i_4|2\rangle & & \cdot \\ \cdot & & & \cdot \\ \cdot & & & \cdot \\ \cdot & & & \cdot \\ \langle 6|i_4|1\rangle & \langle 6|i_4|2\rangle & \cdots & \langle 6|i_4|6\rangle \end{pmatrix} \\
 &= \begin{pmatrix} \cdot & 1 & \cdot & \cdot & \cdot & \cdot \\ 1 & \cdot & \cdot & \cdot & \cdot & \cdot \\ \cdot & \cdot & \cdot & \cdot & \cdot & 1 \\ \cdot & \cdot & \cdot & \cdot & 1 & \cdot \\ \cdot & \cdot & \cdot & 1 & \cdot & \cdot \\ \cdot & \cdot & 1 & \cdot & \cdot & \cdot \end{pmatrix}.
 \end{aligned}
 \tag{4.3.12}$$

Note that the transformed base states  $\{g|1\rangle, g|2\rangle, \dots\}$  such as (4.3.11), can be derived more quickly simply by inspecting Figure 4.3.1 and using Figure 4.1.2, which defines octahedral  $g$ . The  $0_4 \uparrow O$  induced representations will be reduced now to solve the problems diagrammed in Figure 4.3.1. Later on we will discuss other kinds of induced representations.

## B. Model Solving and Induced Representation Reduction

The Newton equations of motion for the classical spring-mass problem are second-order differential equations

$$m \frac{\partial^2}{\partial t^2} |x\rangle = \mathbf{a}|x\rangle,$$

or

$$m \frac{\partial^2 \langle j|x\rangle}{\partial t^2} = \sum_k \langle j|\mathbf{a}|k\rangle \langle k|x\rangle, \tag{4.3.13}$$

coupled by the acceleration matrix (4.3.2). The Schrödinger equations of the quantum problem are first-order differential equations,

$$i\hbar \frac{\partial}{\partial t} |\psi\rangle = \mathbf{H} |\psi\rangle$$

or

$$i\hbar \frac{\partial \langle j|\psi\rangle}{\partial t} = \sum_k \langle j|\mathbf{H}|k\rangle \langle k|\psi\rangle, \tag{4.3.14}$$

coupled by the Hamiltonian matrix (4.3.3). However, either set of equations becomes decoupled if one first solves time-independent eigenvalue equations,

$$\mathbf{a} |e_j\rangle = \alpha_j |e_j\rangle, \tag{4.3.15}$$

for the spring-mass problem and Schrödinger's equation,

$$\mathbf{H} |e_j\rangle = E_j |e_j\rangle, \tag{4.3.16}$$

for the quantum problem. In either problem the eigenvalues determine the energy spectrum. The quantum eigenvalues,

$$E_j = \hbar \omega_j, \tag{4.3.17}$$

are proportional to the spectral frequencies of the quantum system. The square roots

$$(\alpha_j/m)^{1/2} = \omega_j, \tag{4.3.18}$$

of the classical eigenvalues give the resonant frequencies of the spring-mass system.

The eigenvectors  $|e_j\rangle$  can be obtained for either octahedral problem by applying the octahedral elementary  $P$  operators to the first ket  $|1\rangle$ ,

$$|e_j^\alpha\rangle = P_{jk}^\alpha |1\rangle / (N_k^\alpha)^{1/2}, \tag{4.3.19a}$$

where normalization factor  $N_k^\alpha$  is chosen so that

$$\langle e_j^\alpha | e_j^\alpha \rangle = 1,$$

or

$$N_k^\alpha = \langle 1 | P_{jk}^{\alpha\dagger} P_{jk}^\alpha | 1 \rangle = \langle 1 | P_{kk}^\alpha | 1 \rangle. \tag{4.3.19b}$$

There are 24 octahedral  $P$  operators, but only six  $|e_j^\alpha\rangle$  states are possible. One needs a way to tell beforehand whether a projected state  $P_{jk}^\alpha |1\rangle$  is going to have a nonzero norm  $N_k^\alpha$ .

The key is to use only those  $P_{jk}^\alpha$  whose right-hand "bodyguards"  $P_k^\alpha$  are compatible with the state  $|1\rangle$ . Since the state  $|1\rangle$  has local  $C_4$  symmetry condition (4.3.7) of type  $0_4$ , only those  $C_4$ -defined  $P_k^\alpha$  with  $k = 0_4$  are

compatible. Among the  $C_4$ -defined subgroup labels in Eqs. (4.2.37)–(4.2.41), the  $k = 0_4$  label appears under three different octahedral irrep labels, namely,  $\alpha = A_1$ ,  $E$ , and  $T_1$ . For  $\alpha = A_1$  and  $k = 0_4 = j$  [Eq. (4.2.41)] there is one eigenstate,

$$\begin{aligned} |e_{0_4}^{A_1}\rangle &= P_{0_4}^{A_1}|1\rangle/(N^{A_1})^{1/2} \\ &= \frac{1}{24} \sum_g \mathcal{D}^{A_1^*}(g)g|1\rangle/(N^{A_1})^{1/2} \\ &= (|1\rangle + |2\rangle + |3\rangle + |4\rangle + |5\rangle + |6\rangle)/(6)^{1/2}. \end{aligned} \quad (4.3.20)$$

The formula (3.4.19) for  $P^\alpha$  and the irreps  $\mathcal{D}^{A_1}(g) \equiv 1$  from the octahedral characters (4.1.11) are used. For  $\alpha = E$  and  $k = 0_4$  [Eq. (4.2.39)] there is an eigenstate for each value of  $j = 0_4$  and  $2_4$ . For  $j = 0_4$  we have

$$\begin{aligned} |e_{0_4}^E\rangle &= P_{0_4 0_4}^E|1\rangle/(N^E)^{1/2} \\ &= \frac{2}{24} \sum_g \mathcal{D}_{0_4 0_4}^{E^*}(g)g|1\rangle/(N^E)^{1/2} \\ &= \frac{2}{24} \left[ (1 + R_3 + R_3^2 + R_3^3) + (R_1^2 + i_4 + R_2^2 + i_3) \right. \\ &\quad \left. - \frac{1}{2}(r_1 + i_1 + r_4 + R_2) - \frac{1}{2}(r_2 + i_2 + r_3 + R_2^3) \right. \\ &\quad \left. - \frac{1}{2}(r_1^2 + R_1^3 + r_3^2 + i_6) - \frac{1}{2}(r_2^2 + R_1 + r_4^2 + i_5) \right] |1\rangle/(N^E)^{1/2}, \end{aligned} \quad (4.3.21)$$

where formula (3.4.19) is used again, this time with the  $\mathcal{D}^E$  irrep (4.2.19). (Recall that tetragonal standing- and moving-wave  $E$  irreps are the same.) The  $g$  sum is collected into the six  $C_4$  cosets which label the bases  $\{|1\rangle, |2\rangle, \dots, |6\rangle\}$ . Thus we have

$$|e_{0_4}^E\rangle = (2|1\rangle + 2|2\rangle - |3\rangle - |4\rangle - |5\rangle - |6\rangle)/(2\sqrt{3}). \quad (4.3.22)$$

The second  $E$  partner with  $j = 2_4$  is given:

$$\begin{aligned} |e_{2_4}^E\rangle &= P_{2_4 0_4}^E|1\rangle/(N^E)^{1/2} \\ &= \frac{2}{24} \sum_g \mathcal{D}_{2_4 0_4}^{E^*}(g)g|1\rangle/(N^E)^{1/2} \\ &= \frac{2}{24} \left[ \frac{\sqrt{3}}{2}(r_1 + i_1 + r_4 + R_2) + \frac{\sqrt{3}}{2}(r_2 + i_2 + r_3 + R_2^3) \right. \\ &\quad \left. - \frac{\sqrt{3}}{2}(r_1^2 + R_1^3 + r_3^2 + i_6) - \frac{\sqrt{3}}{2}(r_2^2 + R_1 + r_4^2 + i_5) \right] |1\rangle/(N^E)^{1/2}, \\ |e_{2_4}^E\rangle &= (|3\rangle + |4\rangle - |5\rangle - |6\rangle)/2. \end{aligned} \quad (4.3.23)$$

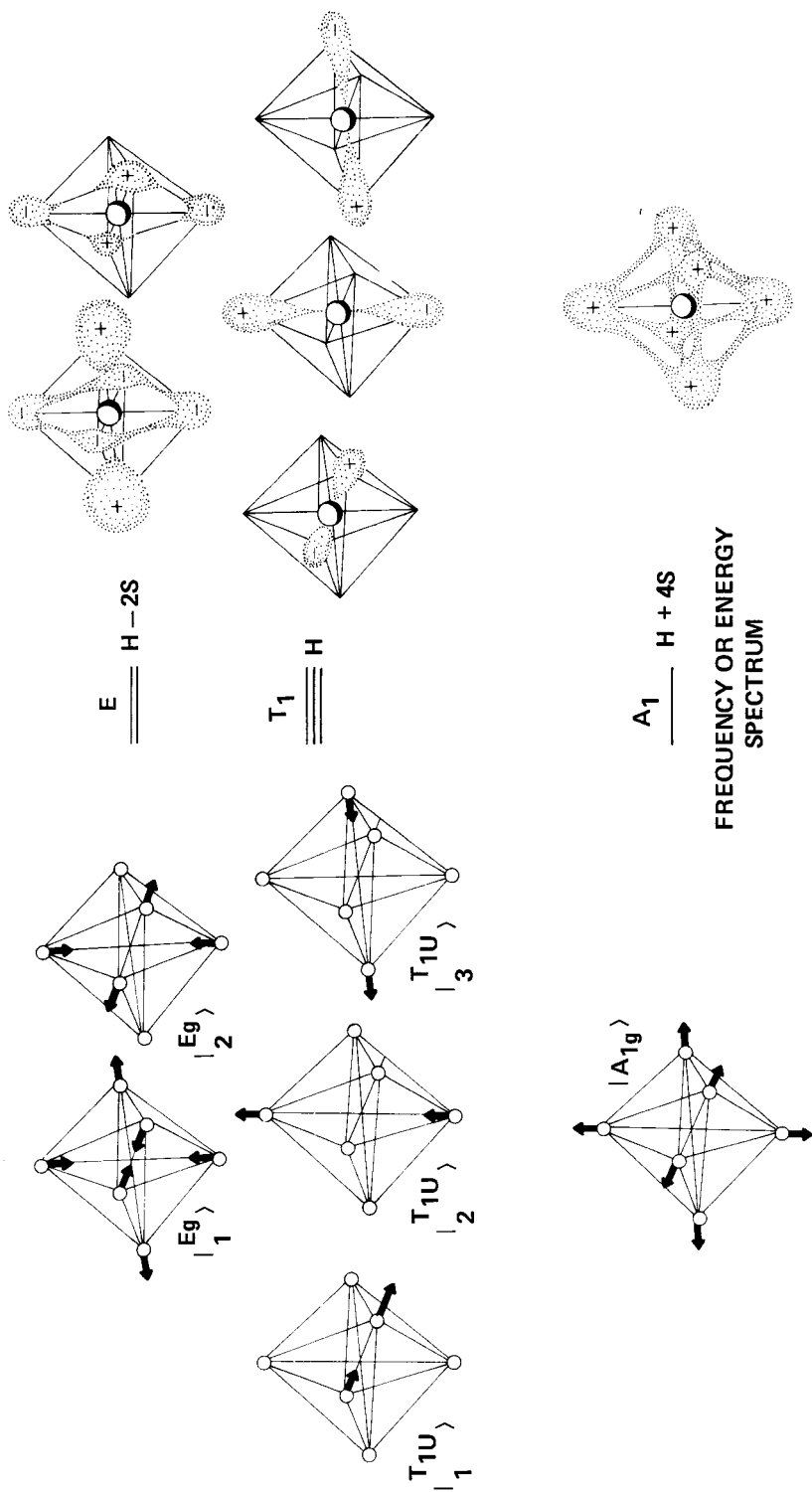


**Figure 4.3.2** Eigensolutions for octahedral systems. (a) Normal vibration modes for classical system. (b) Eigenwaves for quantum system. (Note that tunneling amplitude is negative:  $S < 0$ .)

Finally, for  $\alpha = T_1$  and  $k = 0_4$  [Eq. (4.2.37)], there are three more eigenstates, one for each value of  $j = 1_4, 3_4$ , and  $0_4$ . Putting these together with the  $A_1$  and  $E$  eigenvectors gives all six eigensolutions for the octahedral problems. Sketches of the quantum eigenwaves are given in Figure 4.3.2(b). [The corresponding classical vibration modes are shown in Figure 4.3.2(a).] The  $T_1$  solution for  $j = 1_4$  is

$$\begin{aligned} |e_{1_4}^{T_1}\rangle &= P_{1_4 0_4}^{T_1} |1\rangle / (N^{T_1})^{1/2} \\ &= \frac{3}{24} \sum_g \mathcal{D}_{1_4 0_4}^{T_1*}(g) g |1\rangle / (N^{T_1})^{1/2} \\ &= \frac{3}{24} \left[ -\frac{1}{\sqrt{2}}(r_1 + i_1 + r_4 + R_2) + \frac{1}{\sqrt{2}}(r_2 + i_2 + r_3 + R_3^3) \right. \\ &\quad \left. - \frac{i}{\sqrt{2}}(r_1^2 + R_1^3 + r_3^2 + i_6) + \frac{i}{\sqrt{2}}(r_2^2 + R_1 + r_4^2 + i_5) \right] |1\rangle / (N^{T_1})^{1/2}, \\ |e_{1_4}^{T_1}\rangle &= (-|3\rangle + |4\rangle - i|5\rangle + i|6\rangle)/2. \end{aligned} \quad (4.3.24)$$

The tetragonal moving-wave irreps (4.2.35) were used. Similarly, the other  $T_1$  partners with  $j = 3_4$  and  $0_4$  are found:

$$|e_{3_4}^{T_1}\rangle = (|3\rangle - |4\rangle - i|5\rangle + i|6\rangle)/2, \quad (4.3.25)$$

$$|e_{0_4}^{T_1}\rangle = (|1\rangle - |2\rangle)/\sqrt{2}. \quad (4.3.26)$$

The  $T_1$ -type eigenfunctions sketched in Figure 4.3.2 are the real standing-wave partners,

$$|e_x^{T_1}\rangle = (-|e_{1_4}^{T_1}\rangle + |e_{3_4}^{T_1}\rangle)/\sqrt{2} = (|3\rangle - |4\rangle)/\sqrt{2}, \quad (4.3.27a)$$

$$|e_y^{T_1}\rangle = i(|e_{1_4}^{T_1}\rangle + |e_{3_4}^{T_1}\rangle)/\sqrt{2} = (|5\rangle - |6\rangle)/\sqrt{2}, \quad (4.3.27b)$$

$$|e_z^{T_1}\rangle = |e_{0_4}^{T_1}\rangle = (|1\rangle - |2\rangle)/\sqrt{2}, \quad (4.3.27c)$$

obtained through the transformation (4.2.36).

It is easy to verify that the vectors (4.3.20)–(4.3.27) are all eigenvectors of the Hamiltonian matrix (4.3.3). The energy spectrum,

$$\begin{aligned} E^{A_1} &= H + T + 4S, \\ E^{T_1} &= H - T, \\ E^E &= H + T - 2S, \end{aligned} \quad (4.3.28)$$

is indicated by singlet ( $A_1$ ), triplet ( $T_1$ ), and doublet ( $E$ ) levels next to the wave functions in Figure 4.3.2. For negligible transaxial tunneling ( $T \sim 0$ ) the

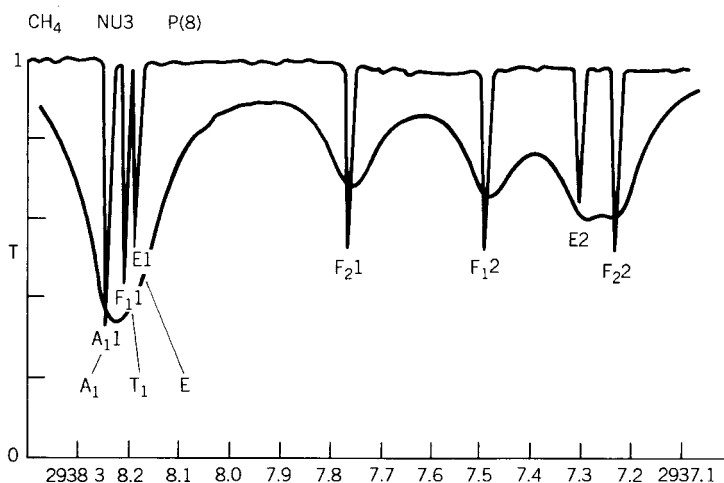


**Figure 4.3.3** Evidence of an  $(A_1T_1E)$  spectral cluster in methane laser spectra. (Courtesy of Dr. Allan Pine, MIT Lincoln Laboratories, from *Journal of Optical Society of America* **66**, 97 (1976)). The ordering and approximate spacing of the  $A_1T_1$  and  $E$  lines is consistent with that of Figure 4.3.2.

$|E^{T_1} - E^{A_1}|$  difference becomes twice the  $|E^E - E^{T_1}|$  difference. This two-to-one splitting is being observed repeatedly in laser spectra of tetrahedral and octahedral molecules. One of the first resolved  $(A_1T_1E)$  “clusters” is shown in part of Allen Pine’s methane spectrum in Figure 4.3.3. (The line intensities actually correspond to nuclear spin and inversion degeneracy and *not* to the octahedral degeneracies.)

Notice that the  $E$  and  $A_1$  wave functions in Figure 4.3.2 have even inversion parity, i.e., they belong to  $E_g$  and  $A_{1g}$  irreps of  $O_h$ . The  $T_1$  wave functions have odd parity and are therefore  $T_{1u}$ -type bases for  $O_h$ . The mathematical significance of the  $(A_{1g}, T_{1u}, E_g)$  combination will be explained in the following section.

### C. Frobenius Reciprocity Theorem and Factored $P$ Operators

It is important to understand the role of subgroup correlation here. The  $A_1$ ,  $T_1$ , and  $E$  octahedral states were the only ones correlated with an  $0_4$  substate. They are therefore the only octahedral irreps to appear in the  $0_4$  column of the  $C_4$  subgroup correlation table (4.2.42b). This is the necessary and sufficient condition that  $A_1$ ,  $T_1$ , and  $E$  should appear in the reduction of  $0_4 \uparrow O$ . We now shall prove that, in general, the  $\alpha$ th column of a  $G \supset H$  correlation table will contain the frequencies  $f^\alpha (D^\alpha \uparrow G)$  of  $G$  irreps  $\mathcal{D}^\alpha$  in an induced representation  $D^\alpha \uparrow G$ . By definition, the  $\alpha$ th row contains the frequencies  $f^\alpha (\mathcal{D}^\alpha \downarrow H)$  of  $H$  irreps  $D^\alpha$  in a subduced representation

$\mathcal{D}^\alpha \downarrow H$ . The beautiful relation

$$f^\alpha(D^a \uparrow G) = f^\alpha(\mathcal{D}^\alpha \downarrow H) \quad (4.3.29)$$

is called the FROBENIUS RECIPROCITY THEOREM. It is easy to understand and prove this theorem using correlated  $P$  operators by generalizing the  $0_4 \uparrow O$  example in the preceding section.

Suppose a base state  $|1\rangle$  satisfies a local symmetry condition,

$$|1\rangle = P^a|1\rangle, \quad (4.3.30a)$$

where

$$P^a = (1/{}^oH) \sum_h D^{a^*}(h)h \quad (4.3.30b)$$

is an irrep projector of subgroup  $H = \{1, h, h', \dots\} \subset G$  for which

$$hP^a = D^a(h)P^a \quad (4.3.31)$$

for all  $h$  in  $H$ . Combining this with condition (4.3.30a) gives

$$h|1\rangle = D^a(h)|1\rangle. \quad (4.3.32)$$

For example, let us consider a local moving-wave state  $|1\rangle$  which satisfies an  $H = C_4$  condition

$$|1\rangle = P^{1_4}|1\rangle, \quad (4.3.30a)_x$$

where

$$P^{1_4} = \frac{1}{4}(1 + iR_3 - R_3^2 - iR_3^3) \quad (4.3.30b)_x$$

and

$$R_3|1\rangle = -i|1\rangle. \quad (4.3.32)_x$$

The sample equations are generalizations of Eqs. (4.3.6) and (4.3.7).

For each coset  $l_2H = \{l_2, l_2h, l_2h', \dots\}, l_3H, \dots$  of subgroup  $H$  let there be one more orthogonal states  $|m\rangle = l_m|1\rangle$ . The  ${}^oG/{}^oH$  orthonormal states

$$\{D^a \uparrow G\} = \{|1\rangle, |2\rangle = l_2|1\rangle, |3\rangle = l_3|1\rangle, \dots, l_{oG/oH}|1\rangle\} \quad (4.3.33)$$

are a basis for the induced representation  $D^a \uparrow G$  of “supergroup”  $G =$



$\{1, g, \dots\}$ . The induced representation is defined by

$$\mathcal{S}_{ij}^{a \uparrow G} = \langle i | g | j \rangle = \begin{cases} D^a(l_i^{-1} g l_j), & \text{if } l_i^{-1} g l_j \text{ is in } H, \\ 0, & \text{if not} \end{cases} \quad (4.3.34)$$

For example, the  $1_4 \uparrow O$  induced representation of  $i_4$  is

$$\mathcal{S}^{1_4 \uparrow O}(i_4) = \begin{pmatrix} \cdot & i & \cdot & \cdot & \cdot & \cdot \\ -i & \cdot & \cdot & \cdot & \cdot & \cdot \\ \cdot & \cdot & \cdot & \cdot & \cdot & -i \\ \cdot & \cdot & \cdot & \cdot & -i & \cdot \\ \cdot & \cdot & \cdot & i & \cdot & \cdot \\ \cdot & \cdot & i & \cdot & \cdot & \cdot \end{pmatrix}. \quad (4.3.34)_x$$

One chooses one element  $l_j$  from each coset to label the bases of an induced representation. We shall call these chosen elements the COSET LEADERS. The same choices were made in the example above as in Eqs. (4.3.10) and (4.3.11).

To reduce  $\mathcal{S}^{a \uparrow G}$  one uses irreducible idempotents  $P_a^\alpha \equiv P_{aa}^\alpha$  and nilpotents  $P_{ba}^\alpha$  of  $G$ . It is convenient to use the ones which are defined by the subgroup  $H$ , i.e., for which

$$P_k^\alpha P^a = \delta^{ka} P_a^\alpha \quad (4.3.35)$$

for all irreducible idempotents  $P^a$  of  $H$ . Now, suppose irrep  $D^a$  of  $H$  is repeated  $f^a(\mathcal{D}^\alpha \downarrow H)$  times in the subduced irrep  $\mathcal{D}^\alpha \downarrow H$  of  $G$ .

$$\mathcal{D}^\alpha \downarrow H = \mathcal{D}^\alpha(h) = \begin{pmatrix} D^a(h) & & & & \\ & \ddots & & & \\ & & D^a(h) & & \\ & & & \ddots & \\ & & & & D^a(h) & \\ & & & & & \ddots \end{pmatrix}. \quad (4.3.36)$$

Each repeat corresponds to a  $G$  idempotent  $\{P_a^\alpha \cdots P_a^\alpha \cdots\}$  whose  $H$  sublabel is  $(a)$ , that is, a base state correlated with  $(a)$ . These are the only idempotents which will not annihilate  $P^a$  or state  $|1\rangle = P^a|1\rangle$  according to Eq. (4.3.35). Each one gives rise to an orthogonal set of states

$$|{}_{ba}^\alpha\rangle = P_{ba}^\alpha |1\rangle / (N_a^\alpha)^{1/2} = (I^\alpha / G) \sum_g \mathcal{D}_{ba}^{\alpha*}(g) g |1\rangle / (N_a^\alpha)^{1/2}, \quad (4.3.37)$$

and another  $\mathcal{D}^\alpha$  in the reduction of  $\mathcal{S}^{a \uparrow G}$ . If the states  $P_{ba}^\alpha |1\rangle$  exist then there are  $f^a$  repeated  $\mathcal{D}^\alpha$  in  $D^a \uparrow G$  which proves the Frobenius theorem (4.3.29). The norm (4.3.19b) of these states works out to be the following

nonzero value:

$$\begin{aligned}
 N_a^\alpha &= \langle 1 | P_{aa}^\alpha | 1 \rangle = (l^\alpha / {}^\circ G) \sum_g \mathcal{D}_{aa}^{\alpha*}(g) \langle 1 | g | 1 \rangle \\
 &= (l^\alpha / {}^\circ G) \sum_h \mathcal{D}_{aa}^{\alpha*}(h) D^a(h) \\
 &= (l^\alpha / {}^\circ G) \mathcal{D}_{aa}^{\alpha*} \left( \sum_h D^a(h) h \right) \\
 &= (l^\alpha / {}^\circ G) {}^\circ H \mathcal{D}_{aa}^{\alpha*}(P^a), \\
 N_a^\alpha &= l^{\alpha \circ} H / {}^\circ G.
 \end{aligned} \tag{4.3.38}$$

Equation (4.3.32) is used to get the second line, while Eq. (4.3.30b) is used for the fourth line. The fact that  $\mathcal{D}_{aa}^\alpha(P^a) = 1$  follows from the assumed form (4.3.36) of  $\mathcal{D}^\alpha$ . For example, by combining the representations (4.2.35) of  $C_4$  one finds

$$\mathcal{D}^{T_1}(P^{1_4}) = \mathcal{D}^{T_1}(1 + iR_3 - R_3^2 - iR_3^3)/4 = \begin{pmatrix} 1 & 0 & 0 \\ 0 & 0 & 0 \\ 0 & 0 & 0 \end{pmatrix}, \tag{4.3.39}$$

and similarly for  $\mathcal{D}^{T_2}(P^{1_4})$ . From this one concludes that  $\mathcal{F}^{1_4 \uparrow 0}$  can be reduced to

$$\mathcal{F}^\dagger \mathcal{F}^{1_4 \uparrow 0} \mathcal{F} = \begin{pmatrix} \boxed{\mathcal{D}^{T_1}} & \cdot & \cdot \\ \cdot & \cdot & \cdot \\ \cdot & \cdot & \boxed{\mathcal{D}^{T_2}} \end{pmatrix}. \tag{4.3.40}$$

Note that only  $T_1$  and  $T_2$  appear in the  $(1_4)$  column of correlation table (4.2.42b).

The projection operator algebra which leads to this reduction can be simplified. Suppose the sum  $\sum_g$  is replaced by a sum and subsum  $\sum_l \sum_h$  over coset leaders  $\{l_1 \equiv 1, l_2, \dots\}$  and subgroup elements  $\{1, h, \dots\}$ , respectively.

$$P_{jk}^a = (l^\alpha / {}^\circ G) \sum_l \sum_h \mathcal{D}_{jk}^{\alpha*}(lh) lh. \tag{4.3.41}$$

The projection operation can be factored if  $\mathcal{D}^\alpha$  is  $H$ -defined. The fundamental definition (3.3.11) gives

$$\begin{aligned}
 \mathcal{D}_{jk}^\alpha(lh) P_{jk}^\alpha &= P_j^\alpha lh P_k^\alpha \\
 &= D^k(h) P_j^\alpha l P_k^\alpha \\
 &= D^k(h) \mathcal{D}_{jk}^\alpha(l) P_{jk}^\alpha,
 \end{aligned} \tag{4.3.42}$$

where Eqs. (4.3.31) and (4.3.35) were used. Then the projection

$$\begin{aligned}
 P_{jk}^\alpha |1\rangle &= (l^\alpha / {}^\circ G) \sum_l \mathcal{D}_{jk}^{\alpha*}(l) l \left[ \sum_h D^{k*}(h) h |1\rangle \right] \\
 &= (l^\alpha {}^\circ H / {}^\circ G) \sum_l \mathcal{D}_{jk}^{\alpha*}(l) l [P^k |1\rangle]
 \end{aligned}
 \tag{4.3.43}$$

is reduced to a sum just over coset leaders  $l$  if  $P^a |1\rangle = |1\rangle$ .

$$|{}^\alpha_{ja}\rangle = P_{ja}^\alpha |1\rangle / (N_a^\alpha)^{1/2} = (l^\alpha {}^\circ H / {}^\circ G)^{1/2} \sum_l \mathcal{D}_{ja}^{\alpha*}(l) |l\rangle.
 \tag{4.3.44}$$

The normalization formula (4.3.38) has been included in this result.

This coset factorization was observed in the previous examples of Eqs. (4.3.21), (4.3.23), and (4.3.24). It cuts the arithmetic labor down by a factor of  ${}^\circ G / {}^\circ H$ , and allows one to tabulate that many fewer  $\mathcal{D}(g)$  matrices. It also simplifies energy matrix formulas such as

$$\begin{aligned}
 \langle {}^\alpha_{ja} | H | {}^\beta_{kb} \rangle &= \langle 1 | P_{ja}^{\alpha\dagger} \mathbf{H} P_{kb}^\beta | 1 \rangle / (N^\alpha N^\beta)^{1/2} \\
 &= \langle 1 | \mathbf{H} P_{aj}^\alpha P_{kb}^\beta | 1 \rangle / (N^\alpha N^\beta)^{1/2} \\
 &= \delta^{\alpha\beta} \delta_{jk} \langle 1 | \mathbf{H} P_{ab}^\alpha | 1 \rangle / N^\alpha.
 \end{aligned}
 \tag{4.3.45}$$

Here  $G$  symmetry of Hamiltonian  $\mathbf{H}$  was assumed so that  $P_{aj}^\alpha = P_{ja}^{\alpha\dagger}$  could commute through it. The coset factorization formula (4.3.43) reduces the nonzero components to a sum

$$\langle {}^\alpha_{ja} | \mathbf{H} | {}^\alpha_{jb} \rangle = \sum_l \langle 1 | \mathbf{H} | l \rangle \mathcal{D}_{ab}^{\alpha*}(l)
 \tag{4.3.46}$$

just over coset leaders  $\{l_1 \equiv 1, l_2, \dots, l_{oG/oH}\}$ . For example, the energy formulas (4.3.28) can be rederived just from one row of matrix (4.3.3). Given

$$\begin{aligned}
 \langle 1 | \mathbf{H} | l \rangle &= (H, T, S, S, S, S), \\
 l &= (1, R_1^2, r_1, r_2, r_1^2, r_2^2),
 \end{aligned}$$

one has for the  $E$  levels (here  $\mathcal{D}^{E*} = \mathcal{D}^E$  is real)

$$\begin{aligned}
 \langle {}^E_{j_{0_2}} | \mathbf{H} | {}^E_{j_{0_4}} \rangle &= H \mathcal{D}_{0_4 0_4}^E(1) + T \mathcal{D}_{0_4 0_4}^E(R_1^2) \\
 &\quad + S \left( \mathcal{D}_{0_2 0_4}^E(r_1) + \mathcal{D}_{0_4 0_4}^E(r_2) + \mathcal{D}_{0_4 0_4}^E(r_1^2) + \mathcal{D}_{0_4 0_4}^E(r_2^2) \right) \\
 &= H - T + 2S,
 \end{aligned}
 \tag{4.3.46}_x$$

and similarly for the  $T_1$  and  $A_1$  levels.

The  $(A_1 T_1 E)$  induced representation is labeled  $(A_{1g} T_{1u} E_g)$  when  $O_h$  inversion is included. Indeed, the first column of the  $O_h \supset C_{4v}$  correlation table (4.2.46c) gives just these irreps. By extending the local symmetry of state  $|1\rangle$  in Section 4.3.B from  $0_4$  (of  $C_4$ ) to  $A'$  (of  $C_{4v}$ ) one obtains the induced representation

$$D^{A'} \uparrow O_h \sim \mathcal{D}^{A_{1g}} \oplus \mathcal{D}^{T_{1u}} \oplus \mathcal{D}^{E_g}. \quad (4.3.47)$$

By specifying the local  $C_{4v}$  reflection symmetry one predicts the overall  $O_h$  inversion symmetry of the induced wave states in Figure 4.3.2.

The moving-wave irreps  $1_4$  and  $3_4$  of  $C_4$  are part of a subduced  $E$  irrep of  $C_{4v}$ . [Recall Eq. (3.6.10).] The induced representations  $1_4 \uparrow O$  and  $3_4 \uparrow O$  both contribute a  $T_1 + T_2$  pair of  $O$  irreps. Therefore it should not be surprising that  $E \uparrow O_h$  contains two such pairs distinguished by opposite parities. The  $E$  column of (4.2.46c) gives

$$D^E \uparrow O_h \sim \mathcal{D}^{T_{1g}} + \mathcal{D}^{T_{2g}} + \mathcal{D}^{T_{1u}} + \mathcal{D}^{T_{2u}}. \quad (4.3.48)$$

Indeed, the Frobenius theorem applies as well to multiply degenerate representations such as  $D^E$ . A physical example of an  $E \uparrow O_h$  representation will appear in the  $SF_6$  vibration problem in Section 4.4. (It is instructive to rework the analysis of this subsection assuming degenerate  $D^a$ . See Problem 4.3.2.)

## D. Spontaneous or Internal Symmetry Breaking

When all the tunneling coefficients,  $S$  as well as  $T$ , go to zero the  $A_1$ ,  $T_1$ , and  $E$  levels in Figure 4.3.2 collapse into a sixfold degeneracy. Then any combination of the base states are eigenvectors, including each one of the original base states  $\{|1\rangle, |2\rangle, \dots, |6\rangle\}$ . One can then imagine that the system is simply six identical disconnected wells, each with a  $C_4$  or  $C_{4v}$  local symmetry. The meaning of the " $O_h$  connection" is lost, even though the Hamiltonian still really has  $O_h$  symmetry. This is a simple example of spontaneous symmetry breaking. Single  $C_4$  symmetric states like  $|1\rangle$  become "frozen in" within a system that intrinsically has a much higher  $O_h$  symmetry. With this freezing or breakdown comes higher (sixfold) degeneracy corresponding to an induced representation.

More complex examples of spontaneous symmetry breaking include ferromagnetism, order-disorder phase transitions, Jahn-Teller distortions, and many other effects both real and imagined in other areas of physics such as high-energy theory. We shall discuss some of these in detail later. For now let us review a simpler example.

By applying the Frobenius theorem to the  $D_6$  correlations (3.6.27), it is possible to understand better the spontaneous symmetry breaking there. The

columns of the  $D_6 \supset C_2$  correlation table give two kinds of induced representations. The first is

$$D^{0_2} \uparrow D_6 \sim A_1 + E_1 + E_2 + B_1, \quad (4.3.49a)$$

which corresponds to  $C_2$  symmetric waves frozen in twofold symmetric valleys. The second is

$$D^{1_2} \uparrow D_6 \sim B_2 + E_2 + E_1 + A_2, \quad (4.3.49b)$$

which corresponds to  $C_2$  antisymmetric waves frozen in twofold valleys. These waves were sketched in Figure 3.6.5, and it is easy to see how they belong to induced representations. In the absence of communication between valleys each set becomes degenerate. Then wave functions which are stuck in a single valley may be eigensolutions.

One should note that the induced representations  $D^{a_6} \uparrow D_6$  are useful for the opposite extreme in which all valleys disappear. The first and fourth columns of  $D_6 \supset C_6$  correlations (3.6.27a) give

$$\begin{aligned} D^{0_6} \uparrow D_6 &\sim A_1 + A_2, \\ D^{3_6} \uparrow D_6 &\sim B_1 + B_2. \end{aligned} \quad (4.3.50)$$

These are the band-gap degeneracies that occur when the potential is constant. The wave states belonging to  $k_m$  for which  $m = \pm 1 \pmod 6$  and  $m = \pm 2 \pmod 6$  are bases for representations

$$\begin{aligned} D^{1_6} \uparrow D_6 &= E_1, \\ D^{2_6} \uparrow D_6 &= E_2, \end{aligned} \quad (4.3.51)$$

respectively. These are both induced and irreducible representations of  $D_6$ .

Finally, one should observe that the regular representation  $\mathcal{R}$  of group  $G$  (recall definition of  $\mathcal{R}$  vis-à-vis  $G = C_{3_v}$  in Section 3.4) is an induced representation  $D^{0_1}$  (of  $C_1 \uparrow G$  induced by the smallest subgroup  $C_1$ . For example, the octahedral regular representation is

$$\mathcal{R} = D^{0_1} \uparrow O = \mathcal{D}^{A_1} \oplus \mathcal{D}^{A_2} \oplus 2\mathcal{D}^E \oplus 3\mathcal{D}^{T_1} \oplus 3\mathcal{D}^{T_2}.$$

According to the Frobenius theorem the frequency of repetition for each irrep must equal its dimension, since  $C_1$  has only one kind of irrep.

The simplest regular or induced representation is  $D^{0_1} \uparrow C_2$  which was the basis of the ammonia two-state inversion model in Section 2.12. In the absence of tunneling or external field perturbation this basis belongs to a twofold degenerate inversion doublet.

## E. External Symmetry Breaking

Degeneracy of spectra for a physical system may correspond to irreducible representations of its symmetry group or to combinations of irreps induced by subgroup irreps. It is generally possible to split any degenerate or nearly degenerate level by introducing external forces of lower symmetry. The splitting or “level-crossing” effect of an electric field on the ammonia doublet was shown in Figure 2.12.8. Let us now consider some more complex level splitting and crossing using the octahedral states as a basis.

**(a) Electric Quadrupole or  $D_{4h}$  Splitting** Suppose the classical or quantum octahedral systems in Figure 4.3.1 are subjected to a  $D_{4h}$  perturbation as indicated in Figure 4.3.4. This perturbation could be two additional identical springs attached to coordinate states  $|1\rangle$  and  $|2\rangle$  along the  $z$  axis of the classical oscillator. Or it could be a change in the masses of the two particles on the  $z$  axis. For the quantum system let us imagine a quadrupole electric potential  $V_Q V(z^2, x^2 + y^2)$  such as one might find at the center of a homogeneously charged  $x$ - $y$  slab. Later, in Chapters 5–7, the definition of “quadrupolarity” will be made more precise. For now we imagine any field that has  $D_{4h}$  symmetry, i.e.,  $90^\circ$  and  $180^\circ$  rotations around the  $z$  axis as well as “vertical”  $xz$ - or  $yz$ -plane reflections and “horizontal”  $xy$ -plane reflections.

Let the Hamiltonian (4.3.3) be perturbed to the form

$$\langle H + V_Q \rangle = \begin{array}{c} \begin{array}{cccccc} |1\rangle & |2\rangle & |3\rangle & |4\rangle & |5\rangle & |6\rangle \end{array} \\ \hline \begin{pmatrix} H + Q & 0 & S & S & S & S \\ 0 & H + Q & S & S & S & S \\ S & S & H & 0 & S & S \\ S & S & 0 & H & S & S \\ S & S & S & S & H & 0 \\ S & S & S & S & 0 & H \end{pmatrix} \end{array}, \quad (4.3.52)$$

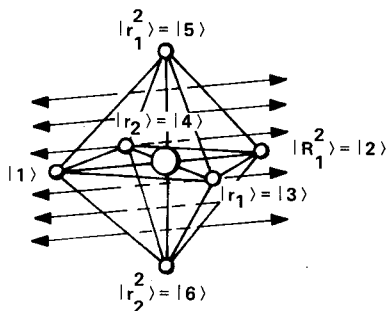


**Figure 4.3.4**  $D_{4h}$  symmetric  $Q$  perturbation of octahedrally symmetric system.

where  $Q$  is the change in energy of potential wells 1 and 2 due to the perturbation. (For simplicity, we assume next-nearest-neighbor tunneling  $T$  is zero.) Let a similar change be made to the acceleration matrix (4.3.2) for the spring-mass problem. More complicated  $D_{4h}$ -symmetric perturbations are possible, but the  $V_Q$  is sufficient for exhibiting the symmetry-breaking effects.

The first task in any symmetry-breaking problem is to see which levels split. According to the  $D_4 \subset O$  correlation (4.2.42a) we have the following for the  $A_1$ ,  $T_1$ , and  $E$  levels in Figure 4.3.2:

$$\mathcal{D}^{A_{1g}} \downarrow D_{4h} = A_{1g}, \quad (4.3.53a)$$

$$\mathcal{D}^{T_{1g}} \downarrow D_{4h} = A_{2u} \oplus E_u, \quad (4.3.53b)$$

$$\mathcal{D}^{E_g} \downarrow D_{4h} = A_{1g} \oplus B_{1g}. \quad (4.3.53c)$$

(Here, the inversion parity subindices  $u$  and  $g$  have been added to label the  $D_{4h} \supset O_h$  correlation completely.) This implies that  $V_Q$  may split the doublet  $E_g$  level into  $A_{1g}$  and  $B_{1g}$  singlets, while the  $T_{1u}$  triplet breaks into an  $A_{2u}$  singlet and a  $E_u$  doublet. Furthermore, there are now two  $D_{4h}$  singlet- $A_{1g}$  levels, one from octahedral  $A_{1g}$  and one from  $E_g$ .

The next task is to find eigenstates and eigenvalues of the new Hamiltonian  $H + V_Q$ . The correlation (4.3.53) implies that four of the six octahedral states are already eigenvectors if they are  $D_{4h}$  defined. Using  $O_h \supset D_{4h} \supset D_{2h}$  chain labels [Section 4.2.A(a)] for these states, it follows that the states (from Figure 4.3.2)

$$\begin{aligned} \left\langle \left\langle \begin{array}{c} T_{1u} \\ [E_u] \\ B_{1u} \end{array} \right\rangle \right\rangle &= \begin{pmatrix} 0 \\ 0 \\ 1/\sqrt{2} \\ -1/\sqrt{2} \\ 0 \\ 0 \end{pmatrix}, & \left\langle \left\langle \begin{array}{c} T_{1u} \\ [E_u] \\ B_{2u} \end{array} \right\rangle \right\rangle &= \begin{pmatrix} 0 \\ 0 \\ 0 \\ 0 \\ 1/\sqrt{2} \\ -1/\sqrt{2} \end{pmatrix}, \\ \left\langle \left\langle \begin{array}{c} T_{1u} \\ [A_{2u}] \\ A_{2u} \end{array} \right\rangle \right\rangle &= \begin{pmatrix} 1/\sqrt{2} \\ -1/\sqrt{2} \\ 0 \\ 0 \\ 0 \\ 0 \end{pmatrix}, & \left\langle \left\langle \begin{array}{c} E_g \\ [B_{1g}] \\ A_{1g} \end{array} \right\rangle \right\rangle &= \begin{pmatrix} 0 \\ 0 \\ 1/2 \\ 1/2 \\ -1/2 \\ -1/2 \end{pmatrix} \end{aligned} \quad (4.3.54)$$

must be eigenvectors of  $H + V_Q$ . This is necessary, since  $H + V_Q$  has  $D_{4h}$  symmetry, and the  $D_{4h} \supset D_{2h}$  labels are all distinct. (Note that the  $D_{4h}$  label is bracketed to indicate the maximal symmetry of  $H + V_Q$ .) On the other

hand, the states

$$\left\langle \left| \begin{array}{c} E_g \\ [A_{1g}] \\ A_{1g} \end{array} \right\rangle \right\rangle = \left( \begin{array}{c} 2 \\ 2 \\ -1 \\ -1 \\ -1 \\ -1 \end{array} \right) / \sqrt{12}, \quad \left\langle \left| \begin{array}{c} A_{1g} \\ [A_{1g}] \\ A_{1g} \end{array} \right\rangle \right\rangle = \left( \begin{array}{c} 1 \\ 1 \\ 1 \\ 1 \\ 1 \\ 1 \end{array} \right) / \sqrt{6} \quad (4.3.55)$$

have the same  $D_{4h}$  labels, and are therefore to be coupled through a  $2 \times 2$ -matrix representation of  $H + V_Q$ .

The representation of  $H + V_Q$  in this basis is easily computed by combining Eqs. (4.3.52), (4.3.54), and (4.3.55),

$$\langle H + V_Q \rangle = \begin{array}{c} \left| \begin{array}{c} T_{1u} \\ [E_u] \\ B_{1u} \end{array} \right\rangle \quad \left| \begin{array}{c} T_{1u} \\ [E_u] \\ B_{2u} \end{array} \right\rangle \quad \left| \begin{array}{c} T_{1u} \\ [A_{2u}] \\ A_{2u} \end{array} \right\rangle \quad \left| \begin{array}{c} A_{1g} \\ [A_{1g}] \\ A_{1g} \end{array} \right\rangle \quad \left| \begin{array}{c} E_g \\ [A_{1g}] \\ A_{1g} \end{array} \right\rangle \quad \left| \begin{array}{c} E_g \\ [B_{1g}] \\ A_{1g} \end{array} \right\rangle \\ \hline \begin{array}{cccccc} H & \cdot & \cdot & \cdot & \cdot & \cdot \\ \cdot & H & \cdot & \cdot & \cdot & \cdot \\ \cdot & \cdot & H + Q & \cdot & \cdot & \cdot \\ \cdot & \cdot & \cdot & H + 4S + Q/3 & \sqrt{2}Q/3 & \cdot \\ \cdot & \cdot & \cdot & \sqrt{2}Q/3 & H - 2S + 2Q/3 & \cdot \\ \cdot & \cdot & \cdot & \cdot & \cdot & H - 2S. \end{array} \end{array} \quad (4.3.56)$$

The eigenvalues of the new matrix are easily found. They are plotted in Figure 4.3.5 as a function of  $Q$  for a fixed negative values of  $S$ . Note the splitting or level shifting of the  $A_{1g}$ ,  $T_{1u}$ , and  $E_g$  levels around  $Q = 0$  in the center of the figure. Sublevels belonging to states

$$\left| \begin{array}{c} T_{1u} \\ 3 \end{array} \right\rangle = \left| \begin{array}{c} T_{1u} \\ [A_{2u}] \end{array} \right\rangle, \quad \left| \begin{array}{c} A_{1g} \\ 1 \end{array} \right\rangle = \left| \begin{array}{c} A_{1g} \\ [A_{1g}] \end{array} \right\rangle, \quad \text{and} \quad \left| \begin{array}{c} E_g \\ 1 \end{array} \right\rangle = \left| \begin{array}{c} E_g \\ [A_{1g}] \end{array} \right\rangle$$

have shifts proportional to  $Q$  for small  $Q$ . These are called FIRST-ORDER energy shifts or splitting. The slopes of the energy-level trajectories are  $1$ ,  $\frac{1}{3}$ , and  $\frac{2}{3}$ , respectively, for these sublevels. The slopes correspond to the diagonal terms  $Q$ ,  $Q/3$ , and  $2Q/3$  in the Hamiltonian matrix (4.3.56).

The  $A_{1g}$  sublevels curve away from each other when  $|Q|$  becomes comparable to  $|S|$ , and the off-diagonal components  $\sqrt{2}Q/3$  take effect. Then the two different  $A_{1g}$ -substates become mixed up in order to be eigenvectors of the  $(2 \times 2)$  submatrix in Eq. (4.3.56). It is instructive to examine the  $A_{1g}$  eigenvectors when  $|Q|$  is much greater than  $|S|$ . Then the  $A_{1g}$  eigenvalue



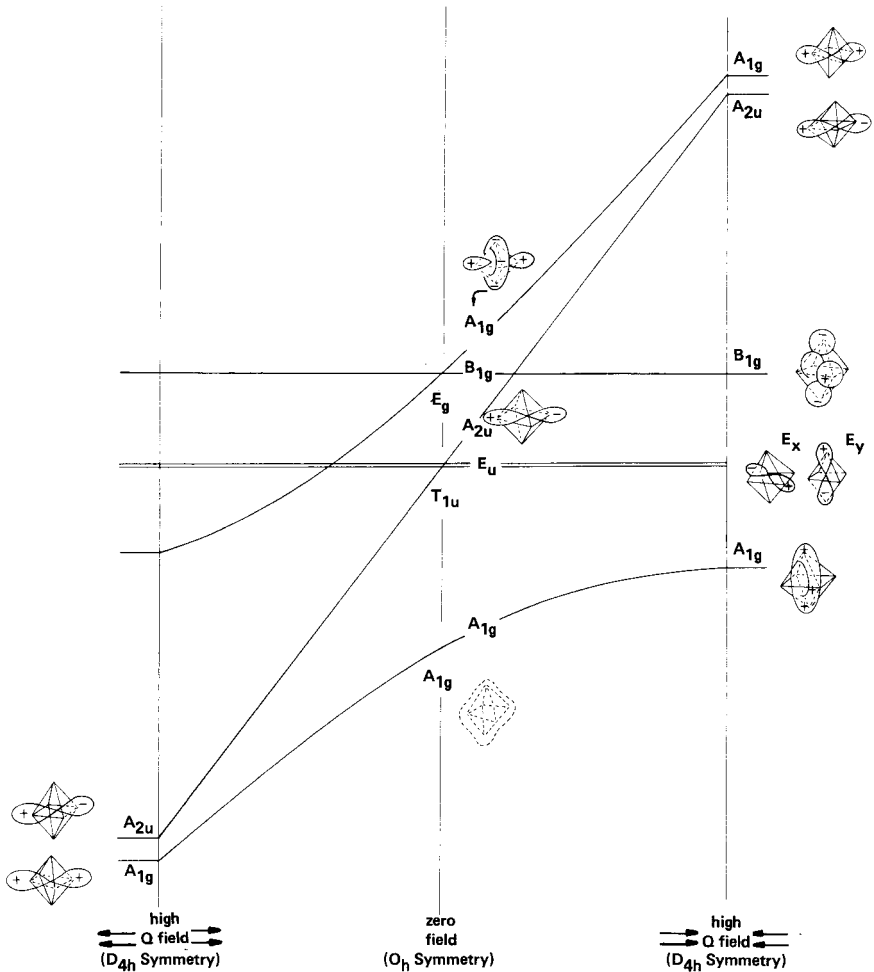


**Figure 4.3.5** Energy-level correlation for  $D_{4h}$   $Q$  perturbation. Eigenvalues and eigenfunctions change as the  $O_h$  symmetry is broken to  $D_{4h}$  by the  $Q$  perturbation.

plots asymptotically approach straight lines, and the eigenvectors are nearly independent of  $Q$ . The  $[A_{1g}]$  eigenvectors of submatrix

$$m = \begin{pmatrix} H + Q/3 & \sqrt{2}Q/3 \\ \sqrt{2}Q/3 & H + 2Q/3 \end{pmatrix} \quad (4.3.57)$$

in Eq. (4.3.56) with  $S \sim 0$  are easily found. The vector belonging to eigen-

value  $H + Q$  is

$$|(H + Q)[A_{1g}]\rangle = \frac{1}{\sqrt{3}} \left| \begin{array}{c} A_{1g} \\ [A_{1g}] \end{array} \right\rangle + \frac{\sqrt{2}}{\sqrt{3}} \left| \begin{array}{c} E_g \\ [A_{1g}] \end{array} \right\rangle, \quad (4.3.58a)$$

which is represented by

$$\frac{1}{\sqrt{3}} \begin{pmatrix} 1 \\ 1 \\ 1 \\ 1 \\ 1 \\ 1 \end{pmatrix} / \sqrt{6} + \frac{\sqrt{2}}{\sqrt{3}} \begin{pmatrix} 2 \\ 2 \\ -1 \\ -1 \\ -1 \\ -1 \end{pmatrix} / \sqrt{12} = \begin{pmatrix} 1 \\ 1 \\ 0 \\ 0 \\ 0 \\ 0 \end{pmatrix} / \sqrt{2} \quad (4.3.58b)$$

in the original  $\{|1\rangle, |2\rangle, \dots, |6\rangle\}$  basis.  $|(H + Q)[A_{1g}]\rangle$  corresponds to a positively phased wave on the two ends ( $|1\rangle$  and  $|2\rangle$ ) of the  $z$  axis as shown in the lower left-hand and upper right-hand sides of Figure 4.3.5. The salient  $[A_{1g}]$  trajectories asymptotically approach the  $A_{2u}$  level as  $|Q|$  grows. The orthogonal  $A_{1g}$  eigenvector whose energy remains close to  $H$  for high  $|Q|$  is

$$|(H)[A_{1g}]\rangle = \frac{\sqrt{2}}{\sqrt{3}} \left| \begin{array}{c} A_{1g} \\ [A_{1g}] \end{array} \right\rangle - \frac{1}{\sqrt{3}} \left| \begin{array}{c} E_g \\ [A_{1g}] \end{array} \right\rangle, \quad (4.3.59a)$$

which is represented by

$$\frac{\sqrt{2}}{\sqrt{3}} \begin{pmatrix} 1 \\ 1 \\ 1 \\ 1 \\ 1 \\ 1 \end{pmatrix} / \sqrt{6} - \frac{1}{\sqrt{3}} \begin{pmatrix} 2 \\ 2 \\ -1 \\ -1 \\ -1 \\ -1 \end{pmatrix} / \sqrt{12} = \begin{pmatrix} 0 \\ 0 \\ 1 \\ 1 \\ 1 \\ 1 \end{pmatrix} / 2. \quad (4.3.59b)$$

The wave function of this  $A_{1g}$  state is confined to the octahedral “equator” ( $|3\rangle, |4\rangle, |5\rangle, \text{ and } |6\rangle$ ) as shown in Figure 4.3.5. Particles residing on the equator are not effected by the  $Q$  perturbation.

It is instructive to transform the  $A_{1g}$  submatrix in Eq. (4.3.56) to the basis [(4.3.58) and (4.3.59)] of high  $|Q|$  eigenstates.

$$\begin{pmatrix} \frac{1}{\sqrt{3}} & \frac{\sqrt{2}}{\sqrt{3}} \\ \frac{\sqrt{2}}{\sqrt{3}} & -\frac{1}{\sqrt{3}} \end{pmatrix} \begin{pmatrix} \frac{H+4S+Q}{3} & \frac{\sqrt{2}Q}{3} \\ \frac{\sqrt{2}Q}{3} & \frac{H-2S+2Q}{3} \end{pmatrix} \begin{pmatrix} \frac{1}{\sqrt{3}} & \frac{\sqrt{2}}{\sqrt{3}} \\ \frac{\sqrt{2}}{\sqrt{3}} & -\frac{1}{\sqrt{3}} \end{pmatrix} = \begin{pmatrix} H+Q & S\sqrt{8} \\ S\sqrt{8} & H+2S \end{pmatrix}. \quad (4.3.60)$$

Then the tunneling amplitude  $S$  appears in the off-diagonal position as well as in the lower diagonal. The lower diagonal  $H + 2S$  gives the expectation value of the  $|(H)[A_{1g}]$  state. The states  $|(H)[A_{1g}]$ ,  $[[E_g]]$ , and  $[[B_{1g}]]$  belong to a  $D_{4h}$  subcluster of eigenvalues  $H + 2S$ ,  $H$ , and  $H - 2S$ , respectively. They all have equatorial wave functions in Figure 4.3.5 and resemble the  $D_4$  molecular orbitals depicted in Figure 2.12.4. Furthermore, the  $\{A_{1g}, A_{2u}\}$  pairs in Figure 4.3.5 are analogous to the inversion doublet discussed in Section 2.12. However, in the limit of high  $Q$  there is no  $A_{1g} - A_{2u}$  splitting as long as next-nearest-neighbor tunneling parameter  $T$  is assumed zero.

Nevertheless, the evolution of  $A_{1g}$  wave functions and energy trajectories with  $Q$  in Figure 4.3.5 is analogous to the avoided crossing discussed in Section 2.12. Here the  $A_{1g}$  waves change continuously from polar waves on one side of the  $Q$  axis to equatorial waves on the other.

**(b) Electric Dipole or  $C_{4v}$  Stark Splitting** Suppose the classical or quantum octahedral systems in Figure 4.3.1 are subjected to a  $C_{4v}$  perturbation as indicated in Figure 4.3.6. This perturbation could be two different  $z$  springs attached to coordinate states  $|1\rangle$  and  $|2\rangle$  of the oscillator. For the quantum system let us imagine a dipolar electric potential  $V_D = V(z, x^2 + y^2)$  such as one might find in a uniform  $E$  field pointing along the  $z$  axis. Such a field has  $C_{4v}$  symmetry, i.e.,  $90^\circ$  and  $180^\circ$  rotations around the  $z$  axis and "vertical"  $x$ - $z$ ,  $y$ - $z$ , and diagonal plane reflections. It no longer has the  $x$ - $y$  plane reflection symmetry which was present in the preceding  $D_{4h}$  example of  $V_Q$ .

Let the Hamiltonian (4.3.3) be perturbed to the form

$$\langle H + V_D \rangle = \begin{array}{c} \begin{array}{cccccc} |1\rangle & |2\rangle & |3\rangle & |4\rangle & |5\rangle & |6\rangle \\ \hline \begin{pmatrix} H - D & 0 & S & S & S & S \\ 0 & H + D & S & S & S & S \\ S & S & H & 0 & S & S \\ S & S & 0 & H & S & S \\ S & S & S & S & H & 0 \\ S & S & S & S & 0 & H \end{pmatrix} \end{array} \end{array}, \quad (4.3.61)$$

where  $D$  is the change in energy of potential wells 1 and 2 due to the electric field. Again, let us ignore the double-tunneling parameter  $T$ .

The level splitting associated with a reduction to  $C_{4v}$  symmetry depends upon the  $O_h \supset C_{4v}$  correlation (4.2.46c). This gives

$$\mathcal{D}^{A_{1g}} \downarrow C_{4v} = A', \quad (4.3.62a)$$

$$\mathcal{D}^{T_{1u}} \downarrow C_{4v} = A' \oplus E, \quad (4.3.62b)$$

$$\mathcal{D}^{E_g} \downarrow C_{4v} = A' \oplus B', \quad (4.3.62c)$$

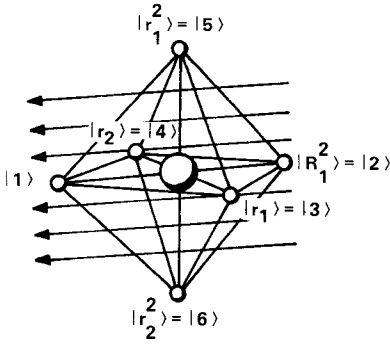


**Figure 4.3.6**  $C_{4v}$  symmetric  $D$  perturbation of octahedrally symmetric system.

which is qualitatively similar to the  $D_{4h}$  splitting (4.3.53). The important difference is that now there are *three* states belonging to the same label  $[A']$  of the  $C_{4v}$  symmetry of the new Hamiltonian. The states

$$\left\langle \begin{matrix} A_{1g} \\ [A'] \\ A' \end{matrix} \right\rangle = \begin{pmatrix} 1 \\ 1 \\ 1 \\ 1 \\ 1 \\ 1 \end{pmatrix} / \sqrt{6}, \quad \left\langle \begin{matrix} E_g \\ [A'] \\ A' \end{matrix} \right\rangle = \begin{pmatrix} 2 \\ 2 \\ -1 \\ -1 \\ -1 \\ -1 \end{pmatrix} / \sqrt{12}, \quad \left\langle \begin{matrix} T_{1u} \\ [A'] \\ A' \end{matrix} \right\rangle = \begin{pmatrix} 1/\sqrt{2} \\ 1/\sqrt{2} \\ 0 \\ 0 \\ 0 \\ 0 \end{pmatrix} \quad (4.3.63)$$

may all be mixed by a general  $C_{4v}$  symmetric perturbation. On the other hand, each of the states

$$\left\langle \begin{matrix} E_g \\ [B'] \\ A' \end{matrix} \right\rangle = \begin{pmatrix} 0 \\ 0 \\ 1/2 \\ 1/2 \\ -1/2 \\ -1/2 \end{pmatrix}, \quad \left\langle \begin{matrix} T_{1u} \\ [E] \\ B' \end{matrix} \right\rangle = \begin{pmatrix} 0 \\ 0 \\ 1/\sqrt{2} \\ -1/\sqrt{2} \\ 0 \\ 0 \end{pmatrix}, \quad \left\langle \begin{matrix} T_{1u} \\ [E] \\ B'' \end{matrix} \right\rangle = \begin{pmatrix} 0 \\ 0 \\ 0 \\ 0 \\ 1/\sqrt{2} \\ -1/\sqrt{2} \end{pmatrix} \quad (4.3.64)$$

is distinguished by one of its  $C_{4v} \supset C_{2v}$  labels, and therefore each one is an eigenstate of  $\langle H + V_D \rangle$ . Note that the same base states are used here as in the preceding  $D_{4h}$  example. Because of inversion commutation the  $D_{4h} \supset D_{2h}$  base states are the same as  $C_{4v} \supset C_{2v} = \{1, R_3^2, IR_2^2, IR_1^2\}$  base states. Therefore, the states [(4.3.54) and (4.3.55)] were simply relabeled by  $C_{4v}$  and  $C_{2v}$  irreps in the preceding equations. The relevant  $C_{2v}$  characters are given by

the following:

$$\begin{array}{c}
 1 \quad R_3^2 \quad IR_2^2 \quad IR_1^2 \\
 \begin{array}{c} A' \\ B' \\ A'' \\ B'' \end{array} \begin{array}{|cccc|} \hline 1 & 1 & 1 & 1 \\ \hline 1 & -1 & 1 & -1 \\ \hline 1 & 1 & -1 & -1 \\ \hline 1 & -1 & -1 & 1 \\ \hline \end{array} \quad (4.3.65)
 \end{array}$$

The representation of  $H + V_D$  in the basis [(4.3.63) and (4.3.64)] is the following:

$$\begin{array}{c}
 \left\langle \begin{array}{c} T_{1u} \\ [E] \\ B' \end{array} \right\rangle \quad \left\langle \begin{array}{c} T_{1u} \\ [E] \\ B'' \end{array} \right\rangle \quad \left\langle \begin{array}{c} T_{1u} \\ [A'] \\ A' \end{array} \right\rangle \quad \left\langle \begin{array}{c} A_{1g} \\ [A'] \\ A' \end{array} \right\rangle \quad \left\langle \begin{array}{c} E_g \\ [A'] \\ A' \end{array} \right\rangle \quad \left\langle \begin{array}{c} E_g \\ [B'] \\ A' \end{array} \right\rangle \\
 \langle H + V_D \rangle = \begin{array}{|cccccc|} \hline H & \cdot & \cdot & \cdot & \cdot & \cdot \\ \cdot & H & \cdot & \cdot & \cdot & \cdot \\ \cdot & \cdot & H & -\frac{D}{\sqrt{3}} & -\frac{\sqrt{2}D}{\sqrt{3}} & \cdot \\ \cdot & \cdot & -\frac{D}{\sqrt{3}} & H - 4S & 0 & \cdot \\ \cdot & \cdot & -\frac{\sqrt{2}D}{\sqrt{3}} & 0 & H - 2S & \cdot \\ \cdot & \cdot & \cdot & \cdot & \cdot & H - 2S \\ \hline \end{array} \quad (4.3.66)
 \end{array}$$

The perturbation  $V_D$  has odd inversion symmetry, since the  $I$  operation reverses any “polar” vectors such as those of a homogeneous electric field:

$$I^\dagger V_D I = I V_D I = -V_D. \quad (4.3.67)$$

Therefore, a matrix component of  $V_D$  between any two states of the same parity must vanish. This includes the component

$$\langle A_{1g} | V_D \left| \begin{array}{c} E_g \\ 1 \end{array} \right\rangle = -\langle A_{1g} | I^\dagger V_D I \left| \begin{array}{c} E_g \\ 1 \end{array} \right\rangle.$$

Since ( $g$ ) denotes inversion symmetry,

$$\left( \langle A_{1g} | I^\dagger = \langle A_{1g} |, I \left| \begin{array}{c} E_g \\ 1 \end{array} \right\rangle = \left| \begin{array}{c} E_g \\ 1 \end{array} \right\rangle \right)$$

the component equals its negative and must therefore be zero:

$$\langle A_{1g} | V_D \begin{matrix} E_g \\ 1 \end{matrix} \rangle = -\langle A_{1g} | V_D \begin{matrix} E_g \\ 1 \end{matrix} \rangle = 0. \quad (4.3.68)$$

The same goes for the diagonal components

$$\langle \begin{matrix} T_{1u} \\ 3 \end{matrix} | V_D \begin{matrix} T_{1u} \\ 3 \end{matrix} \rangle = \langle A_{1g} | V_D | A_{1g} \rangle = \langle \begin{matrix} E_g \\ 1 \end{matrix} | V_D \begin{matrix} E_g \\ 1 \end{matrix} \rangle = 0,$$

which would not otherwise be prohibited by  $C_{4v}$  symmetry. This is quite the opposite of the  $V_Q$  perturbation which has even inversion symmetry and cannot connect any states of different parity.

Elimination of certain matrix components by symmetry analysis belongs to the subject of SELECTION RULES which are to be discussed in Chapters 6 and 7. For now let us see how the absence of  $D$  terms on the diagonal of Hamiltonian (4.3.66) affects the energy levels. In Figure 4.3.7 the Hamiltonian eigenvalues are plotted as a function of  $D$ . Note that for small  $D$  there is little or no splitting of  $T_{1u}$  or  $E_g$ . At  $D = 0$  all energy trajectories have zero slope. The splitting and shifts are said to be SECOND ORDER when diagonal components of a perturbation vanish. The energies do not change until appreciable amounts of different states are mixed to make new eigenstates. The mixing is controlled by the off-diagonal components  $-D/\sqrt{3}$  and  $-2D/\sqrt{3}$  in the Hamiltonian (4.3.66).

As in the preceding  $V_Q$  example it is instructive to study the case in which the perturbation  $V_D$  dominates the Hamiltonian, i.e., the high- $D$  limit. The following transformation diagonalizes the  $D$ -dependent part of the  $[A']$  submatrix.

$$\begin{pmatrix} \frac{1}{\sqrt{2}} & \frac{1}{\sqrt{6}} & \frac{1}{\sqrt{3}} \\ 0 & \frac{2}{\sqrt{6}} & -\frac{1}{\sqrt{3}} \\ -\frac{1}{\sqrt{2}} & \frac{1}{\sqrt{6}} & \frac{1}{\sqrt{3}} \end{pmatrix} \begin{pmatrix} H & -\frac{D}{\sqrt{3}} & -\frac{\sqrt{2}D}{\sqrt{3}} \\ -\frac{D}{\sqrt{3}} & H + 4S & 0 \\ -\frac{\sqrt{2}D}{\sqrt{3}} & 0 & H - 2S \end{pmatrix} \begin{pmatrix} \frac{1}{\sqrt{2}} & 0 & -\frac{1}{\sqrt{2}} \\ \frac{1}{\sqrt{6}} & \frac{2}{\sqrt{6}} & \frac{1}{\sqrt{6}} \\ \frac{1}{\sqrt{3}} & -\frac{1}{\sqrt{3}} & \frac{1}{\sqrt{3}} \end{pmatrix} = \begin{pmatrix} H - D & 2S & 0 \\ 2S & H + 2S & 2S \\ 0 & 2S & H + D \end{pmatrix} \quad (4.3.69)$$

The high- $D$  ground eigenstate of eigenvalue  $(H - D)$  is the original local base state  $|1\rangle$ :

$$|1\rangle = \left( \frac{1}{\sqrt{2}} \right) \begin{matrix} T_{1u} \\ [A'] \\ A' \end{matrix} + \left( \frac{1}{\sqrt{6}} \right) \begin{matrix} A_{1g} \\ [A'] \\ A' \end{matrix} + \left( \frac{1}{\sqrt{3}} \right) \begin{matrix} E_g \\ [A'] \\ A' \end{matrix}. \quad (4.3.70)$$

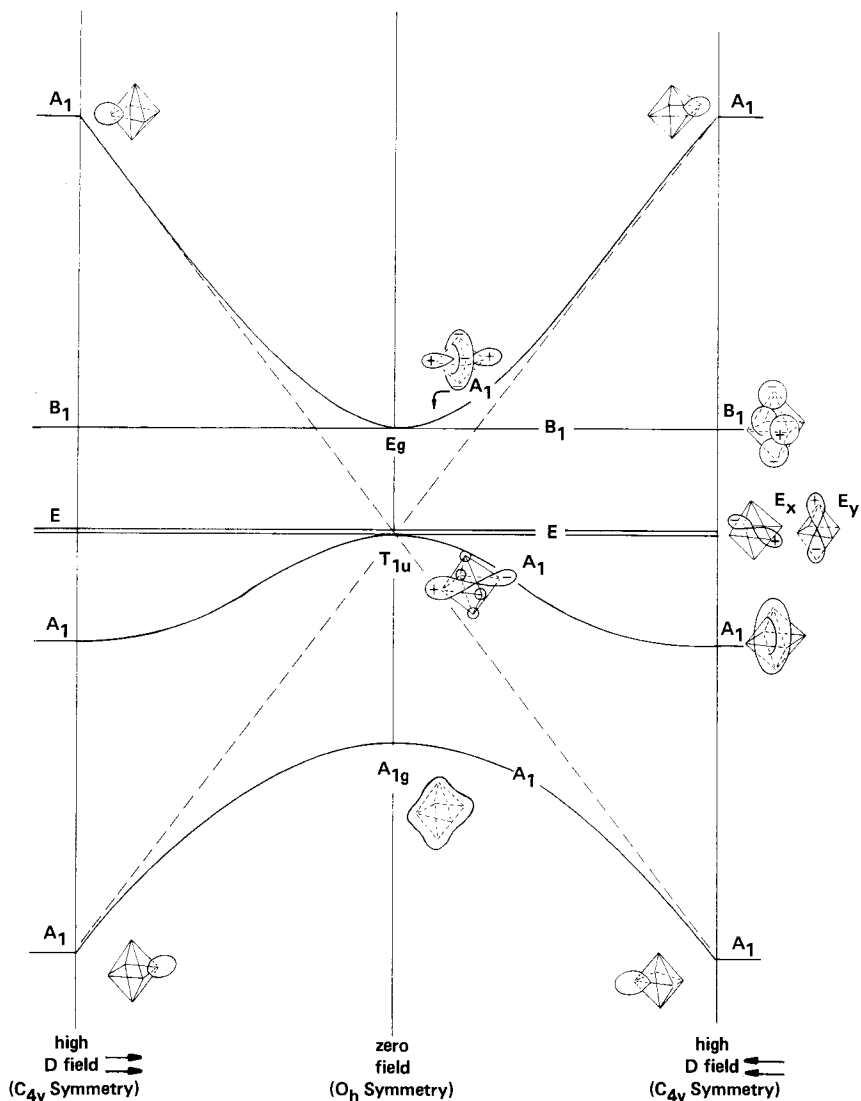


Figure 4.3.7 Energy-level correlation for  $D$  perturbation. Eigenfunction and eigenvalues change as  $O_h$  symmetry is broken to  $C_{4v}$  by the  $D$  field. No first-order splitting (for low  $D$  field) occurs.

This corresponds to a wave function localized on the positive  $z$  axis as shown in the lower right-hand side of Figure 4.3.7. The uppermost eigenfunction on the same side corresponds to the eigenvector

$$|2\rangle = \left(\frac{1}{\sqrt{2}}\right) \begin{vmatrix} T_{1u} \\ [A'] \\ A' \end{vmatrix} + \left(\frac{1}{\sqrt{6}}\right) \begin{vmatrix} A_{1g} \\ [A'] \\ A' \end{vmatrix} + \left(\frac{1}{\sqrt{3}}\right) \begin{vmatrix} E_g \\ [A'] \\ A' \end{vmatrix}, \quad (4.3.71)$$

with eigenvalues  $H + D$ . Of course,  $|1\rangle$  and  $|2\rangle$  switch positions if  $D$  changes sign. The equatorial wave functions belong to the same sort of  $(A, E, B)$  subcluster seen in the preceding example.

The  $[A']$  state,

$$(|3\rangle + |4\rangle + |5\rangle + |6\rangle)/2 = \left(\frac{2}{\sqrt{6}}\right) \begin{vmatrix} A_{1g} \\ [A'] \\ A' \end{vmatrix} - \left(\frac{1}{\sqrt{3}}\right) \begin{vmatrix} E_g \\ [A'] \\ A' \end{vmatrix}, \quad (4.3.72)$$

has energy expectation  $H + 2S$ .

**(c) Magnetic Dipole or  $C_4$  Zeeman Splitting** Suppose a uniform magnetic field is placed along the fourfold  $z$  axis of the octahedral system. Then the symmetry is reduced to the Abelian cyclic group  $C_4$ . A magnetic vector  $\mathbf{B}$  is a pseudovector of axial vector.  $B_z$  is reversed by vertical  $x$ - $z$  or  $y$ - $z$  planar reflections, and so these elements of  $C_{4v}$  are not symmetry operators for magnetic fields. The effects of a uniform magnetic field  $B_z$  are similar to those arising from a uniform rotation about the  $z$  axis, as stated in Larmor's theorem. The symmetry properties of a rotating reference frame are more obvious. It is clear that  $\phi$   $z$  plane reflections reverse the  $z$ -rotational sense of direction and cannot be symmetry operations.

The  $C_4$  correlation table (4.2.42b) tells what can happen to the  $(A_1 T_1 E)$  levels of the  $O_h$  system.

$$\begin{aligned} \mathcal{D}^{A_1} \downarrow C_4 &= O_4, \\ \mathcal{D}^{T_1} \downarrow C_4 &= O_4 \oplus 1_4 \oplus 3_4, \\ \mathcal{D}^E \downarrow C_4 &= O_4 \oplus 2_4. \end{aligned} \quad (4.3.73)$$

According to this all degeneracy is removed. This is called  $C_4$  Zeeman splitting and is analogous to the splitting discussed in Section 3.6.A. Here a  $3 \times 3$  matrix for the  $O_4$  states may have to be diagonalized. Transformations to moving-wave or circularly polarized tetragonal bases are helpful in problems such as these. Physical examples of  $C_4$  splitting will be given in Section 4.4.



**(d) Threefold Axial Perturbations and Basis Changing** Suppose a uniform electric field is placed along the threefold (111) direction or  $r_1$  axis of the octahedral system. Let the Hamiltonian for this field be perturbed to the following form:

$$\langle H + V_d \rangle = \begin{array}{c} \begin{array}{cccccc} |1\rangle & |2\rangle & |3\rangle & |4\rangle & |5\rangle & |6\rangle \\ \hline H-d & 0 & S & S & S & S \\ 0 & H+d & S & S & S & S \\ S & S & H-d & 0 & S & S \\ S & S & 0 & H+d & S & S \\ S & S & S & S & H-d & 0 \\ S & S & S & S & 0 & H+d \end{array} \\ \hline \end{array} \quad (4.3.74)$$

Here the down-field states  $|1\rangle$ ,  $|3\rangle$ , and  $|5\rangle$  have reduced energy expectation values  $(H-d)$ , and the up-field states  $|2\rangle$ ,  $|4\rangle$ , and  $|6\rangle$  have increased values  $(H+d)$ . The symmetry of the Hamiltonian is reduced from  $O_h$  to  $C_{3v} = \{1, r_1, r_1^2, Ii_2, Ii_4, Ii_5\}$ . The broken symmetry includes  $\pm 120^\circ$  rotations around the field direction and reflections through three diagonal planes which are parallel to the field direction.

The  $O \supset C_{3v}$  correlations (4.2.46b) tell qualitatively how the octahedral levels will be split by a  $C_{3v}$  symmetric perturbation:

$$\mathscr{D}^{A_{1g}} \downarrow C_{3v} = A', \quad (4.3.75a)$$

$$\mathscr{D}^{T_{1u}} \downarrow C_{3v} = A' + E, \quad (4.3.75b)$$

$$\mathscr{D}^{E_g} \downarrow C_{3v} = E. \quad (4.3.75c)$$

According to this a  $(2 \times 2)$  Hamiltonian submatrix must be solved for the pair of  $A'$  states and another one solved for the pair of  $E$  states.

In order to reduce  $\langle H + V_d \rangle$  to  $(2 \times 2)$  submatrices one must use base states labeled by  $C_{3v}$  irreps. This is where one must be careful to consistently define all bases and avoid annoying phase errors. The  $(A_{1g}T_{1u}E_g)$  bases we have been using are labeled by tetragonal subgroup chain  $O_h \supset D_{4h} \supset D_{2h}$ . The tetragonal irreps  $\mathscr{D}^{A_{1g}}$  and  $\mathscr{D}^{E_g}$  are already reduced with respect to  $C_{3v}$ . From Section 4.2, and, in particular, Eq. (4.2.19) we have the following:

$$\begin{array}{l} \{ \mathscr{D}^{A_{1g}}(1) = 1, \quad \mathscr{D}^{A_{1g}}(r_1) = 1, \quad \mathscr{D}^{A_{1g}}(r_1^2) = 1, \quad \mathscr{D}^{A_{1g}}(Ii_2) = 1, \quad \mathscr{D}^{A_{1g}}(Ii_4) = 1, \quad \mathscr{D}^{A_{1g}}(Ii_5) = 1 \} \\ \mathscr{D}^{E_g}(1) = \quad \mathscr{D}^{E_g}(r_1) = \quad \mathscr{D}^{E_g}(r_1^2) = \quad \mathscr{D}^{E_g}(Ii_2) = \quad \mathscr{D}^{E_g}(Ii_4) = \quad \mathscr{D}^{E_g}(Ii_5) = \end{array} \left\{ \begin{array}{l} \begin{pmatrix} 1 & 0 \\ 0 & 1 \end{pmatrix}, \quad \begin{pmatrix} -\frac{1}{2} & -\frac{\sqrt{3}}{2} \\ \frac{\sqrt{3}}{2} & -\frac{1}{2} \end{pmatrix}, \quad \begin{pmatrix} -\frac{1}{2} & \frac{\sqrt{3}}{2} \\ -\frac{\sqrt{3}}{2} & -\frac{1}{2} \end{pmatrix}, \quad \begin{pmatrix} -\frac{1}{2} & \frac{\sqrt{3}}{2} \\ \frac{\sqrt{3}}{2} & \frac{1}{2} \end{pmatrix}, \quad \begin{pmatrix} 1 & 0 \\ 0 & -1 \end{pmatrix}, \quad \begin{pmatrix} -\frac{1}{2} & -\frac{\sqrt{3}}{2} \\ -\frac{\sqrt{3}}{2} & \frac{1}{2} \end{pmatrix} \end{array} \right\} \quad (4.3.76)$$

However, the  $T_{1u}$  irreps (4.2.14) are not reduced with respect to  $C_{3v}$ :

$$\begin{aligned} \mathcal{D}^{T_{1u}}(1) = \mathcal{D}^{T_{1u}}(r_1) = \mathcal{D}^{T_{1u}}(r_2) = \mathcal{D}^{T_{1u}}(Ii_2) = \mathcal{D}^{T_{1u}}(Ii_4) = \mathcal{D}^{T_{1u}}(Ii_5) = \\ \begin{pmatrix} \cdot & \cdot & \cdot \\ \cdot & 1 & \cdot \\ \cdot & \cdot & 1 \end{pmatrix}, \begin{pmatrix} \cdot & \cdot & 1 \\ 1 & \cdot & \cdot \\ \cdot & 1 & \cdot \end{pmatrix}, \begin{pmatrix} \cdot & 1 & \cdot \\ \cdot & \cdot & 1 \\ 1 & \cdot & \cdot \end{pmatrix}, \begin{pmatrix} \cdot & \cdot & 1 \\ \cdot & 1 & \cdot \\ 1 & \cdot & \cdot \end{pmatrix}, \begin{pmatrix} \cdot & 1 & \cdot \\ 1 & \cdot & \cdot \\ \cdot & \cdot & 1 \end{pmatrix}, \begin{pmatrix} 1 & \cdot & \cdot \\ \cdot & \cdot & 1 \\ \cdot & 1 & \cdot \end{pmatrix}. \end{aligned} \quad (4.3.77)$$

Hence the tetragonal bases  $\left\{ \left| \begin{smallmatrix} T_{1u} \\ 1 \end{smallmatrix} \right\rangle, \left| \begin{smallmatrix} T_{1u} \\ 2 \end{smallmatrix} \right\rangle, \left| \begin{smallmatrix} T_{1u} \\ 3 \end{smallmatrix} \right\rangle \right\}$  are not yet in a convenient form for a trigonal problem. One needs an  $A'$  and an  $E$  pair of the  $T_{1u}$  bases according to correlation (4.3.75b). What combination of tetragonal  $\left| \begin{smallmatrix} T_{1u} \\ j \end{smallmatrix} \right\rangle$

make a  $C_{3v}$  trigonal  $\left\{ \left| \begin{smallmatrix} E \\ 1 \end{smallmatrix} \right\rangle, \left| \begin{smallmatrix} E \\ 2 \end{smallmatrix} \right\rangle \right\}$  or  $|A'\rangle$  bases?

By applying  $C_{3v}$   $P$  operators to one of the  $T_{1u}$  bases the correct combinations are obtained.  $|A'\rangle$  is found from

$$P^{A'} \left| \begin{smallmatrix} T_{1u} \\ 3 \end{smallmatrix} \right\rangle = (1/6)(1 + r_1 + r_1^2 + Ii_2 + Ii_4 + Ii_5) \left| \begin{smallmatrix} T_{1u} \\ 3 \end{smallmatrix} \right\rangle$$

using

$$g \left| \begin{smallmatrix} T_{1u} \\ 3 \end{smallmatrix} \right\rangle = \sum_{j=1}^3 \mathcal{D}_{j3}^{T_{1u}}(g) \left| \begin{smallmatrix} T_{1u} \\ j \end{smallmatrix} \right\rangle$$

and the tetragonal  $\mathcal{D}^{T_{1u}}(g)$  in Eq. (4.3.77). The normalized result is

$$\left| \begin{smallmatrix} T_{1u} \\ A' \end{smallmatrix} \right\rangle \equiv P^{A'} \left| \begin{smallmatrix} T_{1u} \\ 3 \end{smallmatrix} \right\rangle \sqrt{3} = \left( \left| \begin{smallmatrix} T_{1u} \\ 1 \end{smallmatrix} \right\rangle + \left| \begin{smallmatrix} T_{1u} \\ 2 \end{smallmatrix} \right\rangle + \left| \begin{smallmatrix} T_{1u} \\ 3 \end{smallmatrix} \right\rangle \right) / \sqrt{3}. \quad (4.3.78)$$

Similarly, the  $|E'\rangle$  states are obtained by using the  $P^E$  projectors

$$P_{ij}^E = (I^E / oC_{3v}) \sum_g \mathcal{D}_{ij}^{E*}(g) g$$

and the irreps  $\mathcal{D}^E(g) = \mathcal{D}^{E_s}(g)$  in Eq. (4.3.76). The normalized results are

$$\left| \begin{smallmatrix} T_{1u} \\ E \\ 1 \end{smallmatrix} \right\rangle \equiv P_{11}^E \left| \begin{smallmatrix} T_{1u} \\ 3 \end{smallmatrix} \right\rangle \sqrt{3/2} = \left( - \left| \begin{smallmatrix} T_{1u} \\ 1 \end{smallmatrix} \right\rangle - \left| \begin{smallmatrix} T_{1u} \\ 2 \end{smallmatrix} \right\rangle + 2 \left| \begin{smallmatrix} T_{1u} \\ 3 \end{smallmatrix} \right\rangle \right) / \sqrt{6}, \quad (4.3.79a)$$

$$\left| \begin{smallmatrix} T_{1u} \\ E \\ 2 \end{smallmatrix} \right\rangle \equiv P_{21}^E \left| \begin{smallmatrix} T_{1u} \\ 3 \end{smallmatrix} \right\rangle \sqrt{3/2} = \left( \left| \begin{smallmatrix} T_{1u} \\ 1 \end{smallmatrix} \right\rangle - \left| \begin{smallmatrix} T_{1u} \\ 2 \end{smallmatrix} \right\rangle \right) / \sqrt{2}. \quad (4.3.79b)$$

The Hamiltonian (4.3.74) reduces to a submatrix,

$$\langle H + V_d \rangle^{A'} = \begin{pmatrix} \left\langle \begin{array}{c} A_{1g} \\ A' \end{array} \right\rangle & \left\langle \begin{array}{c} T_{1u} \\ A' \end{array} \right\rangle \\ H + 4S & -d \\ -d & H \end{pmatrix}, \quad (4.3.80)$$

between the  $A'$  states

$$\begin{aligned} \left\langle \begin{array}{c} A_{1g} \\ A' \end{array} \right\rangle &= (|1\rangle + |2\rangle + |3\rangle + |4\rangle + |5\rangle + |6\rangle)/\sqrt{6}, \\ \left\langle \begin{array}{c} T_{1u} \\ A' \end{array} \right\rangle &= (|1\rangle - |2\rangle + |3\rangle - |4\rangle + |5\rangle - |6\rangle)/\sqrt{6}, \end{aligned} \quad (4.3.81)$$

and an identical pair of submatrices,

$$\langle H + V_d \rangle^E = \begin{pmatrix} \left\langle \begin{array}{c} E_g \\ E \\ 1, 2 \end{array} \right\rangle & \left\langle \begin{array}{c} T_{1u} \\ E \\ 1, 2 \end{array} \right\rangle \\ H - 2S & -d \\ -d & H \end{pmatrix}, \quad (4.3.82)$$

between the  $E$  states of the first partners

$$\begin{aligned} \left\langle \begin{array}{c} E_g \\ E \\ 1 \end{array} \right\rangle &= (2|1\rangle + 2|2\rangle - |3\rangle - |4\rangle - |5\rangle - |6\rangle)/\sqrt{12}, \\ \left\langle \begin{array}{c} T_{1u} \\ E \\ 1 \end{array} \right\rangle &= (2|1\rangle - 2|2\rangle - |3\rangle + |4\rangle - |5\rangle + |6\rangle)/\sqrt{12}, \end{aligned} \quad (4.3.83)$$

or else between the  $E$  states of the second partners:

$$\begin{aligned} \left\langle \begin{array}{c} E_g \\ E \\ 2 \end{array} \right\rangle &= (|3\rangle + |4\rangle - |5\rangle - |6\rangle)/2, \\ \left\langle \begin{array}{c} T_{1u} \\ E \\ 2 \end{array} \right\rangle &= (|3\rangle - |4\rangle - |5\rangle + |6\rangle)/2 \end{aligned} \quad (4.3.84)$$

The remaining solution and analysis is left as an exercise.

Note that the  $D_{4h} - C_{3v}$  transformation

$$\mathcal{F} = \begin{pmatrix} \begin{matrix} |E\rangle \\ |1\rangle \end{matrix} & \begin{matrix} |E\rangle \\ |2\rangle \end{matrix} & \begin{matrix} |A'\rangle \\ |3\rangle \end{matrix} \\ \begin{matrix} -\frac{1}{\sqrt{6}} & \frac{1}{\sqrt{2}} & \frac{1}{\sqrt{3}} \\ -\frac{1}{\sqrt{6}} & -\frac{1}{\sqrt{2}} & \frac{1}{\sqrt{3}} \\ \frac{2}{\sqrt{6}} & 0 & \frac{1}{\sqrt{3}} \end{matrix} & \begin{matrix} |T_1\rangle \\ |1\rangle \\ |2\rangle \\ |3\rangle \end{matrix} \end{pmatrix} \quad (4.3.85)$$

obtained in Eqs. (4.3.78) and (4.3.79) differs slightly from the  $D_{4h} - D_{3d}$  transformation (4.2.31). One must use caution when changing between  $D_n$  and  $C_{nv}$  bases.

In fact  $D_{3d}$  symmetry results if a threefold axial quadrupole field fell on the octahedral bases. The  $O_h \supset D_{3d}$  correlations,

$$\begin{aligned} \mathcal{D}^{A_{1g}} \downarrow D_{3d} &= A_{1g}, \\ \mathcal{D}^{T_{1u}} \downarrow D_{3d} &= A_{2u} + E_u, \\ \mathcal{D}^{E_g} \downarrow D_{3d} &= E_g, \end{aligned} \quad (4.3.86)$$

follow from  $D_3$  correlations (4.2.44). It shows that  $D_{3d}$ -defined bases would not mix at all. A  $D_{3d}$ -symmetric quadrupole Hamiltonian  $\langle H + V_q \rangle$  results if one replaces all the  $\pm d$ 's in (4.3.74) with  $q$ 's. However, such a matrix causes no splitting at all. One needs a more "severely" defined Hamiltonian of  $D_{3d}$  symmetry. For example, it is possible that the amplitudes,

$$\langle 1|H|4 \rangle = \langle 2|H|3 \rangle = \cdots = S'(q), \quad (4.3.87)$$

for tunneling along the field might be different from the amplitudes,

$$\langle 1|H|3 \rangle = \langle 2|H|4 \rangle = \cdots = S, \quad (4.3.88)$$

for tunneling transverse to the field. Field-dependent tunneling will effect the splitting predicted in Eq. (4.3.86) as well as changing the spectrum of other problems which have been treated previously in this section. (See Problem 4.3.6.) The variation of tunneling amplitudes with interatomic distance is important in the study of molecular bonding. Electronic energy eigenvalues of symmetric systems are generally quite sensitive to tunneling. The effects of nuclear motion on electronic energy and vice versa will be taken up in Section 6.7 and in subsequent chapters.

## 4.4 VIBRATIONS OF OCTAHEDRAL HEXAFLUORIDE MOLECULES

Octahedral hexafluoride molecules such as  $\text{UF}_6$  have attracted attention because their spectral properties provide a way to separate the isotopes used in reactor fuel. Let us study the first of these properties involving its mechanical vibrations. In Figure 4.4.1 is a drawing of a mechanical model of  $\text{UF}_6$  assuming  $O_h$  symmetry for a molecule, and a coordinate system for its motions. The larger ball represents the U atom of mass  $M$ , and the smaller balls represent F atoms of mass  $m$ . To begin with let us assume only two kinds of central force of "spring" constants:  $k$  for the F—F interaction, and  $j$  for the F—U bond. In order to analyze  $\text{SF}_6$  it is convenient to include a bending constant  $b$  for the F—S bond, as indicated in the figure.

Obviously, a continuous infinity of choices for coordinates exists in problems like this, and one just hopes to pick a fairly convenient system. The choice made in Figure 4.4.1 is adequate for solution of the harmonic equation of motion and for demonstration of some further theoretical points concerning symmetry analysis.

## A. Projection Analysis

As in previous examples it is convenient to obtain eigenvectors from vectors projected by the elementary operators

$$P_{ij}^\alpha = (I^\alpha / {}^0G) \sum_g \mathcal{D}_{ij}^{\alpha*}(g) g \quad (4.4.1)$$

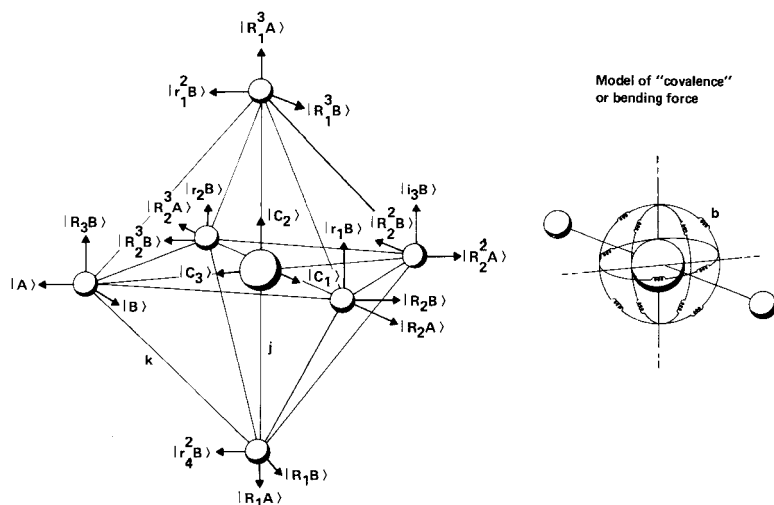


**Figure 4.4.1** Octahedral hexafluoride ( $\text{UF}_6, \text{SF}_6, \dots$ ) molecular model Cartesian coordinates for each atom are labeled by orbit ( $A, B$ , or  $C$ ) and coset leaders. ( $1 = R_3, r_1, R_2, \dots$  etc.) Spring constants are equal to ( $k$ ) for (F—F) bonds and  $j$  for radial (F—central) bonds. Bending spring constant is  $b$ .

of the octahedral groups  $O$  or  $O_h$ . It is important to see how  $P$  operators can be efficiently applied. First of all, our choice of coordinates in Figure 4.4.1 shows which bases are connected by symmetry operations. Sets of base vectors like  $\{|A\rangle, |R_2A\rangle = R_2|A\rangle, \dots\}$  or  $\{|B\rangle, |R_2B\rangle = R_2|B\rangle, \dots\}$  or  $\{|C\rangle, |R_2C\rangle = R_2|C\rangle, |R_3^3C\rangle = R_3^3|C\rangle\}$  are each called ORBITS of symmetry when any two of their bases can be connected by a symmetry operator. Elementary operators  $P_{ij}^\alpha$  need only be applied to the first vector in each orbit. The result of operating on any others is just a linear combination of the first ones, as seen in the following:

$$P_{ij}^\alpha |gA\rangle = P_{ij}^\alpha g|A\rangle = \sum_k \mathcal{D}_{jk}^\alpha(g) P_{ik}^\alpha |A\rangle. \quad (4.4.2)$$

As explained in Sections 4.3.B and 4.3.C, only certain projectors  $P_{jk}^\alpha$  need be applied to a given state such as  $|A\rangle$ . These are the ones for which the right-hand index ( $k$ ) is compatible with a local  $C_4$  symmetry condition such as

$$|A\rangle = P^A |A\rangle = (1/4)(1 + R_3 + R_3^2 + R_3^3)|A\rangle.$$

This is the same as Eq. (4.3.7) involving  $C_4$  irrep  $A \equiv 0_4$ . In fact the orbit  $\{|A\rangle, R_3^2|A\rangle, \dots\}$  is just the basis of the first induced representation

$$D^{0_4} \uparrow O = A_1 \oplus T_1 \oplus E$$

introduced in Section 4.3.A. The full  $C_{4v} \subset O_h$  labeling of this orbit is given by the induced representation

$$D^A \uparrow O_h = A_{1g} \oplus T_{1u} \oplus E_g, \quad (4.4.3)$$

which corresponds to the  $(A_{1g}, T_{1u}, E_g)$  eigenvectors for the octahedral systems in Figure 4.3.1. The mechanical system in Figure 4.3.1 is a constrained version of the  $UF_6$  molecule in which the  $\{|B\rangle \dots\}$  and  $\{|C\rangle \dots\}$  degrees of freedom are absent.

The  $\{|B\rangle \dots\}$  orbit contains 12 base states. The local  $C_2$  rotational symmetry condition for  $|B\rangle$  is

$$|B\rangle = P^B |B\rangle = \frac{1}{2}(1 - R_3^2)|B\rangle, \quad (4.4.4)$$

since  $180^\circ$  rotation of  $|B\rangle$  around the 3 axis is just  $-|B\rangle$ . A more detailed local symmetry condition for  $|B\rangle$  is

$$|B\rangle = P_1^E |B\rangle = \frac{1}{4}(1 - R_3^2 - IR_1^2 + IR_2^2)|B\rangle, \quad (4.4.5)$$

where

$$P_1^E \equiv P_{B_1}^E = \frac{1}{4}(1 - R_3^2 - IR_1^2 + IR_2^2) \quad (4.4.6)$$

is a  $C_{4v} \supset C_{2v}$  projection operator. The full  $O_h$  labeling of the  $\{|B\rangle \dots\}$  orbit is therefore given by the 12-dimensional induced representation

$$\mathcal{D}^E \uparrow O_h = T_{1g} \oplus T_{2g} \oplus T_{1u} \oplus T_{2u}, \quad (4.4.7)$$

according to the  $E$  column of  $C_{4v}$  correlation (4.2.46c).

The three base states of the  $\{|C_1\rangle, |C_2\rangle, |C_3\rangle\}$  orbit involve translation of the central U atom.  $|C_j\rangle$  obviously satisfies the local symmetry condition of a polar vector

$$|C_j\rangle = P_{jj}^{T_{1u}}|C_j\rangle; \quad (4.4.8)$$

i.e., they are ready-made bases of  $O_h$  irrep  $T_{1u}$  in the tetragonal basis. Altogether, the  $UF_6$  coordinates belong to a 21-dimensional representation which reduces to

$$\begin{aligned} A + B + C &= (A_{1g} \oplus T_{1u} \oplus E_g) \oplus (T_{1g} \oplus T_{2g} \oplus T_{1u} \oplus T_{2u}) \oplus (T_{1u}) \\ &= A_{1g} \oplus E_g \oplus T_{1g} \oplus T_{2g} \oplus T_{2u} \oplus 3T_{1u}. \end{aligned} \quad (4.4.9)$$

Each irrep labels a fundamental resonance. All resonances except the three  $T_{1u}$ 's are uniquely labeled.

It will be necessary to account for the 12  $B$ -orbit vectors

$$|e_{jk}^\alpha B\rangle = P_{jk}^\alpha |B\rangle / (N_k^\alpha)^{1/2}. \quad (4.4.10)$$

The tetragonal local symmetry condition (4.4.5) tells which  $k$  to use. If you forget how the  $k$  are labeled it is easy to represent the local symmetry projector (4.4.6) and see which components are nonzero. Using tetragonally defined irreps (4.2.14) the following representations result:

$$\begin{aligned} \mathcal{D}^{T_{1g}}(P_1^E) &= (1/4)(\mathcal{D}^{T_{1g}}(1) - \mathcal{D}^{T_{1g}}(R_3^2) - \mathcal{D}^{T_{1g}}(IR_1^2) + \mathcal{D}^{T_{1g}}(IR_2^2)) \\ &= \left[ \begin{pmatrix} 1 & 0 & 0 \\ 0 & 1 & 0 \\ 0 & 0 & 1 \end{pmatrix} - \begin{pmatrix} -1 & 0 & 0 \\ 0 & -1 & 0 \\ 0 & 0 & 1 \end{pmatrix} - \begin{pmatrix} 1 & 0 & 0 \\ 0 & -1 & 0 \\ 0 & 0 & -1 \end{pmatrix} + \begin{pmatrix} -1 & 0 & 0 \\ 0 & 1 & 0 \\ 0 & 0 & -1 \end{pmatrix} \right] / 4 = \begin{pmatrix} 0 & 0 & 0 \\ 0 & 0 & 0 \\ 0 & 0 & 0 \end{pmatrix} \end{aligned} \quad (4.4.11a)$$

$$\mathcal{D}^{T_{1u}}(P_1^E) = \left[ \begin{pmatrix} 1 & 0 & 0 \\ 0 & 1 & 0 \\ 0 & 0 & 1 \end{pmatrix} - \begin{pmatrix} -1 & 0 & 0 \\ 0 & -1 & 0 \\ 0 & 0 & 1 \end{pmatrix} - \begin{pmatrix} -1 & 0 & 0 \\ 0 & 1 & 0 \\ 0 & 0 & 1 \end{pmatrix} + \begin{pmatrix} 1 & 0 & 0 \\ 0 & -1 & 0 \\ 0 & 0 & 1 \end{pmatrix} \right] / 4 = \begin{pmatrix} 1 & 0 & 0 \\ 0 & 0 & 0 \\ 0 & 0 & 0 \end{pmatrix} \quad (4.4.11b)$$

The first and second diagonal components, respectively, of the  $T_{1u}$  and  $T_{1g}$  matrices are nonzero. Hence,  $T_{1u}$  and  $T_{1g}$  vectors require that  $k = 1$  and  $2$ , respectively,

$$|e_{j1}^{T_{1u}B}\rangle = P_{j1}^{T_{1u}}|B\rangle / (N_1^{T_{1u}})^{1/2}, \quad (4.4.12a)$$

$$|e_{j2}^{T_{1g}B}\rangle = P_{j2}^{T_{1g}}N_2^{T_{1g}}|B\rangle / (N_2^{T_{1g}})^{1/2}. \quad (4.4.12b)$$

As explained in Section 4.3.C the calculation of  $P_{jk}^\alpha|B\rangle$  is simple when  $P_{jk}^\alpha$  matches the local symmetry as per Eq. (4.3.35). In writing out each projected state one needs only to sum over group elements  $l_j$  which label coordinates  $\langle l_j|B\rangle$  in Figure 4.4.1. This result was expressed by Eq. (4.3.44). Using the  $T_1$  irreps (4.2.14) we derive the following:

$$\begin{aligned} |e_{11}^{T_{1u}B}\rangle &= \frac{1}{16}(\mathcal{D}_{11}^{T_1}(1)|B\rangle \\ &\quad + \cdots + \mathcal{D}_{11}^{T_1}(R_1)|R_1B\rangle + \cdots + \mathcal{D}_{11}^{T_1}(R_1^3)|R_1^3B\rangle \\ &\quad + \cdots + \mathcal{D}_{11}^{T_1}(R_2^2)|R_2^2B\rangle) / (N)^{1/2} \\ &= (|B\rangle + |R_1B\rangle + |R_1^3B\rangle - |R_2^2B\rangle) / 2, \end{aligned} \quad (4.4.13a)$$

$$|e_{21}^{T_{1u}B}\rangle = (|R_3B\rangle + |r_1B\rangle + |r_2B\rangle + |i_3B\rangle) / 2, \quad (4.4.13b)$$

$$|e_{31}^{T_{1u}B}\rangle = (-|R_2B\rangle + |R_2^3B\rangle + |r_1^2B\rangle + |r_4^2B\rangle) / 2. \quad (4.4.13c)$$

Figure 4.4.2 shows the first partner state  $|e_{11}^{T_{1u}B}\rangle$  to be a translation relative to the 1 axis of the octahedral equator. Shown also is the state

$$\begin{aligned} |e_{12}^{T_{1g}B}\rangle &= \frac{1}{16}(\cdots + \mathcal{D}_{12}^{T_1}(R_3)|R_3B\rangle + \cdots + \mathcal{D}_{12}^{T_1}(i_3)|i_3B\rangle \\ &\quad + \cdots + \mathcal{D}_{12}^{T_1}(r_1^2)|r_1^2B\rangle + \cdots + \mathcal{D}_{12}^{T_1}(r_4^2)|r_4^2B\rangle) / (N) \\ &= (-|R_3B\rangle + |i_3B\rangle + |r_1^2B\rangle - |r_4^2B\rangle) / 2, \end{aligned} \quad (4.4.14)$$

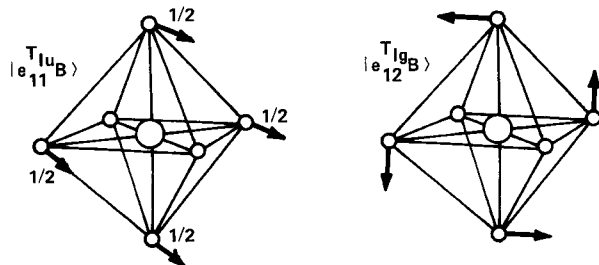
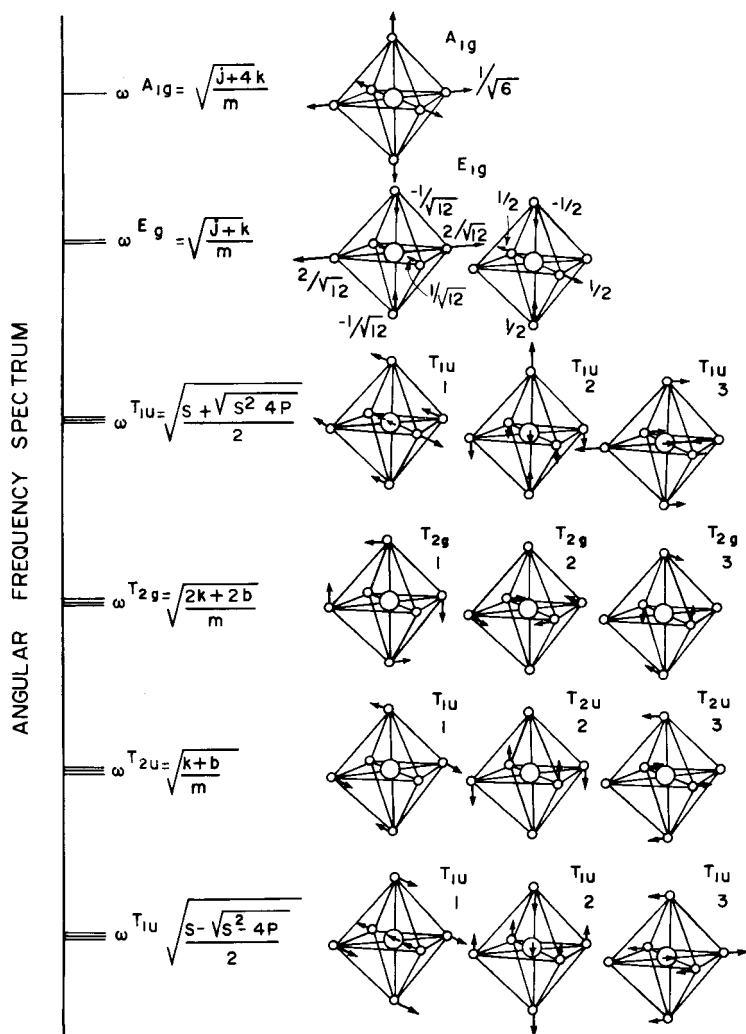


Figure 4.4.2  $T_1$  motions from the  $B$  orbit.





**Figure 4.4.3** Hexafluoride vibrational modes and spectrum.  $T_{1u}$  modes are not drawn precisely, since their form depends upon the choice of constants and rotational perturbations. (See Figure 4.4.7.)

which corresponds to rotation around the 1 axis. This is a nongenuine vibration and so it will not be considered further until rotations are studied in subsequent chapters.

The derivation of the  $T_2$  states

$$|e_{j1}^{T_{2u}}B\rangle = P_{j1}^{T_{2u}}|B\rangle / (N_1^{T_{2u}})^{1/2}, \quad (4.4.15a)$$

$$|e_{j2}^{T_{2g}}B\rangle = P_{j2}^{T_{2g}}|B\rangle / (N_2^{T_{2g}})^{1/2}, \quad (4.4.15b)$$

follows the same lines. The results are shown by the first and second triplets in Figure 4.4.3. Shown also are the  $A$ -orbit states

$$|e^{A_{1g}}A\rangle = P^{A_{1g}}|A\rangle / (N^{A_{1g}})^{1/2}, \quad (4.4.16a)$$

$$|e_{j1}^{E_g}A\rangle = P_{j1}^{E_g}|A\rangle / (N^{E_g})^{1/2}, \quad (4.4.16b)$$

which were derived before in Eqs. (4.3.20)–(4.3.23).

Thus we have accounted for all modes of  $UF_6$  except those labeled by  $T_{1u}$ . Besides the  $T_{1u}$  states (4.4.13) there are axial F-atom translation states

$$|e_{j3}^{T_{1u}}A\rangle = P_{j3}^{T_{1u}}|A\rangle / (N_3^{T_{1u}})^{1/2}, \quad (4.4.17)$$

which were derived before in Eqs. (4.3.27), and the central U-atom translation states (4.4.8). The first partner of each is shown in Figure 4.4.4a. Each of these modes causes the molecular center of mass to translate. If the arrows in Figure 4.4.4(a) stand for velocity, then the linear momentum of  $|e^{T_{1u}}A\rangle$ ,  $|e^{T_{1u}}B\rangle$ , and  $|e^{T_{1u}}C\rangle$  is  $m\sqrt{2}$ ,  $2m$ , and  $M$ , respectively. Clearly, the combination modes

$$\begin{aligned} |c_j^{T_{1u}}\rangle &= \sqrt{2}|e_j^{T_{1u}}A\rangle - |e_j^{T_{1u}}B\rangle \\ &= 2P_{j3}^{T_{1u}}|A\rangle - 2P_{j1}^{T_{1u}}|B\rangle \end{aligned} \quad (4.4.18)$$

and

$$|c_j^{T_{1u'}}\rangle = M\sqrt{2}|e_j^{T_{1u}}A\rangle + 2M|e_j^{T_{1u}}B\rangle - 6m|c_j\rangle \quad (4.4.19)$$

have zero translational momentum and do not move the molecular center of mass. They are drawn in Figure 4.4.4(b). The genuine vibrations will be

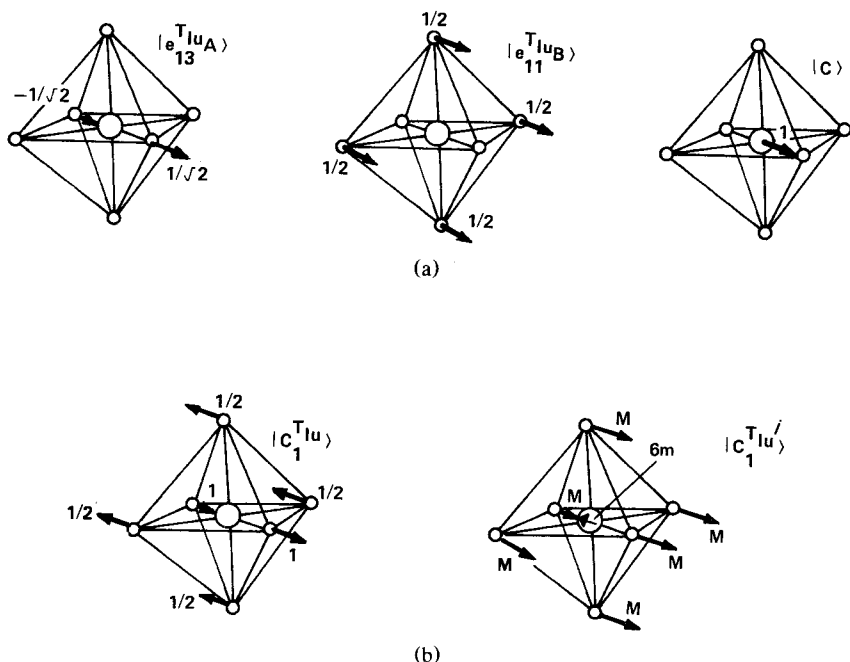


**Figure 4.4.4**  $\left(T_{1u}\right)$  motions. (a) Primitive motions. (b) Constrained motions with zero translation.

combinations of these two constrained states only. Rigid molecular translation corresponds to a third  $T_{1u}$  state,

$$|t_j^{T_{1u}}\rangle = \sqrt{2}|e_j^{T_{1u}A}\rangle + 2|e_j^{T_{1u}B}\rangle + |c_j\rangle, \quad (4.4.20)$$

and this type of motion will not be considered further here.

## B. Solving Equations of Motion

The  $O_h$  symmetry projection provides states which simplify the equation of motion

$$\mathbf{m}|\ddot{x}\rangle = -\mathbf{F}|x\rangle. \quad (4.4.21)$$

The symmetry analysis also tells us exactly how much of the mass matrix  $\langle \mathbf{m} \rangle$  and force matrix  $\langle \mathbf{F} \rangle$  needs to be written. Of the  $(21)^2 = 441$  possible components of  $\langle \mathbf{F} \rangle$  only the 39 entries in Eq. (4.4.22) will be needed. The same is true of the  $\mathbf{m}$  matrix, although its form for this problem is quite simple anyway. In general a row of the matrix is needed for each symmetry orbit. If the matrices are Hermitian as are  $\langle \mathbf{F} \rangle$  and  $\langle \mathbf{m} \rangle$  only the upper-diagonal parts of each row need be written,

$$\langle F \rangle =$$

$\langle A \rangle$	$ R_1^2 A\rangle$	$ R_1 A\rangle$	$ R_2 A\rangle$	$ R_2 A\rangle$	$ R_1 A\rangle$	$ R_3 A\rangle$	$ R_3 A\rangle$	$ B\rangle$	$ r_1 B\rangle$	$ r_2 B\rangle$	$ r_1^2 B\rangle$	$ r_2^2 B\rangle$	$ r_1^2 B\rangle$	$ R_2^2 B\rangle$	$ R_1 B\rangle$	$ R_2 B\rangle$	$ R_3 B\rangle$	$ R_1 B\rangle$	$ R_3 B\rangle$	$ i_3 B\rangle$	$\langle C_1 \rangle$	$\langle C_2 \rangle$	$\langle C_3 \rangle$	
$2k + j$	0	$k/2$	$k/2$	$k/2$	$k/2$	$k/2$	$k/2$	0	0	0	$-k/2$	$-k/2$	0	0	0	0	0	0	0	0	0	0	0	$-j$
$\langle B \rangle$								$k + b$	0	0	0	0	0	0	0	$-\frac{k+b}{2}$	0	0	0	0	0	$-b/2$	0	0
$\langle C_1 \rangle$																								$2(j+b)$

$$\langle m \rangle =$$

$m$	$m$	$m$	$m$	$m$	$m$	$m$	$m$	$m$	$m$	$m$	$m$	$m$	$m$	$m$	$m$	$m$	$m$	$m$	$m$	$m$	$m$	$m$	$m$	$m$	$m$
-----	-----	-----	-----	-----	-----	-----	-----	-----	-----	-----	-----	-----	-----	-----	-----	-----	-----	-----	-----	-----	-----	-----	-----	-----	-----

(4.4.22)

The  $\langle \mathbf{F} \rangle$  components are derived from the spring-coordinate geometry of Figure 4.4.1 according to the small vibration approximations of Section 1.4.B. One should expect a spring-mass model to be only an approximate model for the vibrations of molecules such as  $\text{UF}_6$  or  $\text{SF}_6$ . If more information is gained about the molecular binding then more realistic  $\langle \mathbf{F} \rangle$  components can be given.

The matrix formula (4.3.46) gives the components of  $\langle \mathbf{F} \rangle$  and  $\langle \mathbf{m} \rangle$  matrices in terms of the "primitive" representation (4.4.22). For the bases with distinct irrep labels the resulting components are the desired eigenvalues. From the eigenvalues of  $\langle \mathbf{F} \rangle$  and  $\langle \mathbf{m} \rangle$  one derives the squared eigenfrequencies  $\omega^2 = \langle \mathbf{m}^{-1} \mathbf{F} \rangle$ . As an example consider the  $T_{2u}$  and  $T_{2g}$  eigenfrequency calculations:

$$\begin{aligned} (\omega^{T_{2u}})^2 &= (1/m) \sum_l \langle B | \mathbf{F} | lB \rangle \mathcal{D}_{11}^{T_{2u}}(l) \\ &= [(k+b) \mathcal{D}_{11}^{T_2}(1) - (k/2 + b/2)(\mathcal{D}_{11}^{T_2}(R_2) + \mathcal{D}_{11}^{T_2}(R_3))] / m \\ &= (k+b)/m, \end{aligned} \quad (4.4.23)$$

$$\begin{aligned} (\omega^{T_{2g}})^2 &= (1/m) \sum_l \langle B | \mathbf{F} | lB \rangle \mathcal{D}_{22}^{T_{2g}}(l) \\ &= [(k+b) \mathcal{D}_{11}^{T_2}(1) - (k/2 + b/2)(\mathcal{D}_{22}^{T_2}(R_2) + \mathcal{D}_{22}^{T_2}(R_3))] / m \\ &= 2(k+b)/m. \end{aligned} \quad (4.4.24)$$

Similarly, the eigenfrequencies of the radially moving motions are derived as they were in Section 4.3 [recall Eq. (4.3.36)<sub>x</sub>, for example]:

$$(\omega^{A_{1g}})^2 = (1/m) \sum_l \langle A | \mathbf{F} | lA \rangle \mathcal{D}^{A_{1g}}(l) = (4k+j)/m, \quad (4.4.25)$$

$$(\omega^{E_g})^2 = (1/m) \sum_l \langle A | \mathbf{F} | lA \rangle \mathcal{D}_{11}^{E_g}(l) = (k+j)/m. \quad (4.4.26)$$

This accounts for all genuine vibrational motions in Figure 4.4.4 except the two  $T_{1u}$  modes.

A two-by-two  $\langle \mathbf{F} \rangle$  and  $\langle \mathbf{m} \rangle$  matrix representations in the  $|c_j^{T_{1u}}\rangle$  and  $|c_j^{T_{1u}'}\rangle$  basis [(4.4.18) and (4.4.19)] need to be derived. The first component of operator  $\mathbf{Q} = \mathbf{F}$  or  $\mathbf{Q} = \mathbf{m}$  is computed as follows:

$$\begin{aligned} \langle c_j^{T_{1u}'} | \mathbf{Q} | c_j^{T_{1u}} \rangle &= (2 \langle A | P_{3j}^{T_{1u}} - 2 \langle B | P_{1j}^{T_{1u}} \rangle \mathbf{Q} (2 P_{j3}^{T_{1u}} | A \rangle - 2 P_{j1}^{T_{1u}} | B \rangle) \\ &= 4 \langle A | P_{33}^{T_{1u}} \mathbf{Q} | A \rangle - 4 \langle A | P_{31}^{T_{1u}} \mathbf{Q} | B \rangle \\ &\quad - 4 \langle B | P_{13}^{T_{1u}} \mathbf{Q} | A \rangle + 4 \langle B | P_{11}^{T_{1u}} \mathbf{Q} | B \rangle. \end{aligned} \quad (4.4.27)$$

The projection matrices  $\langle P \rangle$  can be reduced to sums over the labeling coset

leader elements  $l$  for each orbit:

$$\langle c_j^{T_{1u}} | \mathbf{Q} | c_j^{T_{1u}} \rangle = 2Q_{AA} - \sqrt{2}Q_{AB} + Q_{BB} - \sqrt{2}Q_{BA}, \quad (4.4.28)$$

where

$$\begin{aligned} Q_{AA} &= \sum_l \langle A | \mathbf{Q} | lA \rangle \mathcal{D}_{33}^{T_1}(l), \\ Q_{BA} &= Q_{AB} = (1/\sqrt{2}) \sum_l \langle A | \mathbf{Q} | lA \rangle \mathcal{D}_{31}^{T_1}(l), \\ Q_{BB} &= \sum_l \langle B | \mathbf{Q} | lB \rangle \mathcal{D}_{11}^{T_1}(l). \end{aligned}$$

Substituting the primitive  $\langle \mathbf{F} \rangle$  and  $\langle \mathbf{m} \rangle$  components (4.4.22) into the preceding gives the following:

$$\begin{pmatrix} F_{AA} & F_{AB} \\ F_{BA} & F_{BB} \end{pmatrix} = \begin{pmatrix} 2k + j & -\sqrt{2}k \\ -\sqrt{2}k & k + b \end{pmatrix}, \quad \begin{pmatrix} m_{AA} & m_{AB} \\ m_{BA} & m_{BB} \end{pmatrix} = \begin{pmatrix} m & 0 \\ 0 & m \end{pmatrix}. \quad (4.4.29)$$

Hence, the first  $T_{1u}$  components of  $\langle \mathbf{F} \rangle$  and  $\langle \mathbf{m} \rangle$  are

$$\begin{aligned} \langle c_j^{T_{1u}} | \mathbf{F} | c_j^{T_{1u}} \rangle &= 9k + 2j + b \\ \langle c_j^{T_{1u}} | \mathbf{m} | c_j^{T_{1u}} \rangle &= 3m. \end{aligned} \quad (4.4.30)$$

Similarly the other components are computed. The off-diagonal component of  $\mathbf{Q} = \mathbf{F}$  or  $\mathbf{Q} = \mathbf{M}$  is

$$\begin{aligned} \langle c_j^{T_{1u}} | \mathbf{Q} | c_j^{T_{1u}} \rangle &= 2MQ_{AA} + 2\sqrt{2}MQ_{AB} - 12m \langle A | \mathbf{Q} | C_3 \rangle \\ &\quad - \sqrt{2}MQ_{BA} - 2MQ_{BB} + 12m \langle B | \mathbf{Q} | C_1 \rangle, \end{aligned}$$

which yields

$$\begin{aligned} \langle c_j^{T_{1u}} | \mathbf{F} | c_j^{T_{1u'}} \rangle &= 2(j - b)(M + 6m), \\ \langle c_j^{T_{1u}} | \mathbf{m} | c_j^{T_{1u'}} \rangle &= 0. \end{aligned} \quad (4.4.31)$$

The calculation of the second diagonal component completes each matrix since  $\mathbf{F}$  and  $\mathbf{m}$  are Hermitian,

$$\begin{aligned} \langle c_j^{T_{1u'}} | \mathbf{F} | c_j^{T_{1u'}} \rangle &= (2j + 4b)(M + 6m)^2, \\ \langle c_j^{T_{1u'}} | \mathbf{m} | c_j^{T_{1u'}} \rangle &= 6mM(M + 6m). \end{aligned} \quad (4.4.32)$$

The acceleration matrix  $\langle \mathbf{a} \rangle = \langle \mathbf{m}^{-1} \mathbf{F} \rangle$  is then found:

$$\begin{pmatrix} \langle c^{T_{1u}} | \mathbf{a} | c^{T_{1u}} \rangle & \langle c^{T_{1u}} | \mathbf{a} | c^{T_{1u'}} \rangle \\ \langle c^{T_{1u'}} | \mathbf{a} | c^{T_{1u}} \rangle & \langle c^{T_{1u'}} | \mathbf{a} | c^{T_{1u'}} \rangle \end{pmatrix} = \begin{pmatrix} \frac{9k + 2j + b}{3m} & \frac{2(j + b)(M + 6m)}{3m} \\ \frac{j - b}{3mM} & \frac{(j + 2b)(M + 6m)}{3mM} \end{pmatrix}. \quad (4.4.33)$$

The secular equation for the  $T_{1u}$  acceleration matrix is

$$\lambda^2 - S\lambda + P = 0, \quad (4.4.34a)$$

where each root or eigenvalue

$$\lambda = (\omega^{T_{1u}})^2 \quad (4.4.34b)$$

is the square of an eigenfrequency, while

$$S = (3k + j + b)/m + (2j + 4b)/M \quad (4.4.34c)$$

is the sum of eigenvalues, and

$$P = (kj + 2kb + jb)(M + 6m)/m^2M \quad (4.4.34d)$$

is the product of eigenvalues. The  $T_{1u}$  eigenfrequency equation is then

$$\omega_{\pm}^{T_{1u}} = \left( S \pm (S^2 - 4P)^{1/2} \right)^{1/2} / \sqrt{2}. \quad (4.4.34e)$$

The eigenfrequencies  $\omega^\alpha(k/j)$  for  $b = 0$  are plotted in Figure 4.4.5 using the preceding equations and Eqs. (4.4.23)–(4.4.26). The values of  $(k/j)$  which fit the  $A_{1g}$  and upper  $T_{1u}$  lines observed in  $\text{UF}_6$ ,  $\text{NpF}_6$ , and  $\text{PuF}_6$  are indicated each by a line of circles which denote experimental results. Note that the values of  $k/j$  are small; they range between 0.1 and 0.2. For small  $k$  the spectrum breaks into two “clusters.” The high-frequency cluster ( $A_{1g}$ ,  $T_{1u}$ ,  $E_g$ ) involves radial vibrations which stretch the  $j$  spring or radial bonds. This cluster belongs to the induced representation  $A' \uparrow O_h$  as explained in Section 4.3. The low-frequency cluster consists of  $T_{2g}$ ,  $T_{1u}$ ,  $T_{2u}$ , and  $T_{1g}$  if you count rotations. This includes all the angular motions, which arise from the  $B$  orbit and which belong to the induced representation  $E \uparrow O_h$ . Angular or bending motions do not affect the  $j$  springs directly, but they do stretch the  $k$  and  $b$  springs. For  $k = 0 = b$  the bending or  $B$ -orbit

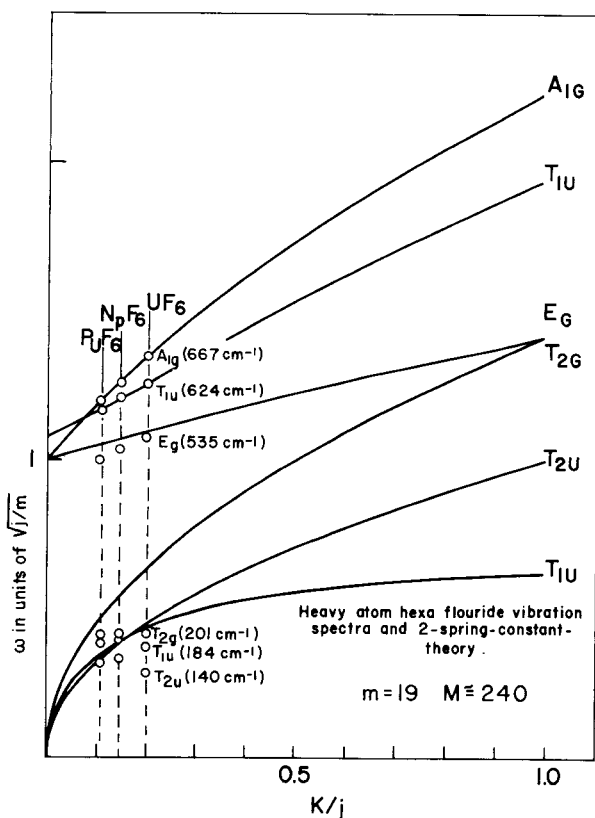


**Figure 4.4.5** Heavy-atom hexafluoride vibration spectra and  $(k, j)$  spring constant theory.

cluster of levels become degenerate with zero frequency. The splitting of the  $A$ -orbit cluster ( $A_{1g}, T_{1u}, E_g$ ) for  $k = 0 = b$  depends on the strength of the  $j$  springs and the mass ratio  $m/M$ . In Figure 4.4.5 ( $m/M$ ) is quite small, since the central atomic mass  $M$  is large compared to  $m$ . The motion of the central atom is part of the  $T_{1u}$  modes, and is involved in the coupling between them for nonzero  $k$  or  $b$ . (Notice how the  $T_{1u}$  curves “repel” each other as  $k$  varies across Figure 4.4.5.) However, even for  $k = 0 = b$  there is coupling between antipodal  $m$  atoms through  $j$  springs connected by the central  $M$  mass. This coupling is analogous to the “transaxial” tunneling described by the  $T$  parameter in Eq. (4.3.28), since it leaves  $E_g$  and  $A_{1g}$  levels degenerate, but splits away the  $T_{1u}$  level.

For a lighter hexafluoride molecule such as  $SF_6$  the distinction between radial and angular states seems to disappear, as shown in Figure 4.4.6. Now a small ( $b = 0.2$ ) value for the bending spring seems to be necessary to even approximately match the observed vibration frequencies. The presence of  $k$



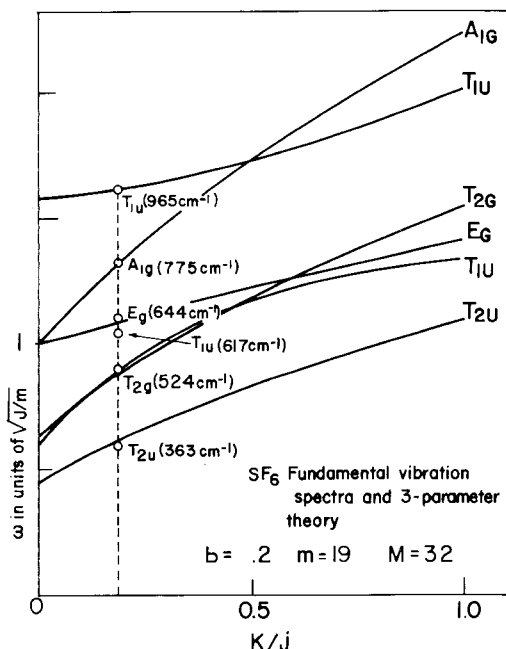


**Figure 4.4.6** Sulfur hexafluoride ( $\text{SF}_6$ ) spectra and theoretical curves. A small bonding constant ( $b = 0.2$ ) has been included.

and  $b$  springs coupling and a light central atom makes the ideas of spectral clusters and localized vibrational modes less useful. Note, however, that the ratio  $\omega^{T_{2g}} : \omega^{T_{2u}}$  is predicted to be

$$\omega^{T_{2g}} / \omega^{T_{2u}} = \sqrt{2}, \quad (4.4.35)$$

independent of  $k$  or  $b$  according to Eqs. (4.4.23) and (4.4.24). This agrees closely with the experimental values for  $\text{UF}_6$  and  $\text{SF}_6$ .

More knowledge of molecular potentials or a more sophisticated arrangement of "springs" is needed to precisely analyze all  $\text{XY}_6$  vibrational spectra. This is particularly true when higher excitations or overtones are observed, and when anharmonic contributions to the potentials need to be considered. However, some information can be learned from the present spring-mass model.

For example, let us derive a prediction for the isotope shift between  $\text{S}^{32}\text{F}_6$  ( $M = 32$ ) and  $\text{S}^{34}\text{F}_6$  ( $M = 34$ )  $T_{1u}$  modes. Setting  $m = 19$ ,  $b = 0.2j$ , and  $k = 0.18j$  as given in Figure 4.4.6 one needs to consider the solutions (4.4.34e) for two different mass values:  $M = 32$  and  $M = 34$ . The ratios for

the high (+) and low (-)  $T_{1u}$  frequencies are predicted to be

$$\omega_{\pm}^{T_{1u}}(M = 32)/\omega_{\pm}^{T_{1u}}(34) = 1.0173, \quad \omega_{\pm}^{T_{1u}}(M = 32)/\omega_{\pm}^{T_{1u}}(34) = 1.0064, \quad (4.4.36a)$$

in close agreement with the experimental values:

$$965 \text{ cm}^{-1}/948 \text{ mm}^{-1} = 1.0179, \quad 615 \text{ mm}^{-1}/612 \text{ mm}^{-1} = 1.0049. \quad (4.4.36b)$$

Isotope shifts for the other modes besides  $T_{1u}$  can be calculated very quickly. There is no shift in the harmonic spectra due to a change of  $M$ . A shift due to changing all the  $m$  nuclei is given by the ratio  $\omega^{\alpha}(m')/\omega^{\alpha}(m) = (m'/m)^{1/2}$ . A general theory of isotope shifts by Teller and Redlich is described in Herzberg's books listed at the end of Chapter 3.

The interest in the hexafluoride molecules has been centered mostly on the  $T_{1u}$  modes. These are the only modes which vibrate the central  $M$  atom and the only ones which have a useful  $M$  isotope shift. It is instructive to see more exactly how the various atoms move in the  $T_{1u}$  vibrational modes. To see this one must find the eigenvectors

$$|e_i^{T_{1u}}(\pm)\rangle = \varepsilon_{\pm}|c_i^{T_{1u}}\rangle + \varepsilon'_{\pm}|c'_i{}^{T_{1u}}\rangle \quad (4.4.37)$$

of the  $T_{1u}$  acceleration submatrix (4.4.33). For the  $S^{32}F_6$  molecular parameter values  $m = 19$ ,  $M = 32$ ,  $b = 0.2j$ , and  $k = 0.18j$ , there is the following eigenequation:

$$j \begin{pmatrix} 0.0670 & 4.1 \\ 0.00044 & 0.112 \end{pmatrix} \begin{pmatrix} \varepsilon_{\pm} \\ \varepsilon'_{\pm} \end{pmatrix} = \lambda_{\pm}^{T_{1u}} \begin{pmatrix} \varepsilon_{\pm} \\ \varepsilon'_{\pm} \end{pmatrix}, \quad (4.4.38a)$$

where the eigenvalues

$$\lambda_{\pm}^T \lambda_{\pm}^{T_{1u}} = (\omega_{\pm}^{T_{1u}})^2 = 0.138j, \quad \lambda_{\pm}^{T_{1u}} = (\omega_{\pm}^{T_{1u}})^2 = 0.0415j \quad (4.4.38b)$$

are found using Eqs. (4.4.34). The eigenvector solutions are

$$|e_i^{T_{1u}}(+)\rangle = 0.068|c_i^{T_{1u}}\rangle + 0.0012|c'_i{}^{T_{1u}}\rangle, \quad (4.4.39a)$$

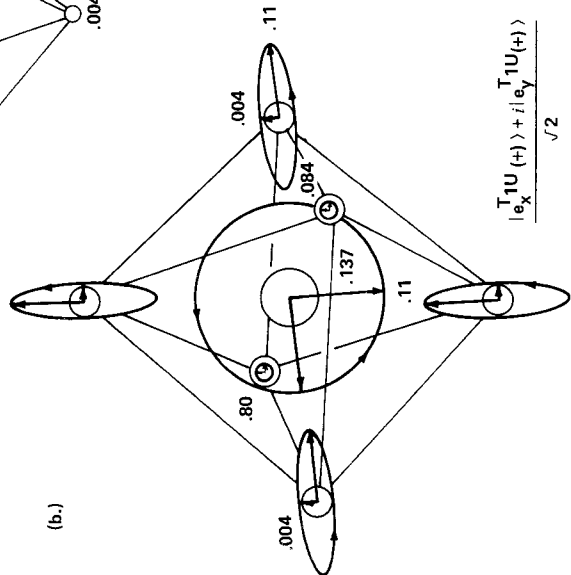
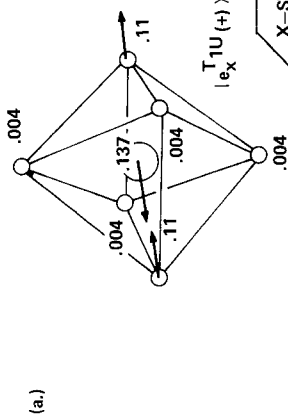
$$|e_i^{T_{1u}}(-)\rangle = 0.114|c_i^{T_{1u}}\rangle - 0.00071|c'_i{}^{T_{1u}}\rangle, \quad (4.4.39b)$$

where the  $m =$  normalization condition

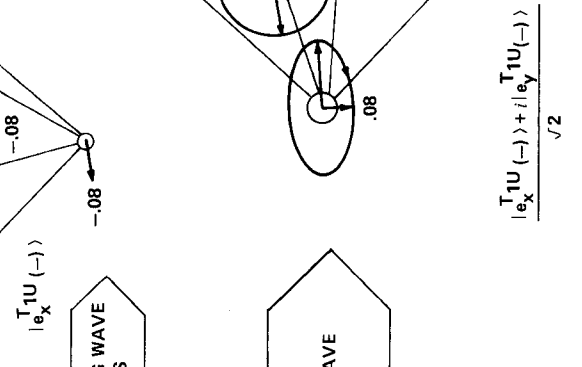
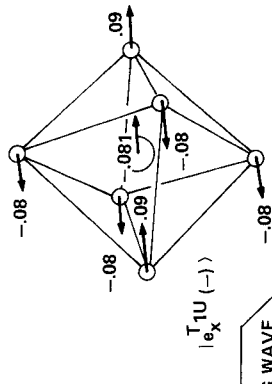
$$\langle (\pm)e | \mathbf{m} | e(\pm) \rangle = 1 \quad (4.4.40)$$

of Eq. (1.4.13a) is used. The first ( $i = 1$ ) partner for the two  $SF_6$  modes is pictured in Figure 4.4.7(a). This was obtained by combining the constrained

HIGH FREQUENCY  
 $T_{1u}$  MODES OF SF<sub>6</sub>  
 ( $\nu_3 \sim 947 \text{ CM}^{-1}$ )



LOW FREQUENCY  
 $T_{1u}$  MODES OF SF<sub>6</sub>  
 ( $\nu_4 \sim 630 \text{ CM}^{-1}$ )



X-STANDING WAVE  
 MODES

X + Y  
 MOVING WAVE  
 MODES

Figure 4.4.7  $T_{1u}$  fundamental motions of  $^{32}\text{SF}_6$  for high-frequency [ $\nu_3$  or (+)] and low-frequency [ $\nu_4$  or (-)] vibrations. (a) Plane-polarized or standing-wave motions. (b) Circularly polarized or moving-wave motions.

motions in Figure (4.4.3(b)) using the coefficients in Eqs. (4.4.39). Note that the displacement of the equatorial fluorine atoms for  $|e_1(+)\rangle$  is

$$\begin{aligned}\langle R_1^3 B | e_1(+)\rangle &= 0.068 \langle R_1^3 B | c_1\rangle + 0.0012 \langle R_1^3 B | c_1'\rangle \\ &= 0.068(-1/2) + 0.0012(32) = 0.004,\end{aligned}\quad (4.4.41)$$

which is quite small compared to the values for the axial atoms. Note that the central atom opposes the axial fluorine atoms in  $|e(+)\rangle$  while it goes along with them in  $|e(-)\rangle$ . Clearly,  $|e(+)\rangle$  has higher frequency because it distorts the strong  $j$  spring more than  $|e(-)\rangle$ . The displacement of the equatorial atoms in  $|e(-)\rangle$  is almost as large as that of the axial atoms. Bear in mind that the precise magnitudes of the  $T_{1u}$  displacements depend on the values of the molecular parameters  $m$ ,  $M$ ,  $b$ ,  $j$ , and  $k$ . The  $T_{1u}$  motions are not entirely fixed by symmetry as are the  $A_{1g}$ ,  $E_g$ ,  $T_{2g}$ , and  $T_{2u}$  motions in Figure 4.4.3.

The  $T_{1u}$  partners  $\{|e_1(\pm)\rangle, |e_2(\pm)\rangle, |e_3(\pm)\rangle\}$  are the same translational distortions pointing along the  $x$ ,  $y$ , and  $z$  directions, respectively. These are the plane-polarized or standing-wave bases. It is important to visualize the motions of the circularly polarized or moving-wave bases,

$$\begin{aligned}|e_{1_4}^{T_{1u}}(\pm)\rangle &= (-|e_1(\pm)\rangle - i|e_2(\pm)\rangle)/\sqrt{2}, \\ |e_{3_4}(\pm)\rangle &= (|e_1(\pm)\rangle - i|e_2(\pm)\rangle)/\sqrt{2}, \\ |e_{0_4}(\pm)\rangle &= |e_3(\pm)\rangle,\end{aligned}\quad (4.4.42)$$

shown in Figure 4.4.7(b). [This transformation of bases was discussed around Eq. (4.2.36).] Notice that each particle has an elliptical orbit. For example, the semimajor and minor orbital axes of the  $xy$ -equatorial fluorine atoms in the  $|e(+)\rangle$  mode are  $a = 0.11$  and  $b = 0.004$ . The classical angular momentum of a mass  $m$  in an elliptical oscillator orbit is

$$l = mab\omega/2.$$

The sum of these momenta for all the atoms in a molecule is the classical VIBRATIONAL ANGULAR MOMENTUM of the system. The coupling of the vibrational momentum to the angular momentum of the molecule as a whole leads to rotational or CORIOLIS splitting of a vibrational line.

### C. Classical Canonical Coordinates

From now on let us demand the  $m$ -normalization conditions

$$\begin{aligned}\langle e_j^\alpha | \mathbf{m} | e_k^\beta \rangle &= \delta^{\alpha\beta} \delta_{jk}, \\ \langle e_j^\alpha | \mathbf{F} | e_k^\beta \rangle &= \delta^{\alpha\beta} \delta_{jk} (\omega^\alpha)^2,\end{aligned}\quad (4.4.43)$$

which were discussed in Section 1.4.A. The  $T_{1u}$  eigenvectors  $|e_j^{T_{1u}}(\pm)\rangle$  have already been made to satisfy this. The other modes  $|e_j^\alpha\rangle$  only involve motion of the mass- $m$  fluorine atoms, and the newly normalized vectors are obtained by affixing a factor  $1/\sqrt{m}$  to the old ones. It is also convenient to use CANONICAL VARIABLES  $(q, p)$  defined by

$$\begin{aligned} q_j^\alpha &= \langle e_j^\alpha | \mathbf{m} | x \rangle, \\ p_j^\alpha &= \langle e_j^\alpha | \mathbf{m} | \dot{x} \rangle. \end{aligned} \tag{4.4.44}$$

The relation between canonical coordinates  $q_j^\alpha$  and “ordinary” coordinates  $X_{lQ} = \langle lQ | X \rangle$  is easily derived:

$$q_j^\alpha = \sum_{Q=A, B, C} \sum_l \langle e_j^\alpha | \mathbf{m} | lQ \rangle \langle lQ | x \rangle. \tag{4.4.45}$$

Here completeness of the original unit states  $|lQ\rangle$  is used. The labeling operator  $l$  ranges over all states in orbit  $Q = A, B,$  and  $C$ .

Expressing the “ordinary” coordinates in terms of the canonical ones is probably more useful. Using the  $m$ -completeness relation (1.4.14) one derives

$$\begin{aligned} X_{lQ} &= \langle lQ | x \rangle = \sum_\alpha \sum_j \langle lQ | e_j^\alpha \rangle \langle e_j^\alpha | \mathbf{m} | x \rangle \\ &= \sum_\alpha \sum_j \langle lQ | e_j^\alpha \rangle q_j^\alpha. \end{aligned} \tag{4.4.46}$$

For example, let us express  $X_{R_3^+ B}$  in terms of  $q_j^\alpha$ . The coefficients  $\langle lQ | e_j^\alpha \rangle$  can be read directly from Figures 4.4.4 and 4.4.7(a):

$$X_{R_3^+ B} = \frac{1}{2\sqrt{m}} q_3^{T_{2g}} - \frac{1}{2\sqrt{m}} q_1^{T_{2u}} + 0.004 q_1^{T_{1u}}(+) - 0.08 q_1^{T_{1u}}(-). \tag{4.4.46}$$

The quantum theory discussed in the following section will give wave functions or statistical distributions for the  $q$ 's. From this one derives an  $X_{lQ}$  wave function through Eq. (4.4.46).

### D. Elementary Quantum Theory of Vibrations

One advantage of the canonical variables (4.4.44) is that they satisfy Hamilton's equations

$$\begin{aligned} \frac{\partial H}{\partial p_i^\alpha} &= \dot{q}_i^\alpha = p_j^\alpha, \\ \frac{\partial H}{\partial q_i^\alpha} &= -\dot{p}_i^\alpha = -(\omega^\alpha)^2 q_j^\alpha, \end{aligned} \tag{4.4.47}$$

for the Hamiltonian

$$H = \sum_{\alpha} \sum_i \left[ (p_i^{\alpha})^2 / 2 + (\omega^{\alpha} q_i^{\alpha})^2 / 2 \right]. \quad (4.4.48)$$

The Hamiltonian describes a collection of independent oscillators each having unit mass and angular frequency  $\omega^{\alpha}$ . According to Dirac's quantization rules the canonical variables  $q_i^{\alpha}$  and  $p_j^{\alpha}$  can be replaced by Hermitian operators  $q_i^{\alpha} = (q_i^{\alpha})^{\dagger}$  and  $p_j^{\alpha} = (p_j^{\alpha})^{\dagger}$  satisfying the commutation relations

$$\left[ q_i^{\alpha}, p_j^{\beta} \right] = \delta^{\alpha\beta} \delta_{ij} 1 \hbar. \quad (4.4.49)$$

These relations and the Hamiltonian (4.4.48) are all that is needed to complete the quantum-mechanical oscillator problem. Most of the work is done once the classical normal modes are found, and the Hamiltonian is reduced to the simple form of Eq. (4.4.48).

An even simpler form can result if the following operators are defined:

$$a_i^{\alpha} \equiv \left( \sqrt{\omega^{\alpha}} q_i^{\alpha} + \frac{i}{\sqrt{\omega^{\alpha}}} p_i^{\alpha} \right) / \sqrt{2\hbar}, \quad (4.4.50a)$$

$$a_i^{\alpha\dagger} \equiv \left( \sqrt{\omega^{\alpha}} q_i^{\alpha} - \frac{i}{\sqrt{\omega^{\alpha}}} p_i^{\alpha} \right) / \sqrt{2\hbar}. \quad (4.4.50b)$$

According to Eq. (4.4.49) they satisfy the following commutation relations:

$$\left[ a_i^{\alpha}, a_j^{\beta\dagger} \right] = \delta^{\alpha\beta} \delta_{ij} 1 \hbar, \quad (4.4.51a)$$

$$\left[ a_i^{\alpha}, a_j^{\beta} \right] = 0 = \left[ a_j^{\beta\dagger}, a_i^{\alpha\dagger} \right]. \quad (4.4.51b)$$

The Hamiltonian is expressed as follows in terms of  $a$  and  $a^{\dagger}$ :

$$H = \sum_{\alpha} \sum_i \frac{\hbar\omega^{\alpha}}{2} \left( a_i^{\alpha\dagger} a_i^{\alpha} + a_i^{\alpha} a_i^{\alpha\dagger} \right) = \sum_{\alpha} \sum_i \hbar\omega^{\alpha} \left( a_i^{\alpha\dagger} a_i^{\alpha} + \frac{1}{2} \right). \quad (4.4.52)$$

The following commutation relations then result:

$$\left[ H, a_i^{\alpha\dagger} \right] = \hbar\omega^{\alpha} a_i^{\alpha\dagger}, \quad \left[ H, a_i^{\alpha} \right] = -\hbar\omega^{\alpha} a_i^{\alpha}. \quad (4.4.53)$$

Operators  $a^\dagger$  and  $a$  are called RAISING and LOWERING operators because of their effect on eigenstates. Suppose eigenstate  $|\varepsilon\rangle$  satisfies  $H|\varepsilon\rangle = \varepsilon|\varepsilon\rangle$ . Then the eigenvalue of  $a^\dagger|\varepsilon\rangle$  will be raised by  $\hbar\omega$  as follows:

$$\begin{aligned} H a_i^{\alpha\dagger} |\varepsilon\rangle &= \left( \left[ H, a_i^{\alpha\dagger} \right] + a_i^{\alpha\dagger} H \right) |\varepsilon\rangle \\ &= (\hbar\omega^\alpha + \varepsilon) a_i^{\alpha\dagger} |\varepsilon\rangle, \end{aligned} \quad (4.4.54)$$

and the eigenvalue of  $a|\varepsilon\rangle$  is lowered by the same amount:

$$H a_i^\alpha |\varepsilon\rangle = (\varepsilon - \hbar\omega^\alpha) a_i^\alpha |\varepsilon\rangle. \quad (4.4.55)$$

It is possible to produce all eigenstates  $|\varepsilon\rangle$  by applying raising operators to the ground state  $|0 \cdots\rangle$ . The ground state is defined to be that state which cannot be lowered.

$$a_i^\alpha |0 \cdots\rangle \equiv 0 \quad (\text{for all } \alpha, i). \quad (4.4.56)$$

Then the eigenstates  $|\varepsilon\rangle = |\cdots n_i^\alpha \cdots n_j^\beta \cdots\rangle$  are

$$|\cdots n_i^\alpha \cdots n_j^\beta \cdots\rangle = \cdots \left( a_i^{\alpha\dagger} \right)^{n_i^\alpha} \cdots \left( a_j^\beta \right)^{n_j^\beta} \cdots |0 \cdots\rangle / \sqrt{N_{\cdots n \cdots n'}}, \quad (4.4.57)$$

where the  $1/\sqrt{N}$  factor normalizes the state so that

$$\langle \cdots n_i^\alpha \cdots n_j^\beta \cdots | \cdots n_i^\alpha \cdots n_j^\beta \cdots \rangle = 1. \quad (4.4.58)$$

Derivation of the normalization and eigenvalues involves the following operator relations whose proofs are left as exercises:

$$\begin{aligned} [a, (a^\dagger)^n] &= n (a^\dagger)^{n-1}, \\ [a^2, (a^\dagger)^n] &= n(n-1)(a^\dagger)^{n-2} + 2n(a^\dagger)^{n-1} a + (a^\dagger)^n a^2, \\ &\vdots \\ [a^m, (a^\dagger)^n] &= \sum_{r=0}^m (n!/(n-m+r)!)(m!/(m-r)!r!)(a^\dagger)^{n-m+r} (a)^r. \end{aligned} \quad (4.4.60)$$

In the preceding the irrep labels  $\binom{\alpha}{i}$  are assumed to be the same and are deleted for typographical simplicity. The normalization is now derived from a

special case of identity (4.4.60):

$$\begin{aligned} \langle 0 \cdots | (a)^n (a^\dagger)^n | 0 \cdots \rangle &= \langle 0 \cdots | [(a)^n (a^\dagger)^n] + (a^\dagger)^n (a)^n | 0 \cdots \rangle \\ &= n! + 0 \cdots . \end{aligned}$$

This holds for each and every  $\begin{pmatrix} \alpha \\ i \end{pmatrix}$ ; hence  $n$  is given:

$$N \dots n_i^\alpha \dots n_j^\beta \dots = \cdots (n_i^\alpha)! \cdots (n_j^\beta)! \cdots . \quad (4.4.61)$$

The general raising and lowering relations result, also:

$$\begin{aligned} a_i^{\alpha\dagger} | \cdots n_i^\alpha \cdots n_j^\beta \cdots \rangle &= \sqrt{n_i^\alpha + 1} | \cdots n_i^\alpha + 1 \cdots n_j^\beta \cdots \rangle, \\ a_i^\alpha | \cdots n_i^\alpha \cdots n_j^\beta \cdots \rangle &= \sqrt{n_i^\alpha} | \cdots n_i^\alpha - 1 \cdots n_j^\beta \cdots \rangle. \end{aligned} \quad (4.4.62)$$

Using these relations it is easy to derive the eigenvalue spectrum of the Hamiltonian (4.4.52):

$$H \cdots | n_i^\alpha \cdots n_j^\beta \cdots \rangle = \left[ \sum_\gamma \sum_k (n_k^\alpha + \frac{1}{2}) \hbar \omega^\gamma \right] | \cdots n_i^\alpha \cdots n_j^\beta \cdots \rangle. \quad (4.4.63)$$

The energy eigenvalues for the hexafluoride molecules are given by

$$\begin{aligned} \varepsilon &= (n^{A_{1g}} + 1/2) \hbar \omega^{A_{1g}} + (n_1^{E_g} + n_2^{E_g} + 1) \hbar \omega^{E_g} \\ &+ (n_1^{T_{1u}}(+) + n_2^{T_{1u}}(+) + n_3^{T_{1u}}(+) + 3/2) \hbar \omega^{T_{1u}}(+) \\ &+ (n_1^{T_{2u}} + n_2^{T_{2u}} + n_3^{T_{2u}} + 3/2) \hbar \omega^{T_{2u}} + (n_1^{T_{2g}} + n_2^{T_{2g}} + n_3^{T_{2g}} + 3/2) \hbar \omega^{T_{2g}} \\ &+ (n_1^{T_{1u}}(-) + n_2^{T_{1u}}(-) + n_3^{T_{1u}}(-) + 3/2) \hbar \omega^{T_{1u}}(-). \end{aligned} \quad (4.4.63)_x$$

A sketch of octahedral hexafluoride energy-levels is shown in Figure 4.4.8. See Figs. 6.6.2–4 for a more complete and accurate diagram of levels for  $\text{SF}_6$ ,  $\text{UF}_6$ , and  $\text{SiF}_4$ . The levels are labeled by a conventional spectroscopic notation  $\nu_1$  for  $A_{1g}$ ,  $\nu_2$  for  $E_g$ ,  $\nu_3$  for  $T_{1u}$ ,  $\nu_4$  for  $T_{2g}$ , and  $\nu_5$  for  $T_{2u}$ . When the  $A_{1g}$ ,  $E_g$ , ... states are doubly excited they are labeled  $2\nu_1, 2\nu_2, \dots$ , etc. These are called double HARMONICS, and similarly for higher excitations.

The number of levels in a given  $n$ th harmonic depends strongly on the degeneracy of the fundamental. A second harmonic of  $E_g$  labeled  $(2\nu_2)$  has three degenerate states:

$$| \dots, n_1^{E_g}, n_2^{E_g}, \dots (2\nu_2) \rangle = \{ | \dots, 2, 0, \dots \rangle, | \dots, 1, 1, \dots \rangle, | \dots, 0, 2, \dots \rangle \},$$



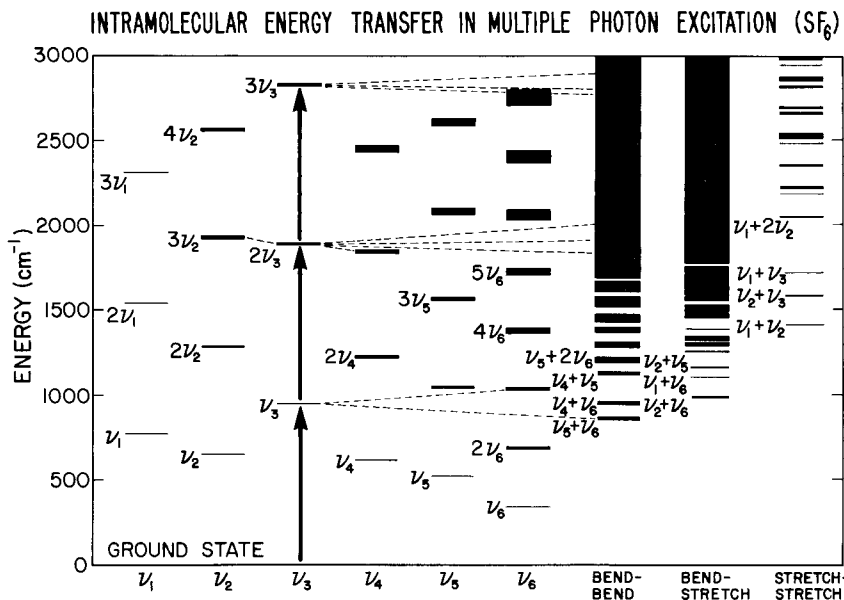


**Figure 4.4.8** Sketch of SF<sub>6</sub> quantum vibration levels. The density of levels increases rapidly at higher energy. Standard spectroscopic notation is used. For example, two quanta of the T<sub>1u</sub>(+) or ν<sub>3</sub> vibration is labeled 2ν<sub>3</sub>. The figure shows expected flow of energy during laser excitation of the ν<sub>3</sub> “ladder.” (Due to Robin S. McDowell and Jay R. Ackerhalt of Los Alamos National Laboratory.)

while a second harmonic of T<sub>1u</sub> (2ν<sub>3</sub>) has six degenerate states:

$$\begin{aligned}
 & | \dots, n_1^{T_{1u}}, n_2^{T_{1u}}, n_3^{T_{1u}}, \dots (2\nu_3) \rangle \\
 & = \{ | \dots, 2, 0, 0, \dots \rangle, | \dots, 0, 2, 0, \dots \rangle, | \dots, 0, 0, 2, \dots \rangle, \\
 & \quad | \dots, 1, 1, 0, \dots \rangle, | \dots, 1, 0, 1, \dots \rangle, | \dots, 0, 0, 1, \dots \rangle \}.
 \end{aligned}$$

In general the *n*th harmonic of an *l*<sup>α</sup>-dimensional fundamental vibration has degeneracy *d*(*n*) equal to a binomial coefficient in Pascals’ triangle:

Fundamental dimension:	<i>l</i> =	1	2	3	4	5					
ground state:	<i>n</i> = 0	<i>d</i> = 1	1	1	1	1	...				
fundamental:	<i>n</i> = 1		1	2	3	4	5	...			
second harmonic:	<i>n</i> = 2			1	3	6	10	15	...		
third harmonic:	<i>n</i> = 3				1	4	10	20	35	...	
fourth harmonic:	<i>n</i> = 4					1	5	15	35	70	...

(4.4.64)

The formula for the degeneracy is

$$d(n^\alpha) = (l^\alpha + n^\alpha - 1)! / n^\alpha!(l^\alpha - 1)! \tag{4.4.65}$$

The general level is a combination of each vibration  $\alpha, \beta, \dots$  excited  $n^\alpha, n^\beta, \dots$  times, respectively. Its degeneracy is simply the product

$$d(n^\alpha, n^\beta, \dots) = d(n^\alpha) d(n^\beta) \cdots \quad (4.4.66)$$

The  $d$  degeneracies are split by anharmonic terms such as  $q^3, q^4, q^3q', \dots$ , etc. as explained in Section 6.6.

Finally, let us consider briefly the wave function of the oscillator eigenstates. The ground-state conditions (4.4.56) take the form

$$\begin{aligned} \langle q \cdots | \sqrt{\omega} q + (i/\sqrt{\omega}) p | 0 \cdots \rangle &= 0, \\ \sqrt{\omega} q + (i/\sqrt{\omega})(\hbar/i) \frac{\partial}{\partial q} \langle q \cdots | 0 \cdots \rangle &= 0, \end{aligned} \quad (4.4.67)$$

in the coordinate representation where  $p \rightarrow (\hbar/i) \partial/\partial q$ . The solution to these differential equations is a product of Gaussian wave functions:

$$\langle q \cdots | 0 \cdots \rangle = \psi_{0\dots}(q \cdots) = (e^{-\omega(q)^2/2\hbar})(\cdots) \quad (4.4.68)$$

For each coordinate  $q = q^{A_{1g}}, q_{1g}^{E_g}, q_{2g}^{E_g}, q_{1u}^{T_{1u}}, \dots$  there is a Gaussian distribution. An excited state is obtained by raising a particular oscillator one unit. Starting with a Gaussian ground-state function one produces the wave function of state  $|1, 0, \dots\rangle$  as follows

$$\begin{aligned} \psi_{1,0,\dots}(q, \dots) &= \left( \sqrt{\omega} q - (\hbar/\sqrt{\omega}) \frac{\partial}{\partial q} \right) \psi_{0,0,\dots}(q, \dots) \\ &= (2\sqrt{\omega} q e^{-\omega(q)^2/2\hbar})(\cdots) \end{aligned} \quad (4.4.69)$$

Finally, the  $n$ th-excited state for one coordinate is

$$\psi_{n,0,\dots}(q, \dots) = ((\omega 2^n \hbar \pi n!) H_n(q\sqrt{\omega}/\hbar) e^{-\omega(q)^2/2\hbar})(\cdots), \quad (4.4.70)$$

where  $H_n(x)$  is the  $n$ th Hermite polynomial.

Oscillator wave functions  $\psi(q)$  die off quickly when  $q$  exceeds the magnitude of the CLASSICAL TURNING POINT  $q(\text{TP})$ . This is the classical point of maximum excursion for  $q$  at which momentum  $\sum_i (p_i^\alpha)^2$  is zero in the Hamiltonian (4.4.48):

$$H = (\omega^\alpha)^2 (q^\alpha(\text{TP}))^2/2;$$

setting  $H$  equal to the oscillator eigenvalue we have

$$(n^\alpha + l^\alpha/2) \hbar \omega^\alpha = (\omega^\alpha)^2 (q^\alpha(\text{TP}))^2/2$$

or

$$q^\alpha(\text{TP}) = [(2n^\alpha + l^\alpha) \hbar / \omega^\alpha]^{1/2}, \quad (4.4.71)$$

where  $l^\alpha$  is the number of partners  $\{q_1^\alpha, q_2^\alpha, \dots, q_{l^\alpha}^\alpha\}$  in mode  $\alpha$  and  $n^\alpha$  is the oscillator quantum number.

## ADDITIONAL READING

It is hard to find a simple physical treatment of induced representations and subgroup coset spaces. The references cited below are not simple to read.

G.W. Mackey, *Induced Representations of Groups and Quantum Mechanics* (Benjamin, New York, 1968).

A.J. Coleman, *Induced Representations and the Symmetric Group*, Queens University Papers on Mathematics (Queens University Press, Kingston, Ontario, 1965).

The first applications of induced representations to tetrahedral and octahedral fine structure are given in the papers listed below.

W.G. Harter and C.W. Patterson, *Phys. Rev. Lett.*, **38**, 224 (1977); *J. Chem. Phys.*, **66**, 4872 (1977).

W.G. Harter, C.W. Patterson, and F.J. Ja Paixao, *Rev. Mod. Phys.*, **50**, 37 (1978).

W.G. Harter and C.W. Patterson, *J. Math. Phys.*, **20**, 1453 (1979).

The excerpt of methane spectra shown in Figure 4.3.3 was given in Allen Pine's article.

A.S. Pine, *J. Opt. Soc. Am.*, **66**, 97 (1976).

A review of the spectroscopy of octahedral and tetrahedral molecules for the laser isotope program is the following:

R.S. McDowell, C.W. Patterson and W.G. Harter, *Los Alamos Science*, **3**, 38 (1982).

A qualitative discussion of symmetry breaking is given in the following: R. Peierls, (Dirac Memorial Lecture) *Contemporary Physics*, **33**, 221 (1992)

## PROBLEMS

### Section 4.1

**4.1.1** Generally one does not need to tabulate representations of all elements of a given group in order to define them. Some smaller number of elements  $\{g_1, g_2, \dots\}$  can be chosen whose products  $\{g_1^2, g_2^2, \dots, g_1 g_2, g_1 g_2^2, \dots, g_1 p_{g_2} q_{g_1}, \dots\}$  finally generate each and every element of the group. Such elements are called *generators* of the group. What are the minimal number of generators of the groups listed below? (Hint: Consider the Hamilton turns.)

- (a)  $C_3$ , (b)  $C_{3v}$ , (c)  $D_4$ , (d)  $O$ , (e)  $O_h$ .

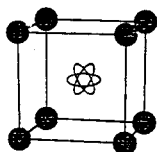
- 4.1.2. (a) How many elements of the octahedral group  $O$  commute with the  $120^\circ$  rotation operator  $r_1$ ? Do these elements form a symmetry group? If so which and why, or why not?
- (b) How many elements of the octahedral group  $O$  commute with the  $90^\circ$  rotation operator  $R_3$ ? Do these elements form a symmetry group? If so which and why, or why not?
- 4.1.3 There are several  $D_2$  symmetry subgroups in the octahedral group. Identify them and tell which if any of these are normal subgroups. Are there any normal  $D_3$  or  $D_4$  subgroups?

## Section 4.2

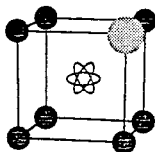
- 4.2.1 Construct correlation tables and level-splitting diagrams for the following tetrahedral ( $T_d$ ) and octahedral ( $O_h$ ) subgroup chains.
- (a)  $T_d \supset C_{3v} \supset C_v$ .      (d)  $O_h \supset D_{4h} \supset D_{2h}$ .  
 (b)  $T_d \supset D_{2d} \supset C_{2v}$ .      (e)  $O_h \supset C_{4v} \supset C_4$ .  
 (c)  $T_d \supset C_{3v} \supset C_3$ .      (f)  $O_h \supset T_h \supset D_2$ .
- 4.2.2 Compare the two different types of  $D_2$  subgroup correlations within  $O$  symmetry by sketching level-splitting diagrams.

$$\begin{array}{c}
 p_x \\
 p_y \equiv \\
 p_z
 \end{array}
 \quad l=1$$

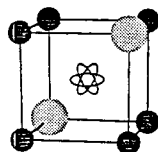
- 4.2.3 Describe and/or label the level splitting that would (or would not) happen to an atomic ( $l = 1$ ) $p$  orbital triplet placed in the center of the following "cages." (Give symmetry group and irreps for each case.)



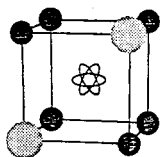
(a) Eight equal charges on cubic vertices.



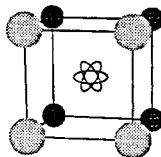
(b) Same as (a) but one extra charge on cubic vertex.



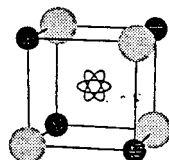
(c) Same as (a) but two equal charges on cubic body diagonal.



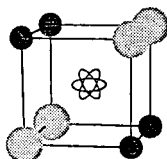
(d) Same as (a) but two equal charges on cubic face diagonal.



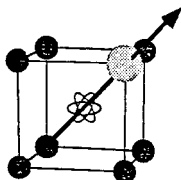
(e) Same as (a) but four equal charges on cubic face.



(f) Same as (a) but four extra charges on alternate vertices.



(g) Same as (a) but four equal charges on cubic body diagonals.



(h) Same as (b) but with a magnetic field along cubic diagonal.

## Section 4.3

**4.3.1** Let each  $C_3$  coset  $\{\mathbf{1}C_3, g_2C_3, g_3C_3, \dots\}$  in octahedral group  $O$  be associated with a ket vector  $\{|1\rangle, |g_2\rangle, |g_3\rangle, \dots\}$ , respectively. Let a representation  $\mathcal{S}(g)$  of each element  $g$  of the group  $O$  be defined by

$$g|g_k\rangle = |gg_k\rangle = |g_jh\rangle,$$

where  $gg_k$  is an element of coset  $g_jC_3$ , or

$$\begin{aligned} \mathcal{S}_{jk}(g) &= \langle g_j|g|g_k\rangle = 1, & \text{if } g_j^{-1}gg_k \text{ is in subgroup } C_3, \\ &= 0, & \text{otherwise.} \end{aligned}$$

[This is the *principal*  $C_3$  induced representation of  $O$ . It is labeled  $\mathcal{S} = D^0(\text{of } C_3) \uparrow O$ .]

- Construct matrices  $\mathcal{S}(\mathbf{1}), \mathcal{S}(r_1), \mathcal{S}(R_1^2), \mathcal{S}(R_1), \mathcal{S}(i_1)$ .
- Use the traces of these representations to compute which and how many irreducible representations of  $O$  will appear if  $\mathcal{S}$  is reduced. Compare with the results predicted using the correlation table between  $C_3$  and  $O$  and the Frobenius reciprocity theorem.
- Do parts (a) and (b) for the cosets  $\{\mathbf{1}D_4, g_2D_4, g_3D_4, \dots\}$  of the subgroup  $D_4$  which contains the  $90^\circ$   $z$  axial rotation  $\mathbf{R}_3$ .

**4.3.2** Let each  $C_{3v}$  coset  $\{\mathbf{1}C_{3v}, g_2C_{3v}, g_3C_{3v}, \dots\}$  in octahedral group  $O_h$  be associated with a pair of ket vectors  $\{|1,1\rangle, |1,2\rangle, |g_2,1\rangle,$

$|g_2, 2\rangle, |g_3, 1\rangle, |g_3, 2\rangle, \dots$ , respectively. Let a representation  $\mathcal{S}(g)$  of each element  $g$  of the group  $O_h$  be defined by

$$g|g_k, 1\rangle = D_{1,1}^E(g_j^{-1}gg_k)|g_j, 1\rangle + D_{2,1}^E(g_j^{-1}gg_k)|g_j, 2\rangle,$$

where  $gg_k$  is in coset  $g_j C_{3v}$ ,

$$g|g_k, 2\rangle = D_{1,2}^E(g_j^{-1}gg_k)|g_j, 1\rangle + D_{2,2}^E(g_j^{-1}gg_k)|g_j, 2\rangle,$$

or  $g_j^{-1}gg_k$  is in subgroup  $C_{3v}$ ,

or

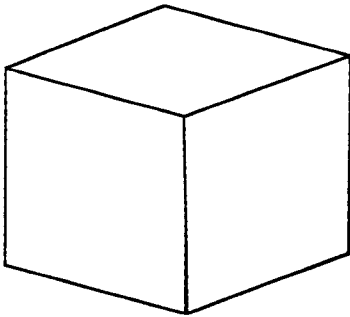
$$\begin{aligned} \mathcal{S}_{j,a;k,b} &= \langle g_j, a | g | g_k, b \rangle = D_{a,b}^E(g_j^{-1}gg_k), & \text{if } g_j^{-1}gg_k \text{ is in subgroup } C_{3v}, \\ &= 0, & \text{otherwise.} \end{aligned}$$

[This is the  $E$  of  $C_{3v}$  induced representation of  $O_h$ . It is labeled  $\mathcal{S} = D^E(\text{of } C_{3v}) \uparrow O_h$ .]

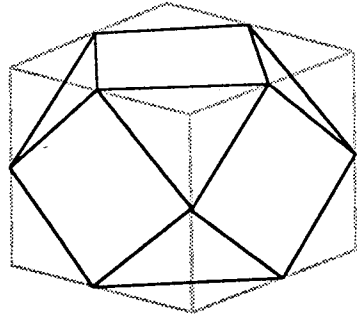
- (a) Construct matrices  $\mathcal{S}(\mathbf{1})$ ,  $\mathcal{S}(r_1)$ ,  $\mathcal{S}(IR_1^2)$ ,  $\mathcal{S}(IR_1)$ , and  $\mathcal{S}(Ii_1)$ .
- (b) Use the traces of these representations to compute which and how many irreducible representations of  $O_h$  will appear if  $\mathcal{S}$  is reduced. Compare with the results predicted using the correlation table between  $C_{3v}$  and  $O_h$  and the Frobenius reciprocity theorem.
- (c) Do parts (a) and (b) for the cosets  $\{1D_{4h}, g_2D_{4h}, g_3D_{4h}, \dots\}$  of the subgroup  $D_{4h}$  which contains the  $90^\circ$   $z$ -axial rotation  $R_3$ . (Use the  $E_g$  representation of  $D_{4h}$ .)

**4.3.3** Suppose a quantum particle can tunnel between eight equilibrium positions or potential wells each being located at the vertices of a cube. Let the local energy of each well be  $H$ , and let the nearest-neighbor tunneling rates be  $-S$ , while the next-nearest-neighbor tunneling rates are equal to  $-T$ . Let the local wave function associated with each well be trigonally symmetric; that is, let:  $\mathbf{r}_1|1\rangle = |1\rangle$  and similarly for each of the local states  $|g_k\rangle$ .

- (a) Label the states using coset elements derived in Problem 4.3.1 or 4.3.2.
- (b) Construct the first two rows of tunneling Hamiltonian matrix in terms of  $H$ ,  $S$ , and  $T$ .
- (c) Construct symmetry defined states  $\mathbf{P}_{ij}^\alpha|1\rangle$  and sketch the wave functions. You may want to compare the states generated by the irreducible representations defined by different subgroup chains  $O_h-C_{3v}-C_c$  and  $O_h-D_{4h}-D_{2h}$  or other.



Cube



Truncated Cube Octahedron

- (d) Display eigenvalue spectrum for the case  $S > 0$  and  $T = 0$ .  
 (e) Display eigenvalue spectrum for the case  $S = 0$  and  $T > 0$ .

**4.3.4** Suppose a quantum particle can tunnel between 12 equilibrium positions or potential wells each being located at the vertices of a cubic octahedron. Let the local energy of each well be  $H$ , and let the nearest-neighbor tunneling rates be  $-S$ , while the next-nearest-neighbor tunneling rates are equal to  $-T$ . Let the local wave function associated with each well be  $C_{2v}$  symmetric; that is, let  $\mathbf{i}_1|1\rangle = |1\rangle$  and similarly for each of the local states  $|\mathbf{g}_k\rangle$ .

- (a) Label the states using coset elements.  
 (b) Construct the first two rows of tunneling Hamiltonian matrix in terms of  $H$ ,  $S$ , and  $T$ .  
 (c) Construct symmetry-defined states  $\mathbf{P}_{ij}^\alpha|1\rangle$  and sketch the wave functions. You may want to compare the states generated by the irreducible representations defined by different subgroup chains  $O_h-C_{2v}-C_v$  and  $O_h-D_{4h}-D_{2h}$  or other.  
 (d) Display eigenvalue spectrum for the case  $S > 0$  and  $T = 0$ .  
 (e) Display eigenvalue spectrum for the case  $S = 0$  and  $T > 0$ .

**4.3.5** The character tables for the icosahedral symmetry  $Y$  and the fivefold dihedral subgroup  $D_5$  are listed in the following.

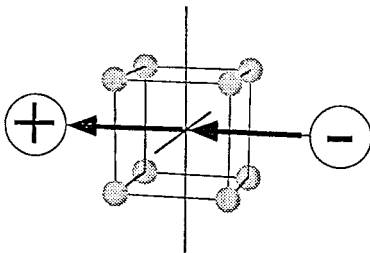
Y classes	$0^\circ$	$72^\circ$	$144^\circ$	$120^\circ$	$180^\circ$
$c_g$ order	1	12	12	20	15
$A$	1	1	1	1	1
$T_1$	3	$G +$	$G -$	0	-1
$T_3$	3	$G -$	$G +$	0	-1
$G$	4	-1	-1	1	0
$H$	5	0	0	-1	1

The numbers  $G +$  and  $G -$  are the “golden ratios”  $G + = (1 + \sqrt{5})/2$  and  $G - = (1 - \sqrt{5})/2$ .

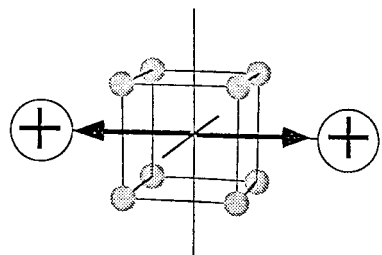
$D_5$ classes	$0^\circ$	$72^\circ$	$144^\circ$	$180^\circ$
$c_g$ order	1	2	2	5
$A_1$	1	1	1	1
$A_2$	1	1	1	-1
$E_1$	2	$-G -$	$-G +$	0
$E_2$	2	$-G +$	$-G -$	0

- (a) Show how the icosahedral levels split when the symmetry is reduced to  $D_5$  and then to  $C_5$ . Construct a correlation table between the  $Y$  group and these two subgroups.
- (b) Show how the icosahedral levels split when the symmetry is reduced to  $D_3$  and then to  $C_3$ . Construct a correlation table between the  $Y$  group and these two subgroups.

**4.3.6** Compute the detailed effects of field perturbations on a charged particle tunneling through the cubic eight-well system (Recall Problem 4.3.3). Plot the energy levels as a function of the field and draw eigenfunction sketches for extreme field limits. Label all levels with appropriate (maximal) symmetry labels.



(a) Dipole field on four-fold axis.



(b) Quadrupole field on four-fold axis.

- (c) Sketch (without detailed calculation) the energy level effects of the same fields on the three-fold axis. Use physical arguments and correlation results.
- (d) Check the results of (c) with detailed diagonalization of the model Hamiltonians.



**Section 4.4**

**4.4.1** Construct and solve a mechanical force model for the methane-like  $XY_4$  tetrahedral molecule. Using the data listed below try to fit your model to  $\text{SiF}_4$ ,  $\text{CF}_4$ ,  $\text{CD}_4$  or  $\text{CH}_4$  fundamental frequencies.

$$\begin{aligned} \text{SiF}_4: \quad & \nu_1 = 801 \text{ cm}^{-1}; & \nu_2 = 264 \text{ mm}^{-1}; & \nu_3, \nu_4 = 382 \text{ cm}^{-1}, 1032 \text{ cm}^{-1}; \\ \text{CF}_4: \quad & \nu_1 = 908 \text{ cm}^{-1}; & \nu_2 = 435 \text{ cm}^{-1}; & \nu_3, \nu_4 = 632 \text{ cm}^{-1}, 1283 \text{ cm}^{-1}; \\ \text{CD}_4: \quad & \nu_1 = 2069 \text{ cm}^{-1}; & \nu_2 = 1092 \text{ cm}^{-1}; & \nu_3, \nu_4 = 996 \text{ cm}^{-1}, 2259 \text{ cm}^{-1}; \\ \text{CH}_4: \quad & \nu_1 = 2917 \text{ cm}^{-1}; & \nu_2 = 1534 \text{ cm}^{-1}; & \nu_3, \nu_4 = 1306 \text{ cm}^{-1}, 3019 \text{ cm}^{-1}. \end{aligned}$$

- 4.4.2 (a)** Construct and solve a mechanical force model for a cubic  $X_8$  molecule using  $O_h$  symmetry.
- (b)** Label the nonzero frequency modes of the cubic molecule  $\text{C}_8\text{H}_8$  (cubane).

## 4 THEORY AND APPLICATIONS OF HIGHER FINITE SYMMETRY AND INDUCED REPRESENTATIONS

- 4.1 Octahedral Symmetries and Their Characters / 227
    - A. Octahedral Group ( $O$ ) / 228
    - B. Full Octahedral Group ( $O_h$ ) / 234
    - C. Full Tetrahedral Symmetry  $T_d$  / 236
    - D. Partial Tetrahedral Symmetries  $T$  and  $T_h$  / 236
  - 4.2 Irreducible Representations of Octahedral Symmetry / 237
    - A. Subgroup Chains and Idempotent Splitting / 237
    - B. More Subgroup Correlations / 231
    - C. Conjugate and Normal Subgroups / 254
  - 4.3 Introduction to Symmetry Breaking and Induced Representations / 255
    - A. Octahedral Models and Induced Representations / 256
    - B. Model Solving and Induced Representation Reduction / 259
    - C. The Frobenius Reciprocity Theorem and Factored  $P$ -Operators / 264
    - D. Spontaneous or Internal Symmetry Breaking / 269
    - E. External Symmetry Breaking / 271
  - 4.4 Vibrations of Octahedral Hexafluoride Molecules / 286
    - A. Projection Analysis / 286
    - B. Solving Equations of Motion / 292
    - C. Classical Canonical Coordinates / 301
    - D. Elementary Quantum Theory of Vibrations / 302
- Additional Reading / 308
- Problems / 308

TABLE F.2.1  $O$ -Group Table

1	$r_1$	$r_2$	$r_3$	$r_4$	$r_1'$	$r_2'$	$r_3'$	$r_4'$	$R_1^1$	$R_2^1$	$R_3^1$	$R_4^1$	$R_1^2$	$R_2^2$	$R_3^2$	$R_4^2$	$i_1$	$i_2$	$i_3$	$i_4$	$i_5$	$i_6$	
$r_1$	$r_1^2$	$-r_2^2$	$-r_3^2$	$r_4^2$	1	$-R_2^2$	$-R_3^2$	$-R_4^2$	$i_3$	$i_6$	$i_1$	$i_2$	$i_4$	$-R_1^1$	$-R_2^1$	$-R_3^1$	$R_1^1$	$i_5$	$R_2^2$	$i_2$	$-i_4$	$R_1^1$	
$r_2$	$-r_3^2$	$r_2^2$	$r_1^2$	$r_4^2$	$R_2^2$	-1	$R_1^2$	$-R_3^2$	$R_3$	$-R_1^1$	$i_3$	$i_6$	$-R_2^1$	$R_2^1$	$-R_3^1$	$R_1^1$	$i_6$	$R_1$	$R_2$	$-i_1$	$R_3^3$	$i_1$	
$r_3$	$-r_4^2$	$-r_1^2$	$r_3^2$	$r_4^2$	$R_3^2$	$-R_1^2$	-1	$R_2^2$	$-i_4$	$R_1$	$-R_2^1$	$R_3^3$	$R_3^1$	$R_1^1$	$i_2$	$i_6$	$i_5$	$R_1^1$	$i_1$	$R_2$	$-i_3$	$R_3$	
$r_4$	$-r_2^2$	$-r_3^2$	$r_1^2$	$r_4^2$	$R_4^2$	$-R_2^2$	-1	$R_3^2$	$-R_3$	$-i_5$	$R_2$	$-i_4$	$-R_3^1$	$R_2^1$	$-R_3^1$	$R_1^1$	$R_1$	$i_6$	$i_2$	$R_2^2$	$R_3$	$i_3$	
$r_1^2$	-1	$R_1^1$	$R_2^1$	$R_3^1$	$-R_1$	$r_3$	$r_4$	$r_2$	$i_2$	$R_3^3$	$R_1^1$	$-i_3$	$-i_6$	$-R_3$	$-R_2^1$	$-R_3^1$	$-R_3$	$-i_4$	$-R_3$	$-R_1^1$	$i_5$	$-i_2$	$-R_2$
$r_2^2$	$-R_1^1$	1	$R_3^1$	$-R_2^1$	$r_4$	$-r_2$	$r_1$	$r_3$	$i_6$	$R_2^1$	$-R_1$	$-i_3$	$-i_6$	$-R_3$	$-R_2^1$	$-R_3^1$	$-R_3$	$i_4$	$-R_3$	$-i_6$	$-i_2$	$-R_2$	
$r_3^2$	$-R_2^1$	$-R_3^1$	-1	$R_1^1$	$r_2$	$r_4$	$-r_3$	$r_1$	$-R_2$	$-i_4$	$-i_6$	$-R_3$	$R_3$	$-R_1^1$	$-R_3^1$	$-R_3$	$-R_3$	$-i_3$	$-R_3$	$-i_6$	$-i_2$	$-R_2$	
$r_4^2$	$-R_3^1$	$R_2^1$	$-R_1^1$	-1	$r_3$	$r_1$	$r_2$	$-r_4$	$-i_1$	$-R_3$	$-i_5$	$-R_2^1$	$-i_4$	$R_1$	$-R_3^1$	$-R_2^1$	$-R_2$	$-R_3^3$	$i_5$	$R_1$	$-i_1$	$-R_2^2$	
$R_1^1$	$-i_4$	$r_3$	$-r_2$	$r_1$	$r_2^2$	$-r_1^2$	$r_4^2$	$-r_3^2$	$R_1^1$	$i_1$	$-i_4$	$-R_1$	$i_2$	$-i_3$	$-R_2^1$	$-R_2^1$	$-R_2$	$-R_2$	$R_3^3$	$R_3$	$-i_6$	$i_5$	
$R_2^1$	$-r_2$	$r_1$	$r_4$	$-r_3$	$r_3^2$	$-r_4^2$	$-r_1^2$	$r_2^2$	$-i_5$	$R_2^1$	$i_3$	$-i_6$	$-R_2$	$-R_2^1$	$-R_3^1$	$-R_2^1$	$-R_2$	$-i_4$	$-R_3$	$R_3^3$	$R_1$	$R_1^1$	
$R_3^1$	$-r_3$	$-r_4$	$r_1$	$r_2$	$r_4^2$	$r_3^2$	$-r_2^2$	$-r_1^2$	$i_6$	$i_2$	$R_3^3$	$-i_5$	$-i_1$	$-R_3$	$-R_2^1$	$-R_3^1$	$-R_3$	$R_2^2$	$R_2^1$	$-i_3$	$R_1^1$	$-R_1$	
$R_1$	$i_1$	$-R_2^2$	$-i_2$	$R_2$	$R_3^3$	$-i_3$	$-R_3$	$i_4$	$R_1^1$	$r_1$	$-r_4^2$	-1	$-R_3$	$R_2^1$	$-R_2^1$	$-R_3^1$	$r_2^2$	$-r_4$	$r_1^2$	$-r_3^2$	$-R_2^2$	$R_3^3$	
$R_2$	$i_3$	$R_3$	$-R_3^3$	$i_4$	$R_1^1$	$i_5$	$-i_6$	$-R_1$	$-r_2^2$	$R_2^1$	$r_1$	$r_3^2$	-1	$-r_4$	-1	$-r_4$	$R_2^1$	$R_3^3$	$-r_2$	$-r_3$	$-r_4^2$	$r_1^2$	
$R_3$	$i_6$	$i_5$	$R_1$	$-R_1^1$	$R_3^3$	$-R_2$	$-i_2$	$-i_1$	$r_1$	$-r_3^2$	$R_3^3$	$-r_2$	$r_4^2$	-1	$-r_4$	$-r_3$	$r_2^2$	$-R_2^1$	$R_2^2$	$-R_1^1$	$-r_4$	$-r_3$	
$R_1^1$	$-R_2$	$-i_2$	$R_2^2$	$i_1$	$-i_3$	$-R_3^3$	$i_4$	$R_3$	-1	$-r_4$	$r_3^2$	$-R_1^1$	$r_2$	$-r_1^2$	$r_2$	$-r_1^2$	$-r_1$	$r_3$	$r_2^2$	$-r_4^2$	$-R_3^3$	$-R_2^2$	
$R_2^1$	$-R_3$	$i_3$	$i_4$	$R_3^3$	$-i_6$	$R_1$	$-R_1^1$	$i_5$	$r_4^2$	-1	$-r_2$	$-r_1^2$	$-R_2^1$	$r_3$	$-R_2^1$	$r_3$	$-R_3^3$	$R_1^1$	$-R_2^1$	$-r_1$	$-r_4$	$-r_2^2$	
$R_3^1$	$-R_1$	$R_1^1$	$i_6$	$i_5$	$-i_1$	$-i_2$	$R_2$	$-R_2^1$	$-r_3$	$r_2^2$	-1	$r_4$	$-r_1^2$	$-R_2^1$	$-R_3^1$	$-R_2^1$	$r_4^2$	$r_3^2$	$-R_1^1$	$-R_2^2$	$-r_2$	$-r_1$	
$i_1$	$R_3^3$	$-i_4$	$i_3$	$R_3$	$-R_1$	$-i_6$	$-i_5$	$-R_1^1$	$r_2^1$	$R_3^3$	$-r_4$	$r_4^2$	$-R_2$	$-R_2$	$-R_1^1$	$-R_1$	-1	$-R_2^2$	$-r_3$	$r_2$	$r_3^2$	$r_2^2$	
$i_2$	$i_4$	$R_3^3$	$R_3$	$-i_3$	$-i_5$	$R_1^1$	$R_1$	$-i_6$	$-r_2^1$	$-r_2^1$	$-r_3$	$-r_2^2$	$-R_3$	$-R_2^1$	$-R_3^3$	$-R_2^1$	$R_2^2$	$-1$	$r_4$	$-r_1$	$r_1^2$	$r_4^2$	
$i_3$	$R_1^1$	$R_1$	$-i_5$	$i_6$	$-R_2$	$-R_2^1$	$-i_1$	$i_2$	$-r_2$	$r_1^2$	$R_1^1$	$-r_1$	$r_2^2$	$-R_2^1$	$-R_2^2$	$-R_2^1$	$r_3^2$	$-r_4^2$	-1	$R_3^3$	$r_3$	$-r_4$	
$i_4$	$-i_5$	$i_6$	$-R_1^1$	$-R_1$	$-i_2$	$i_1$	$-R_2^1$	$-R_2$	$r_4$	$r_4^2$	$R_2^2$	$r_3$	$r_2^2$	$R_1^1$	$r_3^2$	$r_3^2$	$-r_2^2$	$r_1^2$	$-R_3^3$	-1	$r_1$	$-r_2$	
$i_5$	$i_2$	$-R_2$	$i_1$	$-R_2^1$	$i_4$	$-R_3$	$i_3$	$-R_3^3$	$R_3^3$	$r_2$	$r_2^2$	$r_4$	$r_4^2$	$r_4^2$	$r_4^2$	$r_4^2$	$-r_3$	$-r_1$	$-r_3^2$	$-r_1^2$	-1	$-R_1^1$	
$i_6$	$R_2^2$	$i_1$	$R_2$	$i_2$	$-R_3$	$-i_4$	$-R_3^3$	$-i_3$	$R_2^2$	$-r_3$	$r_1^2$	$-R_3^3$	$-r_1$	$r_3^2$	$-r_1$	$r_3^2$	$-r_2$	$-r_4$	$r_4^2$	$r_2^2$	$r_2^2$	-1	



**TABLE F.2.2** (Continued)

 (c) Second-rank Tensor  $E$  Representation

$\mathcal{D}^{E(1)}$	$R_1^2 =$	$r_1 =$	$r_2 =$	$r_1^2 =$	$r_2^2 =$	
$\begin{vmatrix} 1 & 0 \\ 0 & 1 \end{vmatrix}$	$\begin{vmatrix} 1 & 0 \\ 0 & 1 \end{vmatrix}$	$\begin{vmatrix} -1 & -\sqrt{3} \\ 2 & 2 \end{vmatrix}$	$\begin{vmatrix} -1 & -\sqrt{3} \\ 2 & 2 \end{vmatrix}$	$\begin{vmatrix} -1 & \sqrt{3} \\ 2 & 2 \end{vmatrix}$	$\begin{vmatrix} -1 & \sqrt{3} \\ 2 & 2 \end{vmatrix}$	
		$\begin{vmatrix} \sqrt{3} & -1 \\ 2 & 2 \end{vmatrix}$	$\begin{vmatrix} \sqrt{3} & -1 \\ 2 & 2 \end{vmatrix}$	$\begin{vmatrix} -\sqrt{3} & -1 \\ 2 & 2 \end{vmatrix}$	$\begin{vmatrix} -\sqrt{3} & -1 \\ 2 & 2 \end{vmatrix}$	
$\mathcal{D}^{E(R_3^2)}$	$R_2^2 =$	$r_4 =$	$r_3 =$	$r_3^2 =$	$r_4^2 =$	
$\begin{vmatrix} 1 & 0 \\ 0 & 1 \end{vmatrix}$	$\begin{vmatrix} 1 & 0 \\ 0 & 1 \end{vmatrix}$	$\begin{vmatrix} -1 & -\sqrt{3} \\ 2 & 2 \end{vmatrix}$	$\begin{vmatrix} -1 & -\sqrt{3} \\ 2 & 2 \end{vmatrix}$	$\begin{vmatrix} -1 & \sqrt{3} \\ 2 & 2 \end{vmatrix}$	$\begin{vmatrix} -1 & \sqrt{3} \\ 2 & 2 \end{vmatrix}$	
		$\begin{vmatrix} \sqrt{3} & -1 \\ 2 & 2 \end{vmatrix}$	$\begin{vmatrix} \sqrt{3} & -1 \\ 2 & 2 \end{vmatrix}$	$\begin{vmatrix} -\sqrt{3} & -1 \\ 2 & 2 \end{vmatrix}$	$\begin{vmatrix} -\sqrt{3} & -1 \\ 2 & 2 \end{vmatrix}$	
$\mathcal{D}^{E(R_3)}$	$i_4 =$	$i_1 =$	$i_2 =$	$R_1^3 =$	$R_1 =$	
$\begin{vmatrix} 1 & 0 \\ 0 & -1 \end{vmatrix}$	$\begin{vmatrix} 1 & 0 \\ 0 & -1 \end{vmatrix}$	$\begin{vmatrix} -1 & \sqrt{3} \\ 2 & 2 \end{vmatrix}$	$\begin{vmatrix} -1 & \sqrt{3} \\ 2 & 2 \end{vmatrix}$	$\begin{vmatrix} -1 & -\sqrt{3} \\ 2 & 2 \end{vmatrix}$	$\begin{vmatrix} -1 & -\sqrt{3} \\ 2 & 2 \end{vmatrix}$	
		$\begin{vmatrix} \sqrt{3} & 1 \\ 2 & 2 \end{vmatrix}$	$\begin{vmatrix} \sqrt{3} & 1 \\ 2 & 2 \end{vmatrix}$	$\begin{vmatrix} -\sqrt{3} & 1 \\ 2 & 2 \end{vmatrix}$	$\begin{vmatrix} -\sqrt{3} & 1 \\ 2 & 2 \end{vmatrix}$	$\left. \begin{matrix} O: & \begin{vmatrix} T_2 \\ A_1 \end{vmatrix} \\ D_4: & \begin{vmatrix} T_2 \\ B_1 \\ A_1 \end{vmatrix} \\ C_2: & \begin{vmatrix} T_2 \\ B_1 \\ A_1 \end{vmatrix} \end{matrix} \right\} \text{basis}$
$\mathcal{D}^{E(R_3^3)}$	$i_3 =$	$R_2 =$	$R_3^2 =$	$i_6 =$	$i_5 =$	
$\begin{vmatrix} 1 & 0 \\ 0 & -1 \end{vmatrix}$	$\begin{vmatrix} 1 & 0 \\ 0 & -1 \end{vmatrix}$	$\begin{vmatrix} -1 & \sqrt{3} \\ 2 & 2 \end{vmatrix}$	$\begin{vmatrix} -1 & \sqrt{3} \\ 2 & 2 \end{vmatrix}$	$\begin{vmatrix} -1 & -\sqrt{3} \\ 2 & 2 \end{vmatrix}$	$\begin{vmatrix} -1 & -\sqrt{3} \\ 2 & 2 \end{vmatrix}$	
		$\begin{vmatrix} \sqrt{3} & 1 \\ 2 & 2 \end{vmatrix}$	$\begin{vmatrix} \sqrt{3} & 1 \\ 2 & 2 \end{vmatrix}$	$\begin{vmatrix} -\sqrt{3} & 1 \\ 2 & 2 \end{vmatrix}$	$\begin{vmatrix} -\sqrt{3} & 1 \\ 2 & 2 \end{vmatrix}$	

For scalar  $(A_1) \begin{vmatrix} A_1 \\ A_1 \end{vmatrix}$  and pseudoscalar  $(A_2) \begin{vmatrix} A_2 \\ B_1 \\ A_1 \end{vmatrix}$  representations, see the  $O$  character table.



TABLE F.2.4 (Continued)

(b) Second-Rank Tensor Representations

$\mathcal{D}^{T_2(1)} =$	$R_1^2 =$	$r_1 =$	$r_2 =$	$r_1^2 =$	$r_2^2 =$	
$\begin{vmatrix} 1 & \cdot & \cdot \\ \cdot & 1 & \cdot \\ \cdot & \cdot & 1 \end{vmatrix}$	$\begin{vmatrix} 1 & \cdot & \cdot \\ \cdot & -1 & \cdot \\ \cdot & \cdot & -1 \end{vmatrix}$	$\begin{vmatrix} \cdot & \cdot & 1 \\ -1 & \cdot & \cdot \\ \cdot & -1 & \cdot \end{vmatrix}$	$\begin{vmatrix} \cdot & \cdot & -1 \\ -1 & \cdot & \cdot \\ \cdot & 1 & \cdot \end{vmatrix}$	$\begin{vmatrix} \cdot & -1 & \cdot \\ \cdot & \cdot & -1 \\ 1 & \cdot & \cdot \end{vmatrix}$	$\begin{vmatrix} \cdot & -1 & \cdot \\ \cdot & \cdot & 1 \\ -1 & \cdot & \cdot \end{vmatrix}$	
$\mathcal{D}^{T_2(R_3^2)} =$	$R_2^2 =$	$r_4 =$	$r_3 =$	$r_3^2 =$	$r_4^2 =$	
$\begin{vmatrix} -1 & \cdot & \cdot \\ \cdot & -1 & \cdot \\ \cdot & \cdot & 1 \end{vmatrix}$	$\begin{vmatrix} -1 & \cdot & \cdot \\ \cdot & 1 & \cdot \\ \cdot & \cdot & -1 \end{vmatrix}$	$\begin{vmatrix} \cdot & \cdot & 1 \\ 1 & \cdot & \cdot \\ \cdot & 1 & \cdot \end{vmatrix}$	$\begin{vmatrix} \cdot & \cdot & -1 \\ 1 & \cdot & \cdot \\ \cdot & -1 & \cdot \end{vmatrix}$	$\begin{vmatrix} \cdot & 1 & \cdot \\ \cdot & \cdot & -1 \\ -1 & \cdot & \cdot \end{vmatrix}$	$\begin{vmatrix} \cdot & 1 & \cdot \\ \cdot & \cdot & 1 \\ 1 & \cdot & \cdot \end{vmatrix}$	
$\mathcal{D}^{T_2(R_3)} =$	$i_4 =$	$i_1 =$	$i_2 =$	$R_1^3 =$	$R_1 =$	
$\begin{vmatrix} \cdot & -1 & \cdot \\ 1 & \cdot & \cdot \\ \cdot & \cdot & -1 \end{vmatrix}$	$\begin{vmatrix} \cdot & -1 & \cdot \\ -1 & \cdot & \cdot \\ \cdot & \cdot & 1 \end{vmatrix}$	$\begin{vmatrix} \cdot & \cdot & -1 \\ \cdot & 1 & \cdot \\ -1 & \cdot & \cdot \end{vmatrix}$	$\begin{vmatrix} \cdot & \cdot & 1 \\ \cdot & 1 & \cdot \\ 1 & \cdot & \cdot \end{vmatrix}$	$\begin{vmatrix} -1 & \cdot & \cdot \\ \cdot & \cdot & 1 \\ \cdot & -1 & \cdot \end{vmatrix}$	$\begin{vmatrix} -1 & \cdot & \cdot \\ \cdot & \cdot & -1 \\ \cdot & 1 & \cdot \end{vmatrix}$	$O : \begin{vmatrix} T_2 \\ D_4 : E \\ D_2 : B_1 \end{vmatrix} \begin{vmatrix} T_2 \\ E \\ B_2 \end{vmatrix} \begin{vmatrix} T_2 \\ B_2 \\ A_2 \end{vmatrix} \text{ basis}$
$\mathcal{D}^{T_2(R_3^3)} =$	$i_3 =$	$R_2 =$	$R_2^3 =$	$i_6 =$	$i_5 =$	
$\begin{vmatrix} \cdot & 1 & \cdot \\ -1 & \cdot & \cdot \\ \cdot & \cdot & -1 \end{vmatrix}$	$\begin{vmatrix} \cdot & 1 & \cdot \\ 1 & \cdot & \cdot \\ \cdot & \cdot & 1 \end{vmatrix}$	$\begin{vmatrix} \cdot & \cdot & -1 \\ \cdot & -1 & \cdot \\ 1 & \cdot & \cdot \end{vmatrix}$	$\begin{vmatrix} \cdot & \cdot & 1 \\ \cdot & -1 & \cdot \\ -1 & \cdot & \cdot \end{vmatrix}$	$\begin{vmatrix} 1 & \cdot & \cdot \\ \cdot & \cdot & 1 \\ \cdot & 1 & \cdot \end{vmatrix}$	$\begin{vmatrix} 1 & \cdot & \cdot \\ \cdot & \cdot & -1 \\ \cdot & -1 & \cdot \end{vmatrix}$	

$\mathcal{D}^E(1)$	$R_1^2 =$	$r_1 =$	$r_2 =$	$r_1^2 =$	$r_2^2 =$	
$\begin{vmatrix} 1 & 0 \\ 0 & 1 \end{vmatrix}$	$\begin{vmatrix} 1 & 0 \\ 0 & 1 \end{vmatrix}$	$\begin{vmatrix} -1 & -\sqrt{3} \\ 2 & 2 \end{vmatrix}$	$\begin{vmatrix} -1 & -\sqrt{3} \\ 2 & 2 \end{vmatrix}$	$\begin{vmatrix} -1 & \sqrt{3} \\ 2 & 2 \end{vmatrix}$	$\begin{vmatrix} -1 & \sqrt{3} \\ 2 & 2 \end{vmatrix}$	
$\mathcal{D}^E(R_3^2)$	$R_2^2 =$	$r_4 =$	$r_3 =$	$r_3^2 =$	$r_4^2 =$	
$\begin{vmatrix} 1 & 0 \\ 0 & 1 \end{vmatrix}$	$\begin{vmatrix} 1 & 0 \\ 0 & 1 \end{vmatrix}$	$\begin{vmatrix} -1 & -\sqrt{3} \\ 2 & 2 \end{vmatrix}$	$\begin{vmatrix} -1 & -\sqrt{3} \\ 2 & 2 \end{vmatrix}$	$\begin{vmatrix} -1 & \sqrt{3} \\ 2 & 2 \end{vmatrix}$	$\begin{vmatrix} -1 & \sqrt{3} \\ 2 & 2 \end{vmatrix}$	
$\mathcal{D}^E(R_3)$	$i_4 =$	$i_1 =$	$i_2 =$	$R_1^3 =$	$R_1 =$	
$\begin{vmatrix} 1 & 0 \\ 0 & -1 \end{vmatrix}$	$\begin{vmatrix} 1 & 0 \\ 0 & -1 \end{vmatrix}$	$\begin{vmatrix} -1 & \sqrt{3} \\ 2 & 2 \end{vmatrix}$	$\begin{vmatrix} -1 & \sqrt{3} \\ 2 & 2 \end{vmatrix}$	$\begin{vmatrix} -1 & -\sqrt{3} \\ 2 & 2 \end{vmatrix}$	$\begin{vmatrix} -1 & -\sqrt{3} \\ 2 & 2 \end{vmatrix}$	$O : \begin{vmatrix} E \\ D_4 : A_1 \\ D_2 : A_1 \end{vmatrix} \begin{vmatrix} E \\ B_1 \\ A_1 \end{vmatrix} \text{ basis}$
$\mathcal{D}^E(R_3^3)$	$i_3 =$	$R_2 =$	$R_2^3 =$	$i_5 =$	$i_2 =$	
$\begin{vmatrix} 1 & 0 \\ 0 & -1 \end{vmatrix}$	$\begin{vmatrix} 1 & 0 \\ 0 & -1 \end{vmatrix}$	$\begin{vmatrix} -1 & \sqrt{3} \\ 2 & 2 \end{vmatrix}$	$\begin{vmatrix} -1 & \sqrt{3} \\ 2 & 2 \end{vmatrix}$	$\begin{vmatrix} -1 & -\sqrt{3} \\ 2 & 2 \end{vmatrix}$	$\begin{vmatrix} -1 & -\sqrt{3} \\ 2 & 2 \end{vmatrix}$	

For scalar  $(A_1) \begin{vmatrix} A_1 \\ A_1 \\ A_1 \end{vmatrix}$  and pseudoscalar  $(A_2) \begin{vmatrix} A_2 \\ B_1 \\ A_1 \end{vmatrix}$  representations, see the  $O$  character table.





$\mathcal{D}^T(1)$	$r_1 = [12]$	$R_1^2 = [13][24]$	$R_3 = [1423]$
$r_1 = [132]$	$r_5 = [13]$	$r_4 = [234]$	$r_6 = [24]$
$r_1^2 = [123]$	$r_2 = [23]$	$r_2^2 = [142]$	$R_3^2 = [1342]$
$R_2^2 = [14][23]$	$R_3^3 = [1234]$	$R_3^2 = [12][34]$	$r_3 = [34]$
$r_2 = [124]$	$R_1 = [1234]$	$r_3 = [143]$	$R_1^3 = [1432]$
$r_2^2 = [134]$	$r_1 = [14]$	$r_2^2 = [243]$	$R_2 = [1243]$

For scalar  $(A_1)$  and pseudoscalar  $(A_2)$  representations, see the  $O$  character table.

TABLE F.2.6  $O \supset D_4 \supset C_4$  Subgroup Chain Labeled Irreducible Representations (Fourfold Moving-Wave Bases)

(a) Vector  $T_1$  Representation

$\mathcal{D}^T(1) =$	$R_1^2 =$	$r_1 =$	$r_2 =$	$r_3 =$	$r_4 =$	$r_5 =$	$r_6 =$
$\begin{bmatrix} 1 & & & \\ & 1 & & \\ & & 1 & \\ & & & 1 \end{bmatrix}$	$\begin{bmatrix} & & & -1 \\ & & & \\ & & & \\ & & & -1 \end{bmatrix}$	$\begin{bmatrix} i & & & \\ & i & & \\ & & i & \\ & & & i \end{bmatrix}$	$\begin{bmatrix} i & & & \\ & i & & \\ & & i & \\ & & & i \end{bmatrix}$	$\begin{bmatrix} i & & & \\ & i & & \\ & & i & \\ & & & i \end{bmatrix}$	$\begin{bmatrix} i & & & \\ & i & & \\ & & i & \\ & & & i \end{bmatrix}$	$\begin{bmatrix} i & & & \\ & i & & \\ & & i & \\ & & & i \end{bmatrix}$	$\begin{bmatrix} i & & & \\ & i & & \\ & & i & \\ & & & i \end{bmatrix}$
$\mathcal{D}^T(R_3^2) =$	$R_2^2 =$	$r_1 =$	$r_2 =$	$r_3 =$	$r_4 =$	$r_5 =$	$r_6 =$
$\begin{bmatrix} -1 & & & \\ & -1 & & \\ & & -1 & \\ & & & -1 \end{bmatrix}$	$\begin{bmatrix} & & & 1 \\ & & & \\ & & & \\ & & & 1 \end{bmatrix}$	$\begin{bmatrix} i & & & \\ & i & & \\ & & i & \\ & & & i \end{bmatrix}$	$\begin{bmatrix} i & & & \\ & i & & \\ & & i & \\ & & & i \end{bmatrix}$	$\begin{bmatrix} i & & & \\ & i & & \\ & & i & \\ & & & i \end{bmatrix}$	$\begin{bmatrix} i & & & \\ & i & & \\ & & i & \\ & & & i \end{bmatrix}$	$\begin{bmatrix} i & & & \\ & i & & \\ & & i & \\ & & & i \end{bmatrix}$	$\begin{bmatrix} i & & & \\ & i & & \\ & & i & \\ & & & i \end{bmatrix}$
$\mathcal{D}^T(R_3) =$	$i_4 =$	$i_1 =$	$i_2 =$	$R_1^3 =$	$R_1 =$	$r_1 =$	$r_2 =$
$\begin{bmatrix} -i & & & \\ & -i & & \\ & & -i & \\ & & & -i \end{bmatrix}$	$\begin{bmatrix} & & & -i \\ & & & \\ & & & \\ & & & -i \end{bmatrix}$	$\begin{bmatrix} -1 & & & \\ & -1 & & \\ & & -1 & \\ & & & -1 \end{bmatrix}$	$\begin{bmatrix} -1 & & & \\ & -1 & & \\ & & -1 & \\ & & & -1 \end{bmatrix}$	$\begin{bmatrix} 1 & & & \\ & 1 & & \\ & & 1 & \\ & & & 1 \end{bmatrix}$	$\begin{bmatrix} 1 & & & \\ & 1 & & \\ & & 1 & \\ & & & 1 \end{bmatrix}$	$\begin{bmatrix} i & & & \\ & i & & \\ & & i & \\ & & & i \end{bmatrix}$	$\begin{bmatrix} i & & & \\ & i & & \\ & & i & \\ & & & i \end{bmatrix}$

TABLE F.2.6 (Continued)

$\mathcal{D}^{T_1}(R_3^3) =$	$i_3 =$	$R_2 =$	$R_2^3 =$	$i_6 =$	$i_5 =$	
$\begin{vmatrix} i & \cdot & \cdot \\ \cdot & -i & \cdot \\ \cdot & \cdot & 1 \end{vmatrix}$	$\begin{vmatrix} \cdot & i & \cdot \\ -i & \cdot & \cdot \\ \cdot & \cdot & -1 \end{vmatrix}$	$\begin{vmatrix} \frac{1}{2} & \frac{1}{2} & \frac{-1}{\sqrt{2}} \\ \frac{1}{2} & \frac{1}{2} & \frac{1}{\sqrt{2}} \\ \frac{1}{\sqrt{2}} & \frac{-1}{\sqrt{2}} & \cdot \end{vmatrix}$	$\begin{vmatrix} \frac{1}{2} & \frac{1}{2} & \frac{1}{\sqrt{2}} \\ \frac{1}{2} & \frac{1}{2} & \frac{-1}{\sqrt{2}} \\ \frac{-1}{\sqrt{2}} & \frac{1}{\sqrt{2}} & \cdot \end{vmatrix}$	$\begin{vmatrix} \frac{-1}{2} & \frac{1}{2} & \frac{i}{\sqrt{2}} \\ \frac{1}{2} & \frac{-1}{2} & \frac{i}{\sqrt{2}} \\ \frac{-i}{\sqrt{2}} & \frac{-i}{\sqrt{2}} & \cdot \end{vmatrix}$	$\begin{vmatrix} \frac{-1}{2} & \frac{1}{2} & \frac{-i}{\sqrt{2}} \\ \frac{1}{2} & \frac{-1}{2} & \frac{-i}{\sqrt{2}} \\ \frac{i}{\sqrt{2}} & \frac{i}{\sqrt{2}} & \cdot \end{vmatrix}$	basis $\begin{matrix} O : \begin{vmatrix} T_1 \\ E \\ 1_4 \end{vmatrix} \begin{vmatrix} T_1 \\ E \\ 3_4 \end{vmatrix} \begin{vmatrix} T_1 \\ A_2 \\ 0_2 \end{vmatrix} \end{matrix}$

(b) Tensor  $T_2$  Representation

$\mathcal{D}^{T_2}(1) =$	$R_1^2 =$	$r_1 =$	$r_2 =$	$r_1^2 =$	$r_2^2 =$
$\begin{vmatrix} 1 & \cdot & \cdot \\ \cdot & 1 & \cdot \\ \cdot & \cdot & 1 \end{vmatrix}$	$\begin{vmatrix} \cdot & -1 & \cdot \\ -1 & \cdot & \cdot \\ \cdot & \cdot & -1 \end{vmatrix}$	$\begin{vmatrix} \frac{i}{2} & \frac{-i}{2} & \frac{-1}{\sqrt{2}} \\ \frac{i}{2} & \frac{-i}{2} & \frac{1}{\sqrt{2}} \\ \frac{i}{\sqrt{2}} & \frac{i}{\sqrt{2}} & \cdot \end{vmatrix}$	$\begin{vmatrix} \frac{i}{2} & \frac{-i}{2} & \frac{1}{\sqrt{2}} \\ \frac{i}{2} & \frac{-i}{2} & \frac{-1}{\sqrt{2}} \\ \frac{-i}{\sqrt{2}} & \frac{-i}{\sqrt{2}} & \cdot \end{vmatrix}$	$\begin{vmatrix} \frac{-i}{2} & \frac{-i}{2} & \frac{-i}{\sqrt{2}} \\ \frac{i}{2} & \frac{i}{2} & \frac{-i}{\sqrt{2}} \\ \frac{-1}{\sqrt{2}} & \frac{1}{\sqrt{2}} & \cdot \end{vmatrix}$	$\begin{vmatrix} \frac{-i}{2} & \frac{-i}{2} & \frac{i}{\sqrt{2}} \\ \frac{i}{2} & \frac{i}{2} & \frac{i}{\sqrt{2}} \\ \frac{1}{\sqrt{2}} & \frac{-1}{\sqrt{2}} & \cdot \end{vmatrix}$

$\mathcal{D}^{T_2}(R_3^3) =$	$R_2^2 =$	$r_4 =$	$r_3 =$	$r_3^2 =$	$r_2^2 =$
$\begin{vmatrix} -1 & \cdot & \cdot \\ \cdot & -1 & \cdot \\ \cdot & \cdot & 1 \end{vmatrix}$	$\begin{vmatrix} \cdot & 1 & \cdot \\ 1 & \cdot & \cdot \\ \cdot & \cdot & -1 \end{vmatrix}$	$\begin{vmatrix} \frac{-i}{2} & \frac{i}{2} & \frac{-1}{\sqrt{2}} \\ \frac{-i}{2} & \frac{i}{2} & \frac{1}{\sqrt{2}} \\ \frac{-i}{\sqrt{2}} & \frac{-i}{\sqrt{2}} & \cdot \end{vmatrix}$	$\begin{vmatrix} \frac{-i}{2} & \frac{i}{2} & \frac{1}{\sqrt{2}} \\ \frac{-i}{2} & \frac{i}{2} & \frac{-1}{\sqrt{2}} \\ \frac{i}{\sqrt{2}} & \frac{i}{\sqrt{2}} & \cdot \end{vmatrix}$	$\begin{vmatrix} \frac{i}{2} & \frac{i}{2} & \frac{-i}{\sqrt{2}} \\ \frac{-i}{2} & \frac{-i}{2} & \frac{-i}{\sqrt{2}} \\ \frac{1}{\sqrt{2}} & \frac{-1}{\sqrt{2}} & \cdot \end{vmatrix}$	$\begin{vmatrix} \frac{i}{2} & \frac{i}{2} & \frac{i}{\sqrt{2}} \\ \frac{-i}{2} & \frac{-i}{2} & \frac{i}{\sqrt{2}} \\ \frac{-1}{\sqrt{2}} & \frac{1}{\sqrt{2}} & \cdot \end{vmatrix}$

$\mathcal{D}^{T_2}(R_3^3) =$	$i_2 =$	$i_2 =$	$R_1^2 =$	$R_1 =$
$\begin{vmatrix} \cdot & \cdot & \cdot \\ \cdot & \cdot & -i \\ \cdot & -1 & \cdot \end{vmatrix}$	$\begin{vmatrix} \cdot & -i & \cdot \\ i & \cdot & \cdot \\ \cdot & \cdot & 1 \end{vmatrix}$	$\begin{vmatrix} \frac{1}{2} & \frac{1}{2} & \frac{1}{\sqrt{2}} \\ \frac{1}{2} & \frac{1}{2} & \frac{-1}{\sqrt{2}} \\ \frac{1}{\sqrt{2}} & \frac{-1}{\sqrt{2}} & \cdot \end{vmatrix}$	$\begin{vmatrix} \frac{1}{2} & \frac{1}{2} & \frac{-1}{\sqrt{2}} \\ \frac{1}{2} & \frac{1}{2} & \frac{1}{\sqrt{2}} \\ \frac{-1}{\sqrt{2}} & \frac{1}{\sqrt{2}} & \cdot \end{vmatrix}$	$\begin{vmatrix} \frac{-1}{2} & \frac{1}{2} & \frac{-i}{\sqrt{2}} \\ \frac{1}{2} & \frac{-1}{2} & \frac{-i}{\sqrt{2}} \\ \frac{-i}{\sqrt{2}} & \frac{-i}{\sqrt{2}} & \cdot \end{vmatrix}$

$\mathcal{D}^{T_2}(R_3^3) =$	$i_3 =$	$R_2 =$	$R_2^3 =$	$i_7 =$	$i_5 =$	
$\begin{vmatrix} i & \cdot & \cdot \\ \cdot & -i & \cdot \\ \cdot & \cdot & -1 \end{vmatrix}$	$\begin{vmatrix} \cdot & i & \cdot \\ -i & \cdot & \cdot \\ \cdot & \cdot & 1 \end{vmatrix}$	$\begin{vmatrix} \frac{-1}{2} & \frac{-1}{2} & \frac{1}{\sqrt{2}} \\ \frac{-1}{2} & \frac{-1}{2} & \frac{-1}{\sqrt{2}} \\ \frac{-1}{\sqrt{2}} & \frac{1}{\sqrt{2}} & \cdot \end{vmatrix}$	$\begin{vmatrix} \frac{-1}{2} & \frac{-1}{2} & \frac{-1}{\sqrt{2}} \\ \frac{-1}{2} & \frac{-1}{2} & \frac{1}{\sqrt{2}} \\ \frac{1}{\sqrt{2}} & \frac{-1}{\sqrt{2}} & \cdot \end{vmatrix}$	$\begin{vmatrix} \frac{1}{2} & \frac{-1}{2} & \frac{i}{\sqrt{2}} \\ \frac{-1}{2} & \frac{1}{2} & \frac{i}{\sqrt{2}} \\ \frac{-i}{\sqrt{2}} & \frac{-i}{\sqrt{2}} & \cdot \end{vmatrix}$	$\begin{vmatrix} \frac{1}{2} & \frac{-1}{2} & \frac{-i}{\sqrt{2}} \\ \frac{-1}{2} & \frac{1}{2} & \frac{-i}{\sqrt{2}} \\ \frac{i}{\sqrt{2}} & \frac{i}{\sqrt{2}} & \cdot \end{vmatrix}$	basis $\begin{matrix} O : \begin{vmatrix} T_2 \\ E \\ 1_4 \end{vmatrix} \begin{vmatrix} T_2 \\ E \\ 3_4 \end{vmatrix} \begin{vmatrix} T_2 \\ B_2 \\ 2_4 \end{vmatrix} \end{matrix}$

The tensor  $E$  representation is identical to that of  $D_4 \supset D_2$  standing-wave basis.

**TABLE F.2.7**  $O \supset D_3 \supset C_3$  Subgroup Chain Labeled Irreducible Representations (Threefold Moving-Wave Bases)

(a) Vector  $T_1$  Representation

$\mathcal{D}^{T_1}(1) =$	$i_4 = [12]$	$R_1^2 = [13][24]$	$R_3 = [1423]$
$\begin{vmatrix} 1 & & \\ & 1 & \\ & & 1 \end{vmatrix}$	$\begin{vmatrix} & -1 & \\ -1 & & \\ & & -1 \end{vmatrix}$	$\begin{vmatrix} -1 & -1+i\sqrt{3} & i-\sqrt{3} \\ -1 & -1 & i+\sqrt{3} \\ -i-\sqrt{3} & -i+\sqrt{3} & -1 \end{vmatrix}$	$\begin{vmatrix} 1-i\sqrt{3} & 1 & -i+\sqrt{3} \\ 1 & 1+i\sqrt{3} & -i-\sqrt{3} \\ i-\sqrt{3} & i+\sqrt{3} & 1 \end{vmatrix}$
$r_1 = [132]$	$i_5 = [13]$	$r_4 = [234]$	$i_6 = [24]$
$\begin{vmatrix} -1 & i\sqrt{3} \\ 2 & -i\sqrt{3} \\ & & 1 \end{vmatrix}$	$\begin{vmatrix} & 1-i\sqrt{3} \\ 1 & & \\ & & -1 \end{vmatrix}$	$\begin{vmatrix} 1 & i\sqrt{3} & -1-i\sqrt{3} \\ -1 & 1+i\sqrt{3} & 1-i\sqrt{3} \\ 2i & 2i & -1 \end{vmatrix}$	$\begin{vmatrix} -2 & -1+i\sqrt{3} & -i+\sqrt{3} \\ -1 & -i\sqrt{3} & -i-\sqrt{3} \\ i+\sqrt{3} & i-\sqrt{3} & 1 \end{vmatrix}$
$r_1^2 = [123]$	$i_2 = [23]$	$r_2^2 = [142]$	$R_3^2 = [1342]$
$\begin{vmatrix} -1 & i\sqrt{3} \\ 2 & -i\sqrt{3} \\ & & 1 \end{vmatrix}$	$\begin{vmatrix} & 1-i\sqrt{3} \\ 1 & & \\ & & -1 \end{vmatrix}$	$\begin{vmatrix} 1 & i\sqrt{3} & 2 \\ 2 & 1+i\sqrt{3} & i+\sqrt{3} \\ -i+\sqrt{3} & -i-\sqrt{3} & -1 \end{vmatrix}$	$\begin{vmatrix} 1+i\sqrt{3} & -1-i\sqrt{3} & -i+\sqrt{3} \\ -1+i\sqrt{3} & 1-i\sqrt{3} & -i-\sqrt{3} \\ -2i & -2i & 1 \end{vmatrix}$
$R_2^2 = [14][23]$	$R_3^3 = [1324]$	$R_3^2 = [12][34]$	$i_3 = [34]$
$\begin{vmatrix} -1 & -1+i\sqrt{3} & i+\sqrt{3} \\ -1 & -1 & i-\sqrt{3} \\ -i+\sqrt{3} & -i-\sqrt{3} & -1 \end{vmatrix}$	$\begin{vmatrix} 1 & i\sqrt{3} & 1 \\ 1 & 1-i\sqrt{3} & -i+\sqrt{3} \\ i+\sqrt{3} & i-\sqrt{3} & 1 \end{vmatrix}$	$\begin{vmatrix} -1 & 2 & -2i \\ 2 & -1 & -2i \\ 2i & 2i & -1 \end{vmatrix}$	$\begin{vmatrix} -2 & 1 & 2i \\ 1 & -2 & 2i \\ -2i & -2i & 1 \end{vmatrix}$

$r_1 = [124]$	$R_1 = [1234]$	$r_2 = [143]$	$R_3^3 = [1432]$
$\begin{vmatrix} 1 & i\sqrt{3} & 2 \\ -1 & -i\sqrt{3} & i+\sqrt{3} \\ 2 & 1-i\sqrt{3} & i-\sqrt{3} \\ -i-\sqrt{3} & -i+\sqrt{3} & -1 \end{vmatrix}$	$\begin{vmatrix} 1 & i\sqrt{3} & -1-i\sqrt{3} \\ -1 & -i\sqrt{3} & 1+i\sqrt{3} \\ -2i & -2i & 1 \end{vmatrix}$	$\begin{vmatrix} 1 & i\sqrt{3} & -1-i\sqrt{3} \\ -1 & -i\sqrt{3} & 1+i\sqrt{3} \\ -i+\sqrt{3} & -i-\sqrt{3} & -1 \end{vmatrix}$	$\begin{vmatrix} 1 & i\sqrt{3} & -1-i\sqrt{3} \\ -1 & -i\sqrt{3} & 1+i\sqrt{3} \\ i-\sqrt{3} & i+\sqrt{3} & 1 \end{vmatrix}$
$r_3^2 = [134]$	$i_1 = [14]$	$r_2^2 = [243]$	$R_2 = [1243]$
$\begin{vmatrix} 1 & i\sqrt{3} & -1-i\sqrt{3} \\ -1 & -i\sqrt{3} & 1+i\sqrt{3} \\ 2i & 2i & -1 \end{vmatrix}$	$\begin{vmatrix} -2 & -1-i\sqrt{3} & -i-\sqrt{3} \\ -1 & -i\sqrt{3} & -i+\sqrt{3} \\ i & i+\sqrt{3} & 1 \end{vmatrix}$	$\begin{vmatrix} 1 & i\sqrt{3} & -1-i\sqrt{3} \\ -1 & -i\sqrt{3} & 1+i\sqrt{3} \\ -i+\sqrt{3} & -i-\sqrt{3} & -1 \end{vmatrix}$	$\begin{vmatrix} 1 & i\sqrt{3} & -1-i\sqrt{3} \\ -1 & -i\sqrt{3} & 1+i\sqrt{3} \\ i & i+\sqrt{3} & 1 \end{vmatrix}$

$$\begin{matrix} O : & \begin{vmatrix} T_1 \\ E \\ T_1 \end{vmatrix} \\ D_3 : & \begin{vmatrix} E \\ E \\ E \end{vmatrix} \\ C_3 : & \begin{vmatrix} 1_3 \\ 2_3 \\ 2_3 \end{vmatrix} \end{matrix} \begin{matrix} T_1 \\ E \\ T_1 \end{matrix}$$

The  $O \supset D_3 \supset C_3$   $T_1$  representation is obtained from that of  $O \supset D_4 \supset D_2$  by the following transformation matrix:

$\begin{matrix} \langle 1_3   \\ \langle 2_3   \\ \langle 0_3   \end{matrix}$	$\begin{matrix}  x_1\rangle &  x_2\rangle &  x_3\rangle \\ -1 & 1 & -i\sqrt{3} \\ 2 & 2 & -i\sqrt{3} \\ \sqrt{3} & \sqrt{3} & \sqrt{3} \end{matrix}$	$\begin{matrix} \langle 1_3   \\ \langle 2_3   \\ \langle 0_3   \end{matrix}$	$\begin{matrix}  c_1\rangle &  c_2\rangle &  c_3\rangle \\ -1 & i & 0 \\ \sqrt{2} & \sqrt{2} & 0 \\ 0 & 0 & 1 \end{matrix}$	$\begin{matrix} \langle v_1   \\ \langle v_2   \\ \langle v_3   \end{matrix}$	$\begin{matrix}  x_1\rangle &  x_2\rangle &  x_3\rangle \\ 1 & -1 & 0 \\ \sqrt{2} & \sqrt{2} & -2 \\ 1 & 1 & \sqrt{3} \end{matrix}$	where	$\begin{matrix}  x_1\rangle = \begin{vmatrix} T_1 \\ E \\ B_1 \end{vmatrix} \\  v_1\rangle = \begin{vmatrix} T_1 \\ E \\ A \end{vmatrix} \\  1_3\rangle = \begin{vmatrix} T_1 \\ E \\ 1_3 \end{vmatrix} \end{matrix}$	$\begin{matrix}  x_2\rangle = \begin{vmatrix} T_1 \\ E \\ B_2 \end{vmatrix} \\  v_2\rangle = \begin{vmatrix} T_1 \\ E \\ B \end{vmatrix} \\  2_3\rangle = \begin{vmatrix} T_1 \\ E \\ 2_3 \end{vmatrix} \end{matrix}$	$\begin{matrix}  x_3\rangle = \begin{vmatrix} T_1 \\ A_2 \\ A_2 \end{vmatrix} \\  v_3\rangle = \begin{vmatrix} T_1 \\ A_2 \\ B \end{vmatrix} \\  0_3\rangle = \begin{vmatrix} T_1 \\ A_2 \\ 0_3 \end{vmatrix} \end{matrix}$	$\begin{matrix} :O \\ :D_4 \\ :D_2 \end{matrix}$	$\begin{matrix} :O \\ :D_3 \\ :C_2 \end{matrix}$	$\begin{matrix} :O \\ :D_3 \\ :C_3 \end{matrix}$
---	--	---	---	---	---	-------	---	---	---	--	--	--

TABLE F.2.7 (Continued)

(b) Tensor Representation  $T_2$

$\mathcal{L}^{T_2}(1) =$	$i_4 = [12]$	$R_1^2 = [13][24]$	$R_3 = [1423]$
$\begin{vmatrix} 1 & & \\ & 1 & \\ & & -1 \end{vmatrix}$	$\begin{vmatrix} 1 & & \\ & & -1 \end{vmatrix}$	$\begin{vmatrix} -1 & \frac{1}{3} - i\frac{\sqrt{3}}{3} & \frac{-1 - i\sqrt{3}}{3} \\ \frac{1}{3} + i\frac{\sqrt{3}}{3} & -1 & \frac{1 - i\sqrt{3}}{3} \\ \frac{-1}{3} + i\frac{\sqrt{3}}{3} & \frac{1}{3} + i\frac{\sqrt{3}}{3} & -1 \end{vmatrix}$	$\begin{vmatrix} -1 & \frac{1}{3} + i\frac{\sqrt{3}}{3} & \frac{-1}{3} + i\frac{\sqrt{3}}{3} \\ \frac{1}{3} + i\frac{\sqrt{3}}{3} & \frac{-1}{3} + i\frac{\sqrt{3}}{3} & \frac{1}{3} \\ \frac{-1}{3} + i\frac{\sqrt{3}}{3} & \frac{1}{3} & \frac{-1}{3} - i\frac{\sqrt{3}}{3} \end{vmatrix}$
$r_1 = [132]$	$i_5 = [13]$	$r_4 = [234]$	$i_6 = [24]$
$\begin{vmatrix} 1 & & & \\ & \frac{-1}{2} - i\frac{\sqrt{3}}{2} & & \\ & & \frac{-1}{2} + i\frac{\sqrt{3}}{2} & \\ & & & 1 \end{vmatrix}$	$\begin{vmatrix} 1 & & & \\ & \frac{1}{2} + i\frac{\sqrt{3}}{2} & & \\ & & \frac{1}{2} - i\frac{\sqrt{3}}{2} & \\ & & & 1 \end{vmatrix}$	$\begin{vmatrix} -1 & \frac{-2}{3} & \frac{2}{3} \\ \frac{1}{3} + i\frac{\sqrt{3}}{3} & \frac{1}{6} + i\frac{\sqrt{3}}{6} & \frac{1}{3} + i\frac{\sqrt{3}}{3} \\ \frac{-1}{3} + i\frac{\sqrt{3}}{3} & \frac{1}{3} - i\frac{\sqrt{3}}{3} & \frac{1}{6} - i\frac{\sqrt{3}}{6} \end{vmatrix}$	$\begin{vmatrix} -1 & \frac{1}{3} - i\frac{\sqrt{3}}{3} & \frac{-1}{3} - i\frac{\sqrt{3}}{3} \\ \frac{1}{3} + i\frac{\sqrt{3}}{3} & \frac{2}{3} & \frac{-1}{6} + i\frac{\sqrt{3}}{6} \\ \frac{-1}{3} + i\frac{\sqrt{3}}{3} & \frac{-1}{6} - i\frac{\sqrt{3}}{6} & \frac{2}{3} \end{vmatrix}$
$r_1^2 = [123]$	$i_2 = [23]$	$r_2^2 = [142]$	$R_2^3 = [1342]$
$\begin{vmatrix} 1 & & & \\ & \frac{-1}{2} + i\frac{\sqrt{3}}{2} & & \\ & & \frac{-1}{2} - i\frac{\sqrt{3}}{2} & \\ & & & 1 \end{vmatrix}$	$\begin{vmatrix} 1 & & & \\ & \frac{1}{2} - i\frac{\sqrt{3}}{2} & & \\ & & \frac{1}{2} + i\frac{\sqrt{3}}{2} & \\ & & & 1 \end{vmatrix}$	$\begin{vmatrix} -1 & \frac{1}{3} + i\frac{\sqrt{3}}{3} & \frac{-1}{3} + i\frac{\sqrt{3}}{3} \\ \frac{1}{3} + i\frac{\sqrt{3}}{3} & \frac{1}{6} - i\frac{\sqrt{3}}{6} & \frac{-2}{3} \\ \frac{-1}{3} + i\frac{\sqrt{3}}{3} & \frac{-2}{3} & \frac{1}{6} + i\frac{\sqrt{3}}{6} \end{vmatrix}$	$\begin{vmatrix} -1 & \frac{-2}{3} & \frac{2}{3} \\ \frac{1}{3} + i\frac{\sqrt{3}}{3} & \frac{-1}{3} - i\frac{\sqrt{3}}{3} & \frac{-1}{6} - i\frac{\sqrt{3}}{6} \\ \frac{-1}{3} + i\frac{\sqrt{3}}{3} & \frac{1}{6} + i\frac{\sqrt{3}}{6} & \frac{-1}{3} - i\frac{\sqrt{3}}{3} \end{vmatrix}$

$R_1^3 = [124]$	$R_3^3 = [1324]$	$R_2^3 = [12][34]$	$i_3 = [34]$
$\begin{vmatrix} -1 & \frac{1}{3} + i\frac{\sqrt{3}}{3} & \frac{-1}{3} + i\frac{\sqrt{3}}{3} \\ \frac{1}{3} + i\frac{\sqrt{3}}{3} & -1 & \frac{1}{3} + i\frac{\sqrt{3}}{3} \\ \frac{-1}{3} - i\frac{\sqrt{3}}{3} & \frac{1}{3} - i\frac{\sqrt{3}}{3} & -1 \end{vmatrix}$	$\begin{vmatrix} -1 & \frac{1}{3} - i\frac{\sqrt{3}}{3} & \frac{-1}{3} + i\frac{\sqrt{3}}{3} \\ \frac{1}{3} - i\frac{\sqrt{3}}{3} & -1 & \frac{1}{3} + i\frac{\sqrt{3}}{3} \\ \frac{-1}{3} - i\frac{\sqrt{3}}{3} & \frac{1}{3} & \frac{-1}{3} + i\frac{\sqrt{3}}{3} \end{vmatrix}$	$\begin{vmatrix} -1 & -2 & 2 \\ -2 & -1 & -2 \\ 2 & -2 & -1 \end{vmatrix}$	$\begin{vmatrix} -1 & -2 & 2 \\ -2 & 2 & 1 \\ 2 & 1 & 2 \end{vmatrix}$
$r_2 = [124]$	$R_1 = [1234]$	$r_3 = [143]$	$R_1^3 = [1432]$
$\begin{vmatrix} -1 & \frac{1}{3} - i\frac{\sqrt{3}}{3} & \frac{-1}{3} - i\frac{\sqrt{3}}{3} \\ \frac{1}{3} - i\frac{\sqrt{3}}{3} & \frac{1}{6} + i\frac{\sqrt{3}}{6} & \frac{-2}{3} \\ \frac{-1}{3} - i\frac{\sqrt{3}}{3} & \frac{-2}{3} & \frac{1}{6} - i\frac{\sqrt{3}}{6} \end{vmatrix}$	$\begin{vmatrix} -1 & \frac{-2}{3} & \frac{2}{3} \\ \frac{1}{3} - i\frac{\sqrt{3}}{3} & \frac{-1}{3} - i\frac{\sqrt{3}}{3} & \frac{-1}{6} + i\frac{\sqrt{3}}{6} \\ \frac{-1}{3} - i\frac{\sqrt{3}}{3} & \frac{-1}{6} - i\frac{\sqrt{3}}{6} & \frac{-1}{3} - i\frac{\sqrt{3}}{3} \end{vmatrix}$	$\begin{vmatrix} -1 & \frac{1}{3} + i\frac{\sqrt{3}}{3} & \frac{-1}{3} + i\frac{\sqrt{3}}{3} \\ -2 & \frac{1}{6} + i\frac{\sqrt{3}}{6} & \frac{1}{3} - i\frac{\sqrt{3}}{3} \\ 2 & \frac{1}{3} + i\frac{\sqrt{3}}{3} & \frac{1}{6} - i\frac{\sqrt{3}}{6} \end{vmatrix}$	$\begin{vmatrix} -1 & \frac{1}{3} + i\frac{\sqrt{3}}{3} & \frac{-1}{3} + i\frac{\sqrt{3}}{3} \\ -2 & \frac{-1}{3} - i\frac{\sqrt{3}}{3} & \frac{-1}{6} + i\frac{\sqrt{3}}{6} \\ 2 & \frac{-1}{6} - i\frac{\sqrt{3}}{6} & \frac{-1}{3} + i\frac{\sqrt{3}}{3} \end{vmatrix}$
$r_2^2 = [134]$	$i_1 = [14]$	$r_2^2 = [243]$	$R_2 = [1243]$
$\begin{vmatrix} -1 & \frac{-2}{3} & \frac{2}{3} \\ \frac{1}{3} - i\frac{\sqrt{3}}{3} & \frac{1}{6} - i\frac{\sqrt{3}}{6} & \frac{1}{3} - i\frac{\sqrt{3}}{3} \\ \frac{-1}{3} - i\frac{\sqrt{3}}{3} & \frac{1}{6} - i\frac{\sqrt{3}}{6} & \frac{1}{3} - i\frac{\sqrt{3}}{3} \end{vmatrix}$	$\begin{vmatrix} -1 & \frac{1}{3} + i\frac{\sqrt{3}}{3} & \frac{-1}{3} + i\frac{\sqrt{3}}{3} \\ \frac{1}{3} - i\frac{\sqrt{3}}{3} & \frac{2}{3} & \frac{-1}{6} - i\frac{\sqrt{3}}{6} \\ \frac{-1}{3} - i\frac{\sqrt{3}}{3} & \frac{-1}{6} + i\frac{\sqrt{3}}{6} & \frac{2}{3} \end{vmatrix}$	$\begin{vmatrix} -1 & \frac{1}{3} - i\frac{\sqrt{3}}{3} & \frac{-1}{3} - i\frac{\sqrt{3}}{3} \\ -2 & \frac{1}{6} - i\frac{\sqrt{3}}{6} & \frac{1}{3} + i\frac{\sqrt{3}}{3} \\ 2 & \frac{1}{3} - i\frac{\sqrt{3}}{3} & \frac{1}{6} + i\frac{\sqrt{3}}{6} \end{vmatrix}$	$\begin{vmatrix} -1 & \frac{1}{3} - i\frac{\sqrt{3}}{3} & \frac{-1}{3} - i\frac{\sqrt{3}}{3} \\ -2 & \frac{-1}{3} + i\frac{\sqrt{3}}{3} & \frac{-1}{6} - i\frac{\sqrt{3}}{6} \\ 2 & \frac{-1}{6} + i\frac{\sqrt{3}}{6} & \frac{-1}{3} - i\frac{\sqrt{3}}{3} \end{vmatrix}$

$$\begin{matrix} O: \\ D_3: \\ C_3: \end{matrix} \begin{vmatrix} T_2 \\ A_1 \\ 0_3 \end{vmatrix} \begin{matrix} T_2 \\ E \\ 1 \end{matrix}$$

The  $O \supset D_3 \supset C_3 T_2$  representation is obtained from that of  $O \supset D_2 \supset D_2$  by the following transformation matrix:

$$\begin{matrix} \langle 0_3 | \\ \langle 1_3 | \\ \langle 2_3 | \end{matrix} \begin{vmatrix} |x_1\rangle & |x_2\rangle & |x_3\rangle \\ \sqrt{3} & -\sqrt{3} & \sqrt{3} \\ i & i & -\sqrt{3} \\ \frac{1}{2} - i\frac{\sqrt{3}}{6} & \frac{1}{2} - i\frac{\sqrt{3}}{6} & \frac{1}{3} \end{vmatrix} = \begin{matrix} \langle 0_3 | \\ \langle 1_3 | \\ \langle 2_3 | \end{matrix} \begin{vmatrix} |e_1\rangle & |e_2\rangle & |e_3\rangle \\ 1 & 0 & 0 \\ 0 & -1 & i \\ 0 & \frac{1}{\sqrt{2}} & \frac{i}{\sqrt{2}} \end{vmatrix} \cdot \begin{matrix} \langle e_1 | \\ \langle e_2 | \\ \langle e_3 | \end{matrix} \begin{vmatrix} |x_1\rangle & |x_2\rangle & |x_3\rangle \\ 1 & -1 & 1 \\ \sqrt{3} & \sqrt{3} & \sqrt{3} \\ -1 & 1 & 2 \\ \sqrt{6} & \sqrt{6} & \sqrt{6} \end{vmatrix} \quad \text{where} \quad \begin{matrix} |x_1\rangle = \begin{vmatrix} T_2 \\ E \\ B_1 \end{vmatrix} \\ |x_2\rangle = \begin{vmatrix} T_2 \\ E \\ B_2 \end{vmatrix} \\ |x_3\rangle = \begin{vmatrix} T_2 \\ B_2 \\ A_2 \end{vmatrix} \\ |e_1\rangle = \begin{vmatrix} T_2 \\ A_1 \\ A \end{vmatrix} \\ |e_2\rangle = \begin{vmatrix} T_2 \\ E \\ A \end{vmatrix} \\ |e_3\rangle = \begin{vmatrix} T_2 \\ B \\ B \end{vmatrix} \\ |0_3\rangle = \begin{vmatrix} T_2 \\ A_1 \\ 0_3 \end{vmatrix} \\ |1_3\rangle = \begin{vmatrix} T_2 \\ E \\ 1_3 \end{vmatrix} \\ |2_3\rangle = \begin{vmatrix} T_2 \\ E \\ 2_3 \end{vmatrix} \end{matrix} \begin{matrix} :O \\ :D_4 \\ :D_2 \\ :O \\ :D_3 \\ :C_2 \\ :O \\ :D_3 \\ :C_3 \end{matrix}$$

TABLE F.2.7 (Continued)

(c) Tensor Representation  $E$

$$\mathcal{O}^{T_3(1)} =$$

$$\begin{vmatrix} 1 & \cdot \\ \cdot & 1 \end{vmatrix}$$

$$r_1 = [132]$$

$$\begin{vmatrix} \frac{-1}{2} - i\frac{\sqrt{3}}{2} & \\ & \frac{-1}{2} + i\frac{\sqrt{3}}{2} \end{vmatrix}$$

$$r_1^2 = [123]$$

$$\begin{vmatrix} \frac{-1}{2} + i\frac{\sqrt{3}}{2} & \\ & \frac{-1}{2} - i\frac{\sqrt{3}}{2} \end{vmatrix}$$

$$i_4 = [12]$$

$$\begin{vmatrix} \cdot & -1 \\ -1 & \cdot \end{vmatrix}$$

$$i_5 = [13]$$

$$\begin{vmatrix} \cdot & \cdot & \frac{-1}{2} - i\frac{\sqrt{3}}{2} \\ & \frac{-1}{2} + i\frac{\sqrt{3}}{2} & \\ & & \cdot \end{vmatrix}$$

$$i_2 = [23]$$

$$\begin{vmatrix} \cdot & \cdot & \frac{-1}{2} + i\frac{\sqrt{3}}{2} \\ & \frac{-1}{2} - i\frac{\sqrt{3}}{2} & \\ & & \cdot \end{vmatrix}$$

$$R_1^2 = [13][24]$$

$$\begin{vmatrix} 1 & \cdot \\ \cdot & 1 \end{vmatrix}$$

$$r_4 = [234]$$

$$\begin{vmatrix} \frac{-1}{2} - i\frac{\sqrt{3}}{2} & & \\ & \frac{-1}{2} + i\frac{\sqrt{3}}{2} & \\ & & \cdot \end{vmatrix}$$

$$r_2^2 = [142]$$

$$\begin{vmatrix} \frac{-1}{2} + i\frac{\sqrt{3}}{2} & & \\ & \frac{-1}{2} - i\frac{\sqrt{3}}{2} & \\ & & \cdot \end{vmatrix}$$

$$R_3 = [1423]$$

$$\begin{vmatrix} \cdot & -1 \\ -1 & \cdot \end{vmatrix}$$

$$i_6 = [24]$$

$$\begin{vmatrix} \cdot & \cdot & \frac{-1}{2} - i\frac{\sqrt{3}}{2} \\ & \frac{-1}{2} + i\frac{\sqrt{3}}{2} & \\ & & \cdot \end{vmatrix}$$

$$R_2^2 = [1342]$$

$$\begin{vmatrix} \cdot & \cdot & \frac{-1}{2} + i\frac{\sqrt{3}}{2} \\ & \frac{-1}{2} - i\frac{\sqrt{3}}{2} & \\ & & \cdot \end{vmatrix}$$

$$R_2^2 = [14][23]$$

$$\begin{vmatrix} 1 & \cdot \\ \cdot & 1 \end{vmatrix}$$

$$r_2 = [124]$$

$$\begin{vmatrix} \frac{-1}{2} - i\frac{\sqrt{3}}{2} & & \\ & \frac{-1}{2} + i\frac{\sqrt{3}}{2} & \\ & & \cdot \end{vmatrix}$$

$$r_3^2 = [134]$$

$$\begin{vmatrix} \frac{-1}{2} + i\frac{\sqrt{3}}{2} & & \\ & \frac{-1}{2} - i\frac{\sqrt{3}}{2} & \\ & & \cdot \end{vmatrix}$$

$$R_1^2 = [1324]$$

$$\begin{vmatrix} \cdot & -1 \\ -1 & \cdot \end{vmatrix}$$

$$R_1 = [1234]$$

$$\begin{vmatrix} \cdot & \cdot & \frac{-1}{2} - i\frac{\sqrt{3}}{2} \\ & \frac{-1}{2} + i\frac{\sqrt{3}}{2} & \\ & & \cdot \end{vmatrix}$$

$$i_1 = [14]$$

$$\begin{vmatrix} \cdot & \cdot & \frac{-1}{2} + i\frac{\sqrt{3}}{2} \\ & \frac{-1}{2} - i\frac{\sqrt{3}}{2} & \\ & & \cdot \end{vmatrix}$$

$$R_3^2 = [12][34]$$

$$\begin{vmatrix} 1 & \cdot \\ \cdot & 1 \end{vmatrix}$$

$$r_3 = [143]$$

$$\begin{vmatrix} \frac{-1}{2} - i\frac{\sqrt{3}}{2} & & \\ & \frac{-1}{2} + i\frac{\sqrt{3}}{2} & \\ & & \cdot \end{vmatrix}$$

$$r_2^2 = [243]$$

$$\begin{vmatrix} \frac{-1}{2} + i\frac{\sqrt{3}}{2} & & \\ & \frac{-1}{2} - i\frac{\sqrt{3}}{2} & \\ & & \cdot \end{vmatrix}$$

$$i_3 = [34]$$

$$\begin{vmatrix} \cdot & -1 \\ -1 & \cdot \end{vmatrix}$$

$$R_1^3 = [1432]$$

$$\begin{vmatrix} \cdot & \cdot & \frac{-1}{2} - i\frac{\sqrt{3}}{2} \\ & \frac{-1}{2} + i\frac{\sqrt{3}}{2} & \\ & & \cdot \end{vmatrix}$$

$$R_2 = [1243]$$

$$\begin{vmatrix} \cdot & \cdot & \frac{-1}{2} + i\frac{\sqrt{3}}{2} \\ & \frac{-1}{2} - i\frac{\sqrt{3}}{2} & \\ & & \cdot \end{vmatrix}$$

$$\begin{matrix} O: \\ D_3: \\ C_3: \end{matrix} \begin{vmatrix} E \\ E \\ 1_3 \end{vmatrix} \begin{vmatrix} E \\ E \\ 2_3 \end{vmatrix}$$

The  $O \supset D_3 \supset C_3 \supset E$  representation is obtained from that of  $O \supset D_4 \supset D_2$  by the following transformation matrix:

$$\begin{matrix} \langle 1_3 | \\ \langle 2_3 | \end{matrix} \begin{vmatrix} |x_1\rangle & |x_2\rangle \\ \frac{-1}{\sqrt{2}} & \frac{i}{\sqrt{2}} \\ 1 & \frac{i}{\sqrt{2}} \end{vmatrix} = \begin{matrix} \langle 1_3 | \\ \langle 2_3 | \end{matrix} \begin{vmatrix} |e_1\rangle & |e_2\rangle \\ \frac{-1}{\sqrt{2}} & \frac{i}{\sqrt{2}} \\ 1 & \frac{i}{\sqrt{2}} \end{vmatrix} \cdot \begin{matrix} \langle e_1 | \\ \langle e_2 | \end{matrix} \begin{vmatrix} |x_1\rangle & |x_2\rangle \\ 1 & 0 \\ 0 & 1 \end{vmatrix}$$

$$\text{where } \begin{matrix} |x_1\rangle = \begin{vmatrix} E \\ E \\ B_1 \end{vmatrix} \\ |x_2\rangle = \begin{vmatrix} E \\ E \\ B_2 \end{vmatrix} \\ |e_1\rangle = \begin{vmatrix} E \\ E \\ A \end{vmatrix} \\ |e_2\rangle = \begin{vmatrix} E \\ E \\ B \end{vmatrix} \\ |1_3\rangle = \begin{vmatrix} E \\ E \\ 1_1 \end{vmatrix} \end{matrix} \begin{matrix} |x_2\rangle = \begin{vmatrix} E \\ E \\ D_4 \\ D_2 \end{vmatrix} \\ |e_1\rangle = \begin{vmatrix} E \\ E \\ D_3 \\ C_2 \end{vmatrix} \\ |2_3\rangle = \begin{vmatrix} E \\ E \\ 2_3 \\ C_3 \end{vmatrix} \end{matrix} \begin{matrix} :O \\ :D_4 \\ :D_3 \\ :C_2 \\ :D_3 \\ :C_3 \end{matrix}$$